

Design and Prototyping of a High Country Electric Vehicle (HiCEV)

A thesis submitted in partial fulfilment of the requirements for the Degree of Masters of Engineering in
Electronic and Electrical Engineering

By

Pierce L. Hennessy

2016

Abstract

The development of a High Country Electric Vehicle has come about in response to a farmers desire to reduce the dependence on fossil fuels on his station. Electric vehicles have become more prominent in the urban commuter vehicle market over recent years, and are gaining greater acceptance as people look to be more environmentally aware. This project shows that electric vehicles also have a place in the primary sectors in an off-roading, rugged context.

The conversion vehicle of choice is the Toyota Land Cruiser 70 Series, an iconic farming vehicle renowned for its reliability in challenging operating conditions. The vehicle was stripped of components associated with the 1-HZ internal combustion engine (ICE) drivetrain, and electrical drivetrains was scoped, sourced and implemented in the vehicle.

This report investigates the systems integration aspects associated with modern electrical vehicle components. The aspects of integration covered mechanical analysis of shaft coupling, interfacing CANbus systems, high voltage system safety and low voltage wiring loom mapping. The vehicle has reached self-propulsion and validation testing against the initial vehicle modeling is underway.

Acknowledgements

I would like to thank my supervisor Dr Paul Gaynor for his continued support and faith in me and John Shrimpton for his unbounded enthusiasm and foresight to initiate the HiCEV project. Thank you to the technical staff of Canterbury University for your support in locating the vehicle and providing expertise and guidance. Also, thank you to the student groups I have had the pleasure of working with over the last couple of years, you have made HiCEV what it is today.

To Jeff and the Brown family – I cannot thank you enough for the time you have given to me and this project, to say you were generous falls far short of the mark. Your technical expertise and hands on knowledge was critical in forming HiCEV.

Finally thanks to all my friends and family for your undying support, especially when things went pear shaped. There is no chance I would have made this voyage without you.

Table of Contents

1.0 Introduction	8
1.1 Project Motivation	8
1.1.1 Location.....	8
1.2 Electric Vehicles in NZ	9
1.3 Sustainability in NZ Transportation.....	10
2.0 Background	10
2.1 Emissions.....	11
2.1 Electrical Principals	11
2.1.1 Electrical Terminology.....	11
2.1.2 Motor Theory	12
2.1.2.1 DC Motors	12
2.1.2.2 Induction Motors	13
2.1.2.3 BLDC / PMAC Motors	14
2.1.2.4 Motor Losses and Cooling.....	16
2.1.3 Inverter Theory	17
2.1.3.1 Field Orientated Control (FOC)	18
2.1.4 CANbus Communication	18
2.1.4.1 CANbus in Automotive.....	18
2.1.4.2 CAN Terminology	18
2.1.4.3 CAN Operation	19
2.1.5 Battery Theory	19
2.1.5.1 Battery Chemistries.....	20
2.1.6.2 Shielding.....	23
2.1.6 Electro Magnetic Noise	23
2.2. Vehicle Principals	24
2.2.1. Basic Theory of Operation	24
2.2.2. EV Component Configurations.....	25
• BEV	25
• HEV	25
• REEV	25
• FCEV	25
2.2.3. Drivetrain Typologies	25

2.3. Role of Systems Engineer.....	25
3.0 Prototype Specification Design.....	27
3.1. Stakeholder Requirements	27
3.1.1. Costings.....	27
3.2. User Requirements	27
3.2.1. Client and Intended use	27
3.2.2. Donor Vehicle.....	28
3.2.3. Off-Road Operation.....	28
3.2.4. Performance and Drivetrain	29
3.2.4.1. Typology	30
3.3. System Requirements	31
3.3.1. Vehicle Performance.....	31
3.3.1.1. HiCEV Estimated Characteristics	31
3.3.1.2. Regenerative Braking and Range Extension	33
3.4. Component Sourcing	34
3.4.1. Motor and Inverter combination	34
3.4.1.1. Motor Selection	36
3.4.1.2. Inverter Selection.....	37
3.4.2. Remaining Main Components.....	39
3.4.2.1. Battery Pack Sizing	39
3.4.2.2. Remaining main system modules	45
3.5. Main Architectural Design	50
3.5.1. Component Layout.....	51
3.5.2. Electrical Layout.....	53
3.5.3. Mechanical Layout	54
3.5.3.1. Motor to drivetrain	54
3.5.3.2. Battery Boxes	59
3.1 Subsystem Development	61
3.1.1 Thermal Systems.....	62
3.1.2 Motor Cooling	63
3.1.3 Inverter Cooling.....	66
3.1.4 Charger Cooling.....	68
3.1.5 Power Steering.....	68

3.1.6	Dash Cluster	68
3.1.7	Change Over switching unit	68
4.0	Testing and Commissioning.....	68
4.1	Main Modules	68
4.2	Calibration.....	69
4.2.1	Electric Vehicle Control Module (EVCM)	69
4.2.1.1	EVCM Hardware, Control and Implementation	71
4.2.2	Eltek Charger Calibration	81
4.2.3	BMS Calibration.....	85
4.2.4	Rinehart 150 DX inverter Settings.....	88
4.3	Commissioning (Systems integration)	93
4.3.1	Motor Mechanical Development.....	93
4.3.2	Inverter.....	95
4.3.2.1	Interfacing with Remy HVH 250-115 PO.....	96
4.3.2.2	Resolver.....	96
4.3.2.3	HV Safety Circuit	99
4.3.3	CANbus.....	106
4.3.3.1	CANbus Database.....	106
4.3.4	Battery Pack	107
4.3.4.1	Initial BMS Setup	109
4.3.5	Vehicle Analysis.....	110
4.3.6	Cooling	113
5.0	Discussion	115
5.1	Issues Faced	115
5.2	Future for HiCEV.....	115
6.0	Conclusion.....	115
7.0	Appendix.....	116
7.1	Birds eye view of component layout	116
7.2	CAD model of battery boxes	117
7.3	Rinehart Wiring Diagram	118
7.4	Inverter Loom Mapping	119
7.5	Motor Performance Diagrams	123
7.6	Class D Specifications.....	124

8.0 Bibliography	126
-------------------------------	------------

1.0 Introduction

As the demand for electric vehicles (EVs) increases on a global scale largely due to environmental and economic issues, the phasing of electric propulsion systems into different sectors of the vehicle fleet is inevitable. EVs initially found their niche in light urban commuters, but have recently breached into sectors such as racing, long distance commuters and heavy machinery [1, 2, 3, 4, 5]. Tesla Motors has played a major role in increasing the public perception of EVs, with their new model S luxury sedan. The Model S, aside from being a luxury vehicle (capable of 253 mile range), is the fastest on road sedan EV or ICE, with 691 electrical HP and capable of 3.1 second 0-60mph [2]. This move towards EVs has started slow, and faced many challenges but momentum is building behind the EV movement as people become faced with the realities of the issues associated with internal combustion engine (ICE) vehicles. Climate change, oil scarcity combined the fact that the advance of electric propulsion technology to have a desirable vehicle capable of exceeding (ICE) vehicles in performance, price and reduced emissions is quickly coming to fruition.

1.1 Project Motivation

The motivation project arose from the desire of a South Island, New Zealand farm to be more self-sufficient whilst taking the lead with a new application for electric vehicles. Glenthorne Station resides beside Lake Coleridge in the middle of the South Island, is taking the initiative to look into and create an electric vehicle for daily farm use. This high country electric vehicle (HiCEV) uses the shell of a 70 Series Land Cruiser, to retain the durability of a farm vehicle, while not losing any performance. This EV acts as a prototype for the station, with hopes that- down the track, there will be many electric vehicles on the station based on this platform.

Acting as an introduction for electric vehicles into NZ farming, the hope is that there will be a future move towards more self-sustaining agricultural practices in NZ. The requirements for HiCEV were bound initially by the desire to use newly available EV components and the restrictions imposed by the harsh operating conditions.

1.1.1 Location

Glenthorne station is the culmination of two high country stations, lower Ryton station (now ‘Lower Glenthorne’) and the Glenthorne station (now ‘Upper Glenthorne’), whose name was retained. Located off the northern shore of Lake Coleridge, Glenthorne station is the embodiment of ‘High Country Station’. Lower Glenthorne sits at approximately 560m and Upper Glenthorne at 810m meters above sea level and covering 25000 hectares [6]. There are sections of Glenthorne so steep that no pasture grows, and is uninhabitable by cattle, the typology is shown in figure [1]. A public gravel road

runs through the middle of Glenthorne, allowing access to various lakes around the property including Lake Coleridge itself.



Figure 1 Map of Glenthorne Station [6]

The temperature variation is also an interesting parameter to take into account for vehicles on the station, with temperatures that can reach -20°C can make for interesting issues for not only EV's, but ICE vehicles also. At these temperatures, coolant can freeze, oil and battery electrolyte can become viscous and moisture can build in electrical enclosures through condensation.

1.2 Electric Vehicles in NZ

The term Electric Vehicle is a blanket term to describe many types of drivetrain topologies but the two main types are battery electric vehicles (BEV) and hybrid electric vehicles (HEV). BEV's are electric vehicles whose energy storage is wholly electric, in the form of a large capacity battery pack and charged from external electricity supplies [7]. HEV's have both an electric power drivetrain, but also a combustion system that can be used as either a form of on-board battery charging or as an alternative drive train depending on drivetrain typology [8]. HEV's come in with a range of battery capacities, the smallest of which don't require external charging, as the internal system charges the battery pack through the ICE acting as a generator, or energy recapture in the form of regenerative braking. Plug-in HEVs (PHEVs) have a larger battery pack and allow short range travel on battery power alone.

Electric vehicles have made their way into the NZ market, but are still vastly outnumbered by ICE vehicles in both number and advertising. NZ's total light fleet comprises of 589 registered EV's [9] and 8,861 HEVs as of December 2013 [10]. For the past 10 years, the total light vehicle fleet size in NZ has consistently grown fairly consistently, with new vehicles in 2012 comprising 52% of the total travel done in NZ (13% Commercial, 39% Passenger) and 92% of total travel by light vehicle travel [10]

Commercially available EV's are only really available as new vehicles (0-5 years old) as first sales mass EV's to NZ public began in 2011 [7].

To increase the rate of integration of EVs into NZ a major component would be increasing infrastructure to support the new generation of motoring. Options for charging a plugin EV are either; household wall chargers or public charging stations, of which there are 74 public charging stations currently in NZ [9]. Currently, the most common way to charge an EV is at home [11]. With the evolution of the NZ grid towards a 'smart-grid', integrating communication with the current power transmission, chargers should be able to communicate with the grid for the best times to charge for price and also *back-feed* from vehicle to grid (V2G), acting as a network of power supplies for grid stability [12].

This project could form the basis of shifting focus from EVs solely being thought of as light urban commuter vehicles. Main economic NZ sectors associated with heavy work such as agriculture, mining and forestry could start phasing in electric work vehicles with this project in mind. This has several benefits, as these sectors are often associated with trading the environment for economics, by taking EVs into their fleets they will improve their public image while reducing their carbon footprint.

1.3 Sustainability in NZ Transportation

New Zealand already has a majority of renewable sources for power generation with only 30% of generation produced by non-renewables sources [7] which is a good step in the direction towards reducing greenhouse gas emissions and creating an environmentally sustainable future. In the transport sector, the government has placed an exemption for light electric motor vehicles for road user charges (RUC's) until 2020, to give the public some incentive to invest in EVs for public transportation [13].

Policies such as the above are crucial to phasing NZ towards a more sustainable environment. There are going to be have to be more serious changes, in the near future in regards to the general environment. Electric vehicles will play an essential role in any sustainability model that takes into account the future of personal transportation, to reduce the fossil fuel usage and thus the greenhouse gas emissions. Energy security will also play a major role in NZ's energy sustainability model. Oil reserves are depleting globally with time, moving towards an electrified fleet reduces the dependency on oil prices beyond our control becomes less of an issue [7].

Personal transportation has grown to be an essential part of many peoples everyday life to go wherever they want any time they choose. Sustaining this becomes essential in applications such as farming work, where patrolling large areas or land is essential for the upkeep of the station. This factor requires electric vehicles to have the capacity for long duration travel, even if the average distance traveled daily in NZ is 40km [10] which isn't quite there yet for readily available BEVs. That being said, R&D into newer higher capacity batteries with a relatively low cost per kWh is being investigated thoroughly worldwide currently to reduce this hindering factor for potential EV buyers [14].

2.0 Background

Electric vehicles (EVs) are widely viewed as the vehicle of choice in an environmentally responsible society. They are available for personal use (private sales) and are being incorporated into fleet purchases [15]. It should not be surprising that they are also being considered in other areas previously dominated by fossil fueled vehicles.

Historically, vehicle evolution has enabled the human race to expand, interconnect and grow at a rate exponentially faster than would have been possible without them, but this has come hand in hand with crippling effects on the global environment. One of the major contributing factors is combustion engine emissions [16]. To enable the human race to progress, while reducing the environmental impact of vehicles, the proposed solution by many is to phase in low-to-zero pollution emitting electric vehicles. This EV drivetrain technology is becoming increasingly prevalent, starting mainly in the light vehicle transportation sector, but also heavy machinery as efficiency and torque delivery characteristics become more widely acknowledged. The aim of this section is to highlight the main characteristics of EVs, such as their low ground-to-road emission values comparatively with ICE vehicles, but also the drivetrain technology in terms of common componentry and vehicle analysis.

2.1 Emissions

The ‘Greenhouse Effect’ is a naturally occurring effect whereby gases in the atmosphere act as a blanket, keeping the earth warm. Without this effect, the earth would be 33°C lower than it is now, and the life that we have now would not have been possible [17]. Ideal global temperature is under threat as mankind has exaggerated Greenhouse Effect by producing large quantities of CO₂ – vehicle emissions are a major contributor. People are questioning the widespread use of fossil fuels and the danger posed to life on earth as a consequence of this.

As of 2012, the Transport sector in New Zealand (NZ) currently contributes 20% of total greenhouse emissions by sector, second only to the Agricultural Methane emissions at 32% [18] and the current fleet of EVs in NZ have saved 277 tons of CO₂ emissions [9].

2.1 Electrical Principals

Electricity is a secondary form of energy, generated from either renewable sources, fossil fuels or nuclear primary source, and is arguably the most usable form of energy due to its ease of manipulation, transmission and storage [19]. Electrical energy is the driving force of most societies today, with the vast majority of people around the world heavily reliant on it for daily use. Personal transport has relied on electricity since its conception, including powering sub-systems and communication in ICE vehicles, and now the driving force in EV’s and Hybrids.

2.1.1 Electrical Terminology

A list of terminology is given below for reference:

Subscripts

DC	– Direct Current
AC	– Alternating Current
RMS	– Root Mean Squared
p	– Peak
a, b, c	– Phases in AC
m	- Mechanical
e	- Electrical
t	- Torque
s	- Synchronous
heat	

Parameters and Units

V	- Voltage	(Volts)
I	- Current	(Amps)
P	- Power	(Watts)
E	- Back EMF	(Volts)
B	- Magnetic field strength	(Tesla)
λ	- Flux	(Weber)
F	- Force	(Newton)
τ	- Torque	(Newton.meter)
θ	- Angle	(radian)
ω	- Angular Velocity	(radian.second ⁻¹)
t	- Time	(second)
K	- Constant	
p	- Pole Pairs	
BLDC	- Brushless DC	
PMAC	- Permanent Magnet AC	

2.1.2 Motor Theory

The core of an electric vehicle is the motor, transforming electrical energy into motive force. The electric motor is a remarkable piece of engineering, perfect for vehicle use: it has high power density, it is robust and it is capable of regenerative braking. In an ICE system modeled by the Otto cycle, approximately 20% of the energy from the hydrocarbon based fuel is converted to motive energy, with the remaining 80% lost as heat, with a theoretical maximum thermal efficiency of 35% [20]. When the ICE system has to slow down, brakes must be used which dissipate more kinetic energy as heat in the brake rotor. An electric motor can act as a generator (regenerative braking) and feed energy back into the battery pack to slow the vehicle, thus regaining some of the energy used to accelerate the vehicle.

Appropriate choice of motor for any application is crucial, and with many different electric motors available in today's market place, narrowing down to a specific motor can become difficult. Many factors impact this choice: the mains ones being price, availability, load and compatibility. The motor typologies discussed in this section have been narrowed down to those most often used in consumer and hobbyist electric vehicles. Since each topology has unique features commonly associated with it, by first having a sound understanding of motor operation the last two factors with regards to motor choice above become much easier to assess.

2.1.2.1 DC Motors

DC motors are the simplest motor available for EV drive applications, and are not considered by larger scale manufacturers, rather enthusiasts and hobbyists. DC brushed motors are relatively bulky, require maintenance on the commutator brushes, can generate large amounts of EMI and are generally less efficient than other motors. However, DC brushed motors often suit hobbyists, as their cost, along with their associated components makes them the cheapest option for an electric vehicle conversion. Most of the pitfalls for DC motors are often associated with their mechanical commutation - brushes contribute to voltage drop in the system, leading to a reduced efficiency. EMI is generated from arcing from the brushes on the commutator and since friction needs to occur for commutation to take place, the brushes wear down and need to be replaced, with carbon build up in the motor/on the commutator needing to be removed to prevent unwanted conduction [21].

2.1.2.2 Induction Motors

The simplest AC motor construction that is implemented in EV/HEV applications is the induction motor. Although generally having a lower operating efficiency and lower torque density than BLDC/PMAC AC motors, induction makes up for it with generally a more robust design and reduced cost. [8]

As with all AC motors, an inherent benefit is that the mechanical commutation of DC motors is not required, thus reducing maintenance requirements significantly, while increasing efficiency by having no brush voltage drop [22].

The construction of an induction motor consists of; a housing enclosure, a stator, a rotor, a mechanical shaft, bearings, sensors (position and temperature) and cooling (fan or liquid). The main aim of the housing enclosure is sealing the motor while providing structural support for the machine and ease of mounting [23]. The housing specification of a motor is crucial in some applications, such as those where water ingress can become problematic without sufficient sealing, such as with HiCEV. Construction of the stator and rotor is generally stamped, laminated steel stacks to avoid eddy current losses. The windings on the stator are then placed in the stamped slots with ends of each phase exposed for connection. The rotor can be cast in aluminum [8].

AC Motors used in automotive applications are 3-phase stator construction. The basic operating principle of induction motors is that the magnetic field generated by the stator currents *induces* current in the rotor and thus a magnetic field. The induced rotor field lags that of the stator, so that the AC stator magnetic field *drags* the rotor field around (asynchronous), creating motion. Electrically, the three phase stator phase currents are 120deg electrically out of phase, with equal amplitude of I_m and electrical angle (ωt). This is depicted in as:

$$\begin{aligned} i_a &= I_m \cos(\omega_e t) \\ i_b &= I_m \cos(\omega_e t - 120) \\ i_c &= I_m \cos(\omega_e t - 240) \end{aligned} \quad (1.0)$$

The above equations show that the currents vary with time, meaning the current peaks of each phase at any moment in time will have rotated around the stator, but retain their 120deg difference. Since current is directly proportional to magnetic field strength B , shown by:

$$B = K I \quad (1.1)$$

Where K is constant, each of the phase currents in Equations 1.0 can be shown as their sinusoidal magnetic field equivalents:

$$\begin{aligned} B_a &= K i_a \cos(\omega_e t) \\ B_b &= K i_b \cos(\omega_e t - 120) \\ B_c &= K i_c \cos(\omega_e t - 240) \end{aligned} \quad (1.2)$$

And thus magnetic field distribution in the air gap is given by substituting Equations 1.0 into 1.2, and using product-to-sum trigonometric identity $2 \cos(\omega t) \cos(\Theta) = \cos(\omega t - \Theta) + \cos(\omega t + \Theta)$ to give:

$$B_{gap} = B_m \cos(\omega t - \Theta) \quad (1.3)$$

Where Θ represents the field angle and

$$B_m = \frac{3}{2} K I_m \quad (1.4)$$

This shows that the total magnetic field distribution can be shown as a sinusoidal field that travels on the stators inside surface at speed ω radians. Since the supply frequency is proportional to this speed by $\omega = 2\pi f$, the speed of the rotor in rpm is $n_s = \frac{60f}{p}$ where p is the number of pole pairs.

The maximum motor speed is limited by the synchronous speed of the stator field. When the rotor reaches synchronous speed, there is no relative angle between the rotor and stator fields, thus no relative speed difference. Since the induced electromotive force (EMF) on the rotor bars that enables a current flow in the rotor is proportional to the relative movement between mechanical rotor and stator field, EMF drops to zero, and so does force on the rotor. This difference between rotor speed and synchronous speed is called *slip* and is directly proportional to torque.

[2.1.2.3 BLDC / PMAC Motors](#)

Permanent magnet AC (PMAC) or synchronous machines are electric motors that have rotors comprised of permanent magnets and operate at synchronous speed with the line frequency. There are a few types of synchronous motors, but the ones focused on in this paper are; Brushless DC (BLDC) and PMAC type motors, as these are most often found in EVs [8]. Induction motors do not have brushes, but operate on the principle of asynchronous slip, and therefore are not included in this category. There is a confusion associated with the difference between PMAC and BLDC configurations, but in essence it is attributed to motor constant waveform shape (AC and Trapezoidal respectively) arising from mechanical configuration. These motors are popular in electric vehicles as they can easily have large power densities, including high torque at low speeds which is useful in traction applications. Other properties such as high operating efficiencies, compact size and ease of regenerative braking make them an ideal candidate for vehicle applications [8].

The construction of a typical PMAC motor consists of rotor comprised of permanent magnets, wound stator, bearings, rotor position sensor and generally some form of cooling i.e. hoses for liquid. The rotor can either be on the outside of the motor- as in small quad copters and larger hub motors or the rotor can be on the inside- typical of larger vehicle motors.

When the windings are on the outside, heat dissipation is improved since the majority of the power dissipated as heat is proportional to the square of the current, this heat can be easily dispersed into the ambient environment with the addition of liquid cooling to help at larger power operations. The basic layout of the internal and external rotor configurations is given in Figure 2. The permanent magnets (blue) are always the rotor, and hence the wound rotor is always the stator (orange), with the air gap (black) between them.

There are also two common configurations for the rotor magnets in electric vehicles; SPM, or surface



Figure 2 (a) SPM rotor magnets, (b) IPM rotor magnets

mount permanent magnets and IPM or interior permanent magnets. In the case of the SPM, magnets are mounted to the surface of a solid steel rotor whereas IPM motors have the magnets embedded in a laminated stainless steel rotor, shown in figure 2;

The color code for the above picture has the magnets in grey, iron core in white and non-magnetic barriers in tan, where the arrows are depicting the direction of the magnetic field directions. These two magnet configurations have many tradeoffs including manufacturing costs, direct and quadrature axis reactances, and thus reluctance torques.

For a rotor with more than two rotor poles, the difference between mechanical angle and electrical changes. The mechanical angle measurement of the rotor is the same regardless of number of poles with one full rotation as 360° , whereas each magnetic pole-pair represents a magnetic period and is referred to as 360° electrical angle. This can be shown by Equation 1.5:

$$\omega_e = p \omega_m \quad (1.5)$$

Where angular frequencies ω_e and ω_m represent electrical and mechanical respectively, and p is the number of pole pairs [24].

The basic electrical circuit of a three-phase PMAC motor can be modeled by a single phase ideal transformers for each phase, shown in figure 3:

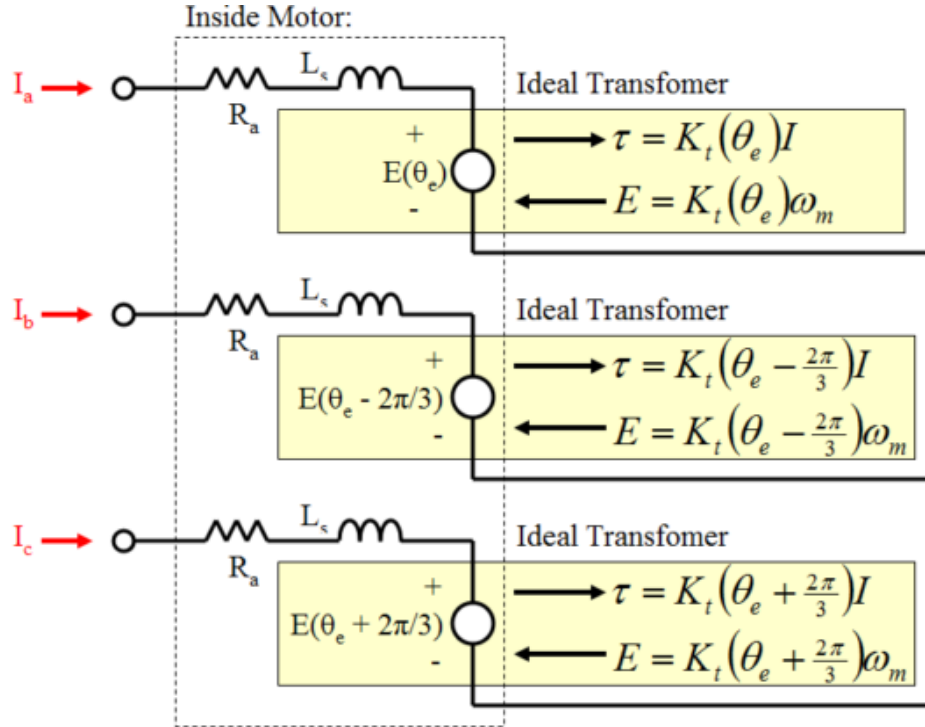


Figure 3 Three phase PMAC electrical model, figure from Shane W. Colton, [8]

From this, it can be seen that torque t is proportional to current, and the back EMF over the load E is proportional to rotor speed ω_m , with motor constant K_t relating both these respective terms, and dependent on the electrical angle θ_e . What can also be derived from this figure, is that ideally all phases have the same series resistive and inductive components per phase to be balanced, and currents I_a , I_b , and I_c are all 120° ($2\pi/3$) out of phase with respect to each other. The two equations

$$t = K_t(\theta_e)I \quad (1.6)$$

$$E = K_t(\theta_e)\omega_m \quad (1.7)$$

Form the basis of the PMAC Motor theory, as they give indicative knowledge of how the machine operates through its spectrums of speed and torque, such that torque generated is directly proportional to current, and BEMF is proportional to rotor speed.

2.1.2.4 Motor Losses and Cooling

The thermal efficiency of a components is the ability to convert energy for its desired use. In the case of a motor, converting energy to motive force is the primary goal. Alternatively a light bulb converts electrical energy to light, but what these two conversions have in common, is unwanted bi-products, usually in the energy form of heat. Heat and vibration in a system are generally two unwanted forms of energy that arise from electrical and mechanical phenomena.

Heat in motors is one of main design considerations and constraints for engineers both designing the motor and those designing the system in which it is used. Heat generated electrically is proportional to resistance of the windings and the current running through it:

$$P_{heat} = I^2 R$$

As shown, the power released as heat is proportional to the resistance, but it is also proportional to the current *squared*. Thus at high currents, and therefore high torque regions, heat can contribute significantly to the motor inefficiencies.

If the heat is allowed to build up unhindered, insulation on windings can be broken down and magnets can start to denature as their Curie temperature is reached. These factors will cause motor failure. Fortunately however, since it can be shown that the concentration of heat is dissipated in the windings for a PM machine, all that is needed to keep the motor operating in the desired torque region without motor failure is sufficient cooling around the windings. Since rotor poles are electromagnets in Induction machines (i.e. there is current flow), heat dissipation on the rotor has to be additionally considered.

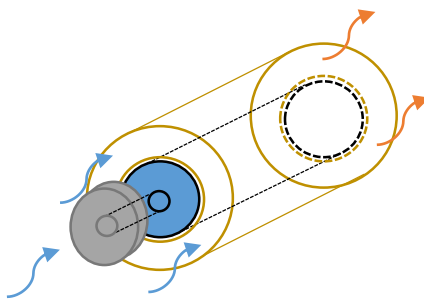


Figure 4 fan cooling

Cooling in an unsealed motor is the simplest scenario shown in figure 4, a simple solution being a fan attached to the rotor, forcing ambient air over the windings. This works in basic applications, but as a fan's loading curve is proportional to angular velocity cubed [25], at high speeds and thus performance applications it is not suitable. In a sealed motor enclosure, cooling becomes a more difficult task, especially since these are usually performance motors with high power requirements. Using an internal rotor type motor enables the stator windings to have a large contact area around their outer circumference and also on each end, perpendicular to the axis of rotation. In many systems, this fact is utilized to provide sufficient cooling through ambient air conduction and is called 'passive air cooling'.

2.1.3 Inverter Theory

The inverter does not create or store energy, but rather converts it from DC battery form, to usable AC for the motor. It is one of the most important components of an EV build, and also a major cost component for a vehicle.

Inverters can have a range of output AC waveforms, varying from a square wave to a sinusoidal waveform. These two types are at each end of the inverter waveform spectrum and are the output waveforms for trapezoidal BLDC and PMAC type motors respectively.

2.1.3.1 Field Orientated Control (FOC)

The concept of FOC is to transform three time variant phases into a two co-ordinate (**Direct** and **Quadrature**) time invariant system (Clarke Transform). The Q-axis current magnitude is linearly proportional to torque development and D-axis current proportional to the flux component [26]. The combination of motor feedback sensors to provide rotor position and the user accelerator input determines the magnitude the Q-axis current when in torque control mode.

2.1.4 CANbus Communication

Effective communication between modules in a vehicle is vital for passenger safety and ease of use, the type of communication should be robust and simplistic to reduce the chance of data loss or corruption. CAN is a communication standard in vehicles and machinery that is well tested, fast communication, is robust and can have many different modules on a single network.

2.1.4.1 CANbus in Automotive

CANbus is a robust protocol designed for in-vehicle communication by Bosch in 1985 [27]. As Vehicle manufacturers started using an increasing amount of interconnected electrical modules, the standard IO wiring harnesses took up more space, along with adding additional weight and expense. BMW was the first to implement the in vehicle network [ref] reducing the overall weight of the vehicle by 100 pounds with sensors working significantly faster than they previously had [28]. CANbus emerged as an industry standard, becoming the international standard known as ISO 11898 in 1993. [27]

The main benefits of CANbus over other serial communication are:

1. Low-Cost
2. Lightweight Network
3. Broadcast Communication Arbitration
4. Custom Message Priority
5. Ease of Error Checking

2.1.4.2 CAN Terminology

Each device on the network is called a **node**, with each node either sending or listening to other nodes message packets called **frames**. Each CAN frame consists of a complete CAN transmission, as shown in order below:

- Start of Frame (SOF)
- Arbitration ID
- SRR
- Identifier Extension bit (IDE)
- Remote Transmission Request bit (RTR)
- Data Length Code (DLC)
- Data Field
- Cyclic Redundancy Check (CRC)
- ACKnowledgement slot (ACK)

-End Of Frame bit (EOF)

Where figure 5 shows the format of a single CAN message starting from left to right.

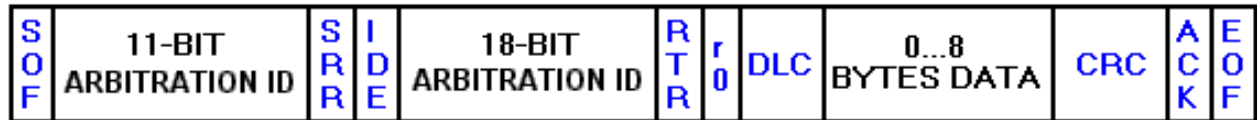


Figure 5 CAN Frame Format (national instruments)

2.1.4.3 CAN Operation

The CAN operation base is, Non-Return-Zero (NRZ) physical signaling with Carrier Sense Multiple Access with Collision Avoidance (CSMA/CA) messaging protocol. Multiple nodes broadcast onto a network with no master arbitrator, but rather an ID arbitrator in the message. To transmit, a node on a network checks the bus and delays transmission if the bus is active, and will wait for the EOF of current message to start transmission. If two messages attempt to transmit simultaneously, the message that has the first '0' bit wins transmission [29].

2.1.5 Battery Theory

Batteries are a storage device for electrical energy. The different combinations of anode, cathode and electrolyte material attribute to the battery cell characteristics. A list of standard battery chemistries is given below in figure 6.

	NiCd	NiMH	Lead Acid	Li-ion	Li-ion polymer	Reusable Alkaline
Gravimetric Energy Density(Wh/kg)	45-80	60-120	30-50	110-160	100-130	80 (initial)
Internal Resistance (includes peripheral circuits) in mΩ	100 to 200 ¹ 6V pack	200 to 300 ¹ 6V pack	<100 ¹ 12V pack	150 to 250 ¹ 7.2V pack	200 to 300 ¹ 7.2V pack	200 to 2000 ¹ 6V pack
Cycle Life (to 80% of initial capacity)	1500 ²	300 to 500 ^{2,3}	200 to 300 ²	500 to 1000 ³	300 to 500	50 ³ (to 50%)
Fast Charge Time	1h typical	2-4h	8-16h	2-4h	2-4h	2-3h
Overcharge Tolerance	moderate	low	high	very low	low	moderate
Self-discharge / Month (room temperature)	20% ⁴	30% ⁴	5%	10% ⁵	~10% ⁵	0.3%
Cell Voltage(nominal)	1.25V ⁶	1.25V ⁶	2V	3.6V	3.6V	1.5V
Load Current						
- peak	20C	5C	5C ⁷	>2C	>2C	0.5C
- best result	1C	0.5C or lower	0.2C	1C or lower	1C or lower	0.2C or lower
Operating Temperature(discharge only)	-40 to 60°C	-20 to 60°C	-20 to 60°C	-20 to 60°C	0 to 60°C	0 to 65°C
Maintenance Requirement	30 to 60 days	60 to 90 days	3 to 6 months ⁸	not req.	not req.	not req.
Typical Battery Cost (US\$, reference only)	\$50 (7.2V)	\$60 (7.2V)	\$25 (6V)	\$100 (7.2V)	\$100 (7.2V)	\$5 (9V)
Cost per Cycle (US\$) ¹¹	\$0.04	\$0.12	\$0.10	\$0.14	\$0.29	\$0.10-0.50
Commercial use since	1950	1990	1970	1991	1999	1992

Figure 6 General Battery Comparison [30]

2.1.5.1 Battery Chemistries

There are many different battery chemistries, each suitable for different applications. The battery chemistries that are discussed further are applicable to the field of EV's, to keep an appropriately narrow scope.

2.1.5.1.1. Lead Acid

Lead acid has been around for over 130 years, the basic chemical composition hasn't changed, but the design has been refined to allow for higher energy densities, increased life expectancies and reliability. Lead acid is still used in many traction devices today either as auxiliary 12-24V supply for systems or for traction applications [ref]. With a low upfront cost, this topology comes as a more appealing option compared to its expensive lithium counterparts, but comes at the cost of battery life-expectancy, performance and environmental concerns [ref].

Lead is an ongoing issue in China, with an excess of 130 million electric bikes (ebikes) in the vehicle fleet using lead-based batteries [31], lead-based pollution has become a serious issue. This is largely due to the uncontrolled disposal of batteries, which can seep into waterways or ground waste. The result of lead-poisoning includes attacking central nervous systems and birth defects [31].

The structure can vary slightly between different topologies of lead-acid batteries, but in essence lead acid batteries consist of lead plates immersed in an electrolyte bath acidic solution.

2.1.5.1.3. Lithium Iron

Lithium based battery chemistries are generally accepted as the battery of choice for electric vehicles. Lithium Iron Yttrium Phosphate (LiFeYtPO_4) shown in figure 7 is the primary focus for this conversion as

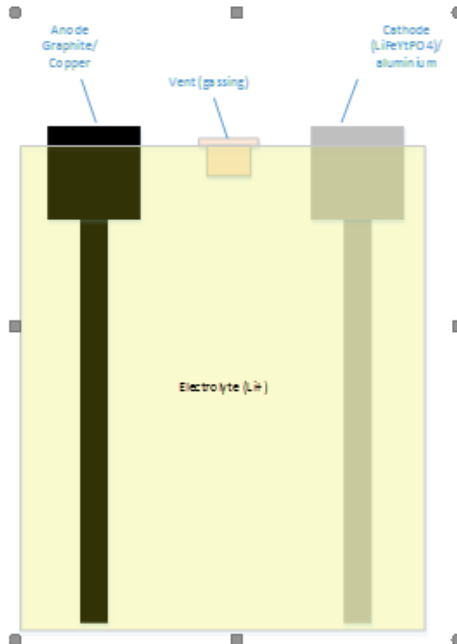


Figure 7 LiFeYtPO_4 battery

Lithium is currently the base material for electric vehicle batteries. Lithium exists in amounts of 20 parts per million in the earth's crust [32] and is never found in its elemental form, due to the inherent high

reactivity in metallic form. When mined, Lithium can be located in indigenous rocks (mainly sodumene) and from chlorine salts from brine pools.

Lithium has one oxidation state: Li^+ the discharge reaction is shown below in the equation {X}



Where one mole of electrons is $26.801 \text{ A}^* \text{h}/\text{mole}$ (Faraday constant) and one mole of Lithium weighs $6.941 \times 10^{-3} \text{ kg}$, specific energy density can be calculated as:

$$G_{\text{Specific theoretical limit}} = E_{\text{mole}} / \text{mass}_{\text{mole, Li}} = 26.801 \text{ Ah} / 6.941 \times 10^{-3} \text{ kg} = 3861 \text{ Ah/kg}$$

Note that this is the theoretical maximum limit for lithium chemistry based batteries, and doesn't include the other components such as doping metals, electrolyte and enclosure in the mass calculation.

To calculate the theoretical energy capacity, the nominal voltage of the battery is required which is 3.2V for LiFePO₄ chemistry. Assuming the voltage doesn't change, and efficiency factor of 49% [33] is used to cover impurities in the electrodes gives a specific power:

$$P_{\text{specific}} = 3.2V * 3861 \text{ Ah/kg} * 0.49 = \sim 6 \text{ kWh/kg (pure lithium)}$$

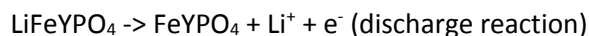
Thus for a battery size of 24 kWh there is roughly 4kg of lithium, which is the size of the Nissan leaf battery pack. For Nissan Leaf's alone, sales in 2014 reached 30,200 [33] – thus 120800kg (or 120.8 tonne) of lithium was consumed in these vehicles alone.

The theoretical specific energy of Lithium Yttrium Iron Phosphate is calculated from table 8.

	Value	Unit
Li	6.941	g/mol
Fe	55.845	g/mol
Y	88.9058	g/mol
P	30.9737	g/mol
O	15.9994	g/mol
LiFeYPO ₄	246.6632	g/mol

Figure 8 Molar mass of battery elements

Where the discharge reaction of losing an electron is:



And thus

$$G_{\text{Specific theo Lim}} = 26.801 \text{ Ah} / 246.6 \times 10^{-3} \text{ kg} = 108.65 \text{ Ah/kg}$$

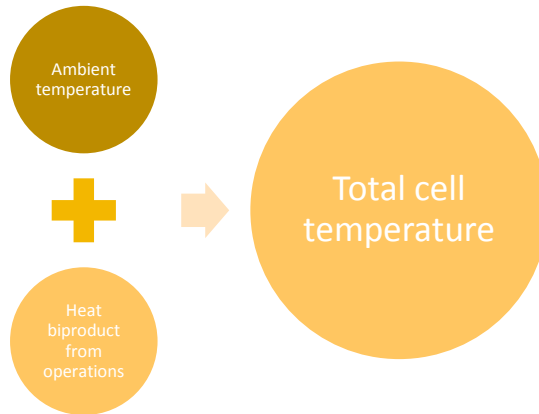
Which gives a theoretical specific energy of $\sim 348 \text{ Wh/kg}$ at a nominal discharge voltage of 3.2V.

2.1.5.1.3.1 State of Charge

State of Charge is the percentage value of capacity in the battery.

2.1.5.1.3.2. Effects of temperature

Every battery has an ideal operating temperature range. For lithium ion, this range is around -20 to 60 °C, where exposure to temperatures outside this range can lead to degradation in performance, capacity and safety. There are two main factors leading to battery temperatures exceeding these thresholds; internal heating of battery during operation and the ambient temperature of the battery enclosure.



If the environment in which a battery is operating is outside the recommended temperature range of the battery, a temperature control system could be implemented to bring the cells back into the optimal range.

2.1.5.1.3.4. Vehicle-to-Grid Technology

An electric vehicle is essentially a rolling power source. Much like in the early days of using powered equipment to drive farming equipment, battery power can be used in a similar but more useful way. Belts from tractor PTOs (Power Take Offs) could be detached to drive anything from threshers to workshop drills [ref], in the same way but many decades later battery power can supply farming equipment with the power needed.

Vehicle-to-grid or (V2G) is the principal of the bidirectional energy transfer from vehicle to grid, where the battery can be used for a back-up power source for a building [8]. As the number of plug-in EVs increases, the combined battery capacity from the vehicles can be used for grid stability, and voltage/frequency regulation [8] providing a lumped network of available energy for the grid to draw from. In a farm environment, this concept can be taken further to provide bi-directional energy flow for operating electrically driven tools in remote environments.

Farms or stations that are isolated can benefit from this the most. If a power outage occurs, the time lost can be economically significant relative compared to that of an urban outage.

Absence of basic utilities such as heating, lighting and ability to use equipment can affect work deadlines. Having a network of EVs on a station could provide a house or shearing shed with the energy required to wait out the mains power reconnection, shown in figure 9.

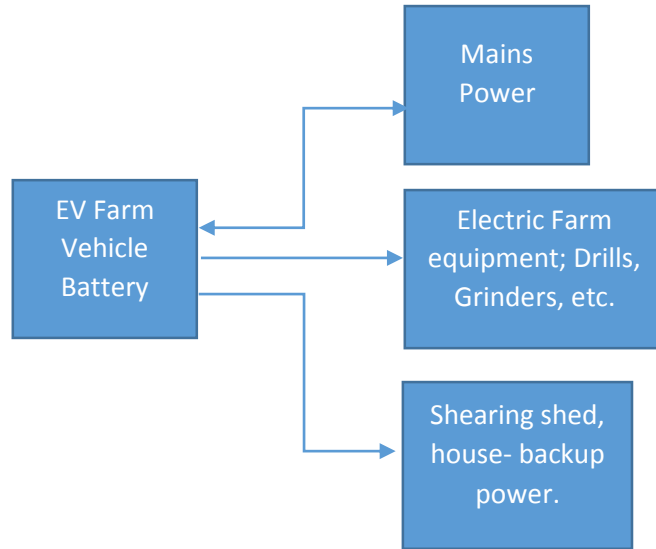


Figure 9 HiCEV V2G Potential

2.1.6.2 Shielding

2.1.6 Electro Magnetic Noise

Electromagnetic noise is the field components produced by varying voltage and current fields. If not carefully considered, EMI from either HV switching or high frequency switching can impair or damage susceptible low voltage components in the vicinity. In a vehicle scenario, this could have a range of consequences, from basic equipment malfunction through to injury of personnel onboard if not properly dealt with. Fortunately, EMI is widely known and mitigation techniques such as shielding and appropriate grounding have been developed.

Induced electromagnetic noise can come from high power switched or high frequency devices. By shielding the source, the victim, or both cables from EMI through faraday screens, minimized corruption of data in LV systems or component damage can be achieved.

The shield of a CANbus network should only be connected at one location to avoid ground loops, that is, if the shields are used on the BMS connector, there shouldn't be a connection anywhere else. If there is any unshielded CANbus cable, it should be kept to a length of a couple of inches maximum – and less in high noise environments. [34]

All devices on the CANbus network should share a common, star-point ground, as different ground potentials between modules can damage the CAN transceivers.

Two 120Ω resistors are required at the ends of the CANbus network, so that, for the utilized system with a centralized six point connector such as the SmartCraft Delphi connector, the longest cables from the node must have the termination resistors. The resistor should be as close to the end as possible-many modules have optional CANbus lines with inbuilt termination resistors in one line and another line

without. Even if the network ‘appears’ to work with one resistor, there may be significant issues down the track or when exposed to a higher noise environment.

2.2. Vehicle Principles

Equations of motion lay the fountain for the basic theory of vehicle motion.

2.2.1. Basic Theory of Operation

The basic theory behind automobiles has not been altered since the shift to electric vehicles, there is still a power source which is depleted by an actuator, in the form of a motor, to provide a torque at the wheel. There are however, as in Internal Combustion Engine (ICE) configurations, many different topologies for connecting the source to the actuator, and many different components that have to be looked at and considered to ensure the automotive systems works well as a unit.

In the case of an electric land vehicle, the model for road loading F_{RL} , includes the force generated from the drive train. It has to overcome the rolling resistance F_{rr} , aerodynamic drag F_{ad} , the force associated with vehicle weight coined as the ‘climbing weight’ and also the acceleration force of the vehicle [8].

$$F_{RL} = F_{rr} + F_{ad} + F_{rg}$$

From above, the theory for analyzing the vehicle can be broken down into further components. If the vehicle is stationary with respect to the ground (velocity $v=0$), and power is being supplied to the drivetrain, then the traction force F_{te} is equal and opposite to the rolling resistance;

$$\text{if } v=0, \quad F_{te} = -F_{rr}$$

Otherwise, the traction force is larger than the rolling resistance ($F_{te} > F_{rr}$) and movement is the result:

$$F_{rr} = -C_f M_v g \cos(a.pi/180^{\circ})$$

And therefore:

$$F_{te} < C_f M_v g \cos(a.pi/180^{\circ})$$

Here RHS represents the rolling resistance, broken down into components: C_f is the co-efficient of rolling friction between tire and ground and $M_v g$ represents the normal force F_N due to the vehicle mass M_v and gravitational acceleration g .

Now, looking at the traction force:

$$F_{te} = T_{ax,e}/r_{yre}$$

It can be shown that the tractive force is inversely proportional to the radius of the tire and directly proportional to the torque at the axle, T_{axle} which is the product of the torque from the motor, the gear ratios of transmission and differentials with their respective efficiencies:

$$T_{axle} = T_{ICE} \cdot GR_{trans} \cdot GR_{diff} \cdot n_{trans} \cdot n_{diff}$$

In the scenario presented, these equations are directly interchangeable between ICE and electric traction motors and are used to give a basic analysis of pre-vehicle performance.

2.2.2. EV Component Configurations

- BEV
- HEV
- REEV
- FCEV

2.2.3. Drivetrain Typologies

Every stage in which energy changes form involves losses, and thus reduces total system efficiency. Relating this to an electric vehicle, by removing the gear box and differentials by placing the electric motors on the wheels of the vehicle, two sources of energy loss due to power transmission have been eliminated. The electric motors can then operate as a differential by controlling electrical power flow to the motors with modern processor driven power electronics.

2.3. Role of Systems Engineer

The role of the author in this master's thesis can best be described as systems design engineer. Interfacing as the 'middle-man' with the client and supervisor for both technical and business needs from both, but also with potential clients, undergraduate student work groups and outsourcing work to many different parties. INCOSE (International Council on Systems Engineering) describes the role of system engineering as a process that 'integrates all the disciplines and specialty groups into a team effort forming a structured development process that proceeds from concept to production to operation. Systems engineering considers both the business and technical needs of all customers with the goal of providing a quality product that meets the user needs.'

A model was found that gave guidance into the structuring of a systems integration project such as HiCEV called the V-diagram, shown below in figure 10:

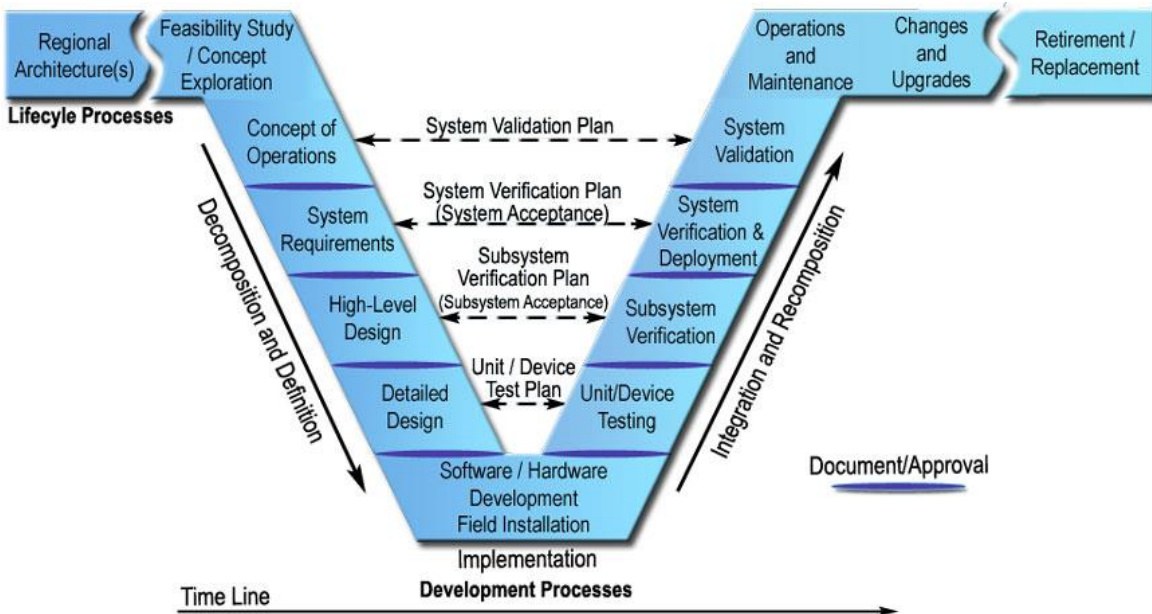


Figure 10 V – Diagram [35]

The V-diagram describes the development of any system, where the x-axis refers to the duration of a project's timeline. The dip in the 'V' allows sections to be directly compared to a coupled section from the concept and design phase to the testing and validation phases through planning. The author felt as though the V-Diagram could be modified for a better fit for the particular system in this thesis, following the same themes per above. This is shown below:

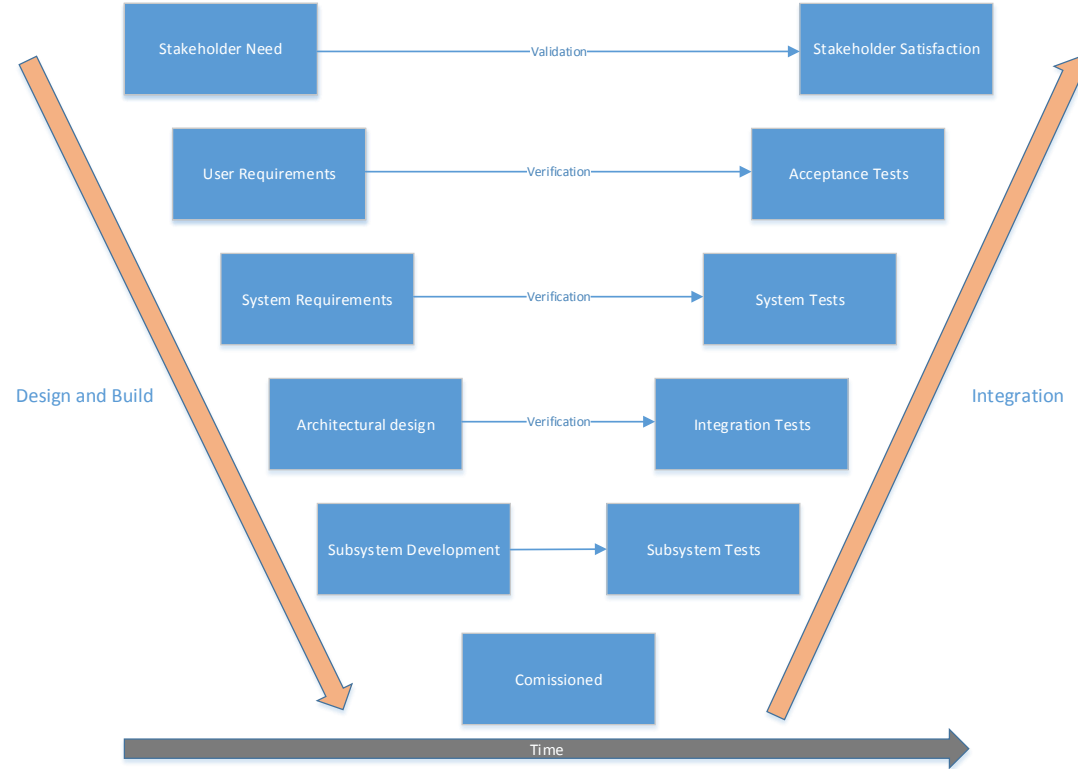


Figure 11 HiCEV V-Diagram

These sections highlighted in the above V diagram in figure 11 formed the basis of the HiCEV Project and are looked at in further depth in the following sections.

3.0 Prototype Specification Design

The majority of work conducted in this project was in the areas of ‘Component Selection’ and in ‘Systems Integration’. Testing the vehicle would ideally have the equivalent time allocated as the other two areas, but due to the nature of the project and time constraints only a few of the many vehicle aspects were able to be tested and evaluated.

3.1. Stakeholder Requirements

The HiCEV project began in 2013 as a collaboration between the Department of Electrical and Computer Engineering and Glenthorne Station, a high country station in central Canterbury, South Island of New Zealand situated on the northern side of Lake Coleridge. The client approached the university identifying their need of a vehicle that would serve as a prototype electric vehicle for farming applications, with the potential to convert further vehicles in the fleet in the future.

There was a list of initial core requirements for the end product as specified by the client as follows:

- Must be capable of farm work
- Must be usable by any farmer
- Must be fully sealed
- Must be capable of regenerative braking
- Must be certifiable

These were the base requirements of the project to give an overarching reference when specific engineering design solutions were being implemented.

3.1.1. Costings

Pricing has been omitted from the report. This being due to the fact that HiCEV is a prototype vehicle by nature thus is generally subject to a great amount of variability as the project progresses.

3.2. User Requirements

The following sections detail in depth the requirements laid out by both the client and farmers that will be using the vehicle.

3.2.1. Client and Intended use

The end user group was determined to be both the owner of the farming station and also the farmers.

The three main functions of the vehicle are:

1. Station ‘errand’ vehicle

The station is 25,233.00 hectares in area, and is comprised of two former stations with a twenty minute drive separating the two. Both stations have their primary use, the lower used for reception, lodging, vehicle yard and mechanics workshop – the upper used for lodging and managerial purposes.

2. Station working vehicle

Daily tasks include; carrying fence piles, moving cattle, or a dog-carrying truck for high country musterers. These are examples of light duty, but the vehicle must also be able to tow loads of

fertilizer and possibly other vehicles if required.

3. Prototype show vehicle for events

The client desires the vehicle to be a platform vehicle to show industry that electric vehicles are able to perform in rough environments. New Zealand has the potential to be a leader in the field of agricultural EV's as NZ farmers have proven to be open to using innovative technology enhance farming practices.

3.2.2. Donor Vehicle

A 70 Series Land Cruiser was the donor vehicle in this project shown in figure 11 This vehicle was not being used extensively in the way of farm work, and was being used as more of a farm run around. It was in an overall good working condition when the conversion process got underway. Aside from this, it was the vehicle that the client requested. Toyota Land Cruisers are known as robust 'workhorses' in the NZ farming community. This is important as farmers are familiar with these vehicles thus making the comparison between the EV and ICE drivetrains easy to distinguish.



Figure 12 HiCEV Donor Vehicle

Originally an 80 Series SUV Land Cruiser frame was intended for conversion, but this was revised and changed as having a deck on the vehicle enabled features that are unique, eye-catching and practical. By being able to detach the deck, much of the planning for component locations could take place with ease, and later on in the project, accessing these vital components easily was a necessity that would have been impractical to implement in an SUV.

3.2.3. Off-Road Operation

Specific requirements are associated with off-road vehicle operation. The following factors separate HiCEV from urban EV commuters such as the Nissan Leaf:

- Un-sealed road operation (high vibration exposure)
- Effective function at low speeds
- Operate in rough terrain (and climatic extremes)

- High power High torque
- Off-Road vehicles are generally associated with mining, construction, forestry, military and agriculture. HiCEV is a hybrid of both on-road and off-road effective vehicle; the expectation is that HiCEV will achieve both requirements at a higher level than the combustion counterpart.

3.2.4. Performance and Drivetrain

A change to a vehicles drivetrain is generally the result of a desire for an increase in performance. Although not the core driving force for the conversion, sufficient performance is required for usability and product image. Although the client did not have specific performance requirements, it was clear the user would be discontent with an underpowered system. Hence, the performance factor was driven from the farmer's perspective. After consulting with spokesmen for the farmers, the following two requirements were agreed upon:

- **More Power than the Original ICE**

The farmers reasoning for this was twofold; Firstly, after explaining that the vehicle will gain some weight due largely to the battery pack, increased electrical power compared to the original ICE drivetrain is required to obtain similar performance in order to be used as a work vehicle. Secondly, the farmer that corresponded most with the author was also a mechanic and quite rightly stated that public interest will increase if it has noticeable performance improvement. This is in the interest of the client too as the vehicle is to be used as a show piece. To calculate power requirements, a straight power-to-mass ratio was used to obtain a target threshold electrical power:

$$\frac{P_{ice}}{M_{ice}} = \frac{P_{elec}}{M_{elec}}$$

Where $P_{ice} = 96\text{kW}$ and $M_{ice} = 2010\text{kg}$ for the combustion drivetrain. A vehicle mass increase of $\sim 200\text{-}300\text{kg}$ is regularly observed in conversions using lithium chemistry battery packs. P_{elec} can thus be estimated as:

$$P_{elec} = \frac{96\text{kW}}{2000\text{kg}} \cdot 2400\text{kg} = 115\text{ kW}$$

Using the upper end of vehicle conversion weight (300kg) to be conservative, an electrical power *minimum* of 115kW was calculated to give similar performance as the original vehicle.

- **Regenerative Braking is Required**

Although less common amongst most electric car conversions due to associated costs, regenerative braking was set out as a requirement by the farmers. The reason for this is twofold; Firstly, after explaining the vehicle would likely have a run time (at full power) of approximately one hour, the farmers wanted the system to employ ways to extend this. The concept of regenerative braking is simplistic – instead of dissipating energy as heat in traditional friction brakes, the linear kinetic energy of the moving vehicle (momentum) is converted to electric energy through rotational couplings to the motor (wheels, differentials, gears and shafts) where the motor operation shifts to the generating quadrant, providing a retarding torque to slow the vehicle. The energy cycle 'round-trip' (from battery to motor and back to battery) efficiency is important to determining the percentage of recaptured energy. AC motors and controllers are able to run in the 90-95% energy efficiency range [36], but there are other losses in the cycle such as the resistance of cabling and internal impedance of batteries. Below is a simple model

that was used to determine, without datasheets, the kinetic energy conversion through assigning component efficiencies from motor to battery:

$$e_{b-m} = e_b \cdot e_{hvr,tot} \cdot e_i \cdot e_{hvr,tot} \cdot e_m$$

Where e_{m-b} is total efficiency from motor to batteries. To make the calculations simpler, the cable and battery efficiencies were set to 98%. Thus:

$$e_{b-m} = 0.98 \cdot 0.95 \cdot 0.97 \cdot 0.98 \cdot 0.95 = 85\%$$

The mechanical rolling efficiency of the vehicle (affected by components producing heat when the vehicle moves; bearings, CV joints, differentials, gears, wheels) is estimated to be $e_{mech} = 70\%$. For electrical round-trip from batteries, e_{b-m} is squared (losses on both power transmission to motor, and on returning from motor, $e_{b-m} = e_{m-b}$) back to and is multiplied by the mechanical efficiency which is always present:

$$e_{tot} = e_{m-b}^2 \cdot e_{mech} = 0.85 * 0.85 * 0.70 = 51\%$$

Thus giving a potential maximum of 51% of total transmitted energy (e_{tot}) recapture. However, in practice, this number tends to be more in the region of 20% energy recapture [37]. Although this number seems low, it effectively adds approximately an additional 12 minutes to the drive time for a one hour cycle (depending on average proportion of time and magnitude of braking in that hour).

3.2.4.1. Typology

The series electric drivetrain typology was selected from possible configurations shown in figure 13. This involves one electric motor which takes the place of the original ICE. In this configuration, the gearbox can either be retained or removed where a directly coupled single fixed-gear ratio is implemented. Fixed-gearing couples the electric motor directly to a shaft that is fed to the differential, reducing weight and mechanical complexity by removing flywheel, clutch and gearbox assembly. The short-comings associated with fixed gear arises especially for low-speed, high-torque applications where the ability to use 1st gear in combination of the transfer box ratios is of particular benefit.

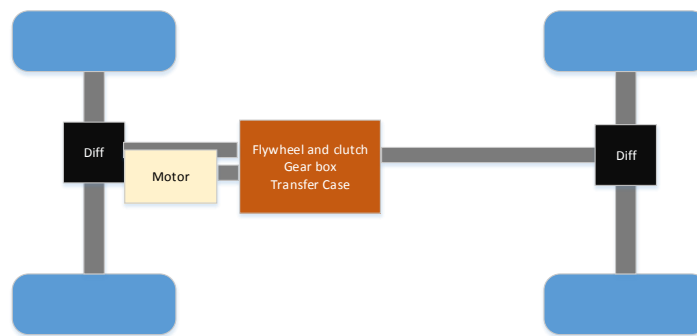


Figure 13 Series BEV Typology

As low-speed off-road applications has been defined as one of the requirements; retaining the gear-box allows for high-ratio gearing ($X >> 1$) for high torque low speed applications and four wheel drive (4WD) which is difficult to implement without a gearbox. The major short comings of this arrangement include both the mechanical coupling and electrical implementation on terms of gear sensing for vehicle speed equations and sensing clutch, both of which are explored in further detail in sections.

3.3. System Requirements

The prior qualitative analysis highlights the client and user needs, further mathematical definition is required to give a quantitative analysis. This is achieved through analyzing the vehicle through equations of motion and modeling electrical and mechanical characteristics, a better understanding of vehicle performance can be realized before purchasing and implementing a system.

3.3.1. Vehicle Performance

Vehicle performance can be modelled by using the kinematic equations of motion for a vehicle. For light urban vehicles (<2000kg), performance benchmarks. Vehicles which are tested through modeling can have results compared to these benchmarks to give an indication of relative performance. Commonly used urban vehicle benchmarks are listed below:

- 0-97 km/hr: < 12 seconds
- 64-97 km/hr: < 5.3 seconds
- 0-140 km/hr: < 23.4 Seconds

These are defined by US Partnership for a New Generation of Vehicle's (PNGV). Although these benchmarks do not carry equivalent importance in the case of HiCEV, which will be spending majority of running time in a low speed off road environment, it will still be on the road at times and as such the benchmarks are worth evaluating.

3.3.1.1. HiCEV Estimated Characteristics

A performance model of HiCEV offers a low cost vehicle assessment, forming the basis of component selection. This is achieved through vehicle equations of motion (EoM) where unknown vehicle parameters have been estimated as accurately as possible. A list of vehicle parameters for HiCEV is shown below in Table. Beginning with evaluating the final vehicle mass:

$$M_{final} = M_{original} - M_{ice} + M_{ev}$$

Where the curb weight ($M_{original}$) for the vehicle was measured as 2065kg. The mass of internal combustion components (M_{ice}) removed consist of the motor and associated components which is approximated to be 300kg. On the EV side of the conversion, the motor, mounting, and accessories are approximated to be 150kg and battery packs with a weight of around 400kg (Winston 0.1-0.09 kw/kg (100Ar and 90Ar respectively [38])) gives an EV component mass of approximately 550kg. This gives an M_{final} of 2315 kg. The addition of passenger(s) increases total weight to approximately 2400kg. The rolling friction, aerodynamic drag coefficient and rolling friction are sourced from a Land Rover Discovery [39].

Predicted Vehicle stats			
Mass	M_{veh}	2400	kg
Acceleration (gravity)	a_g	9.81	ms^{-2}
Rolling Friction	C_{rf}	0.015	
Air Density	P	1.225	kgm^{-3}
Aerodynamic Drag Co	C_d	0.44	
Frontal Area	A_{fr}	1.62	m^2
Wheel inertia	I_{wh}	3.5	kgm^{-2}
Wheel Radius	r_{wh}	0.4	m

Headwind	v_{wind}	0	m/s
3rd Gear			
Torque (engine)	T_{ice}	122	Nm
Gear Ratio transmission	GR_{trans}	1.49	
Gear Ratio Differential	GR_{diff}	4.11	
Gear Ratio Transfer Case	GR_{tcase}	1	
	GR_{tot}	10.1106	
Efficiency transmission	e_{trans}	0.95	%
Efficiency differential	e_{diff}	0.95	%
Efficiency tcase	e_{tcase}	0.95	%

From the original estimate of over 115kW, more vehicle parameters can be refined and base performance characteristics can be defined. Listed above in Table are the predicted vehicle statistics in which to calculate the vehicle forces for the HiCEV vehicle model. To determine the vehicle performance characteristics, firstly F_{rl} (forces due to road loading) must be determined. F_{rl} is the sum forces of rolling resistance, tractive effort, road grade and aerodynamics. Rolling resistance force is defined below:

$$F_{rr} = 0.015 * 2400 * 9.81 * \cos\left(\frac{\Phi\pi}{180}\right) = 353.16 * \cos\left(\frac{\Phi\pi}{180}\right) N$$

Since vehicle velocity is greater than zero. Aerodynamic drag force at 90km/hr is given as:

$$F_{ad} = 0.5 * 1.225 * 0.44 * 1.62 * 25^2 = 272.90 N$$

And force due to road grade is:

$$F_{rg} = -2400 * 9.81 * \sin\left(\frac{\Phi\pi}{180}\right) = -23544 * \sin\left(\frac{\Phi\pi}{180}\right) N$$

Where tractive effort force is defined as $F_{te} = F_{rg} + F_{acc}$ and Tractive force from the motor is calculated as

$$F_{te} = \frac{T_{axle}}{r_{wheel}} = \frac{1768.6}{0.37} = 4780 N$$

Then rearranging eqn above to give acceleration at zero road angle, $\Phi = 0$ from standstill ($F_{ad} = 0$):

$$a_{veh} = \frac{4780 - 353.16}{2400} = 2.0 ms^{-2}$$

Thus, it can be found for a drivetrain of 320 Nm that the acceleration time to get to 100 km/hr (27.78m/s) is roughly 14 seconds. The energy required to accelerate from 0 – 97 km/hr (27m/s or 60mph) is:

$$E_{acc} = \frac{1}{2} m_{veh} \cdot v_{veh}^2 = 2400 \cdot \frac{729}{2} = 880 kJ$$

For an acceleration time of 14 seconds for 0-97 km/hr, the average power required is:

$$P_{av} = \frac{E_{acc}}{t} = \frac{874800}{14} \sim 62 kW$$

And a peak power of:

$$P_{max} = F_{te} * V = 4780 * 27 = 129kW$$

Where this peak power forms the basis of the motor performance requirement.

3.3.1.2. Regenerative Braking and Range Extension

Current electric vehicles, conversions in particular, do not have the range to compete with their ICE counterparts in a market sense. As such, methods of extending maximum range capabilities are crucial in making electric vehicles a competitive solution. Two current ways of extending range aside from increasing effective battery capacity are regenerative braking and hybridization ICE modules to charge batteries whilst in operation. These are discussed below.

Regenerative braking converts the vehicle's kinetic energy to electrical energy which is fed back to the battery bank. This helps recover some of the energy lost due to friction (road, mechanical, air) and acceleration, increasing overall system efficiency. Without taking losses into account, the kinetic energy and thus the amount of energy recapture of a vehicle moving at 97km/hr is given as:

$$E_{kin,veh} = \frac{1}{2} \cdot m \cdot v^2 = 0.5 * 2400 * 27 = 874800J = 0.24 kWh$$

Which is the same amount as above used for calculating the amount of energy to accelerate to 97km/hr. Assuming the vehicle has an average speed during deceleration of $27/2 = 13.5m/s$, correlating to an average drag force of 130 N and the rolling resistance is 350N at zero road angle, the energy losses due to these retarding forces can be calculated as:

$$F * x = \frac{1}{2} * m * a^2 * t^2 = \Delta E_{kin}$$

$$\Delta E_{kin} = 430 * 135 = 58050 J = 0.0161kWh$$

At a stopping time of 10 seconds. Without taking mechanical losses into account, (difficult to guess without a roll down test) the energy that can potentially be recovered from acceleration is $0.24 - 0.016 = 0.23 kWh$. This result may, however, be misleading into the reader thinking that ~90% of energy may be recovered from general commuting, but this however only takes into account the 10 seconds of change in velocity, and not the time spent overcoming frictional forces at a constant velocity such as for a motorway drive cycle (no decelerating). For the motorway drive cycle, range extension can only be achieved by an additional energy source to the batteries – a generator.

Implementing a 3kW petrol generator can act as a range extender element by supplementing energy to the batteries continuously with the effect of giving a higher effective battery capacity. For an effective battery capacity of 30kWh, this can be characterized by:

$$E_{eb} = \frac{E_b}{E_b - (P_{gen} * t_{gen,run})}$$

And thus:

$$t_{veh,run} = \frac{E_b}{P_{b,inst} - P_{gen}}$$

Where:

$$P_{m,inst\ av} = P_{b,inst} - P_{gen}$$

Where $t_{gen,run}$ and $t_{veh,run}$ denote the operation runtime of the generator and the vehicle motor respectively. Combining both range extension and regen braking gives the total effective battery capacity

$$E_{tot,eb} = E_{gen,eb} + 0.2 * E_{eb}$$

Where the regenerative energy is 20% of the effective battery capacity ($0.2 * E_{eb}$). This results in a total effective battery capacity ($E_{tot,eb}$) of approximately 39kWh, an increase in 9kWh from an hour's operation under the above conditions. From the derivations above, the significant impact that the combination of a range extender and regenerative braking has on effective battery capacity and thus run-time.

3.4. Component Sourcing

The decision of purchasing main modules consists of locating suitable technologies and employing a weighting system to choose the best solution for the application. A focus is maintained on the main components for the vehicle, as the subsystems were evaluated by undergraduate student groups working on the vehicle.

3.4.1. Motor and Inverter combination

A system of reliance is considered to evaluate an appropriate drivetrain solution. This is shown in figure [14] below, where the system initiates from user requirements which influences specific components. The vehicle performance analysis above provides a base approximate sizing of the motor and inverter combination – these two components are one of the major design decisions.

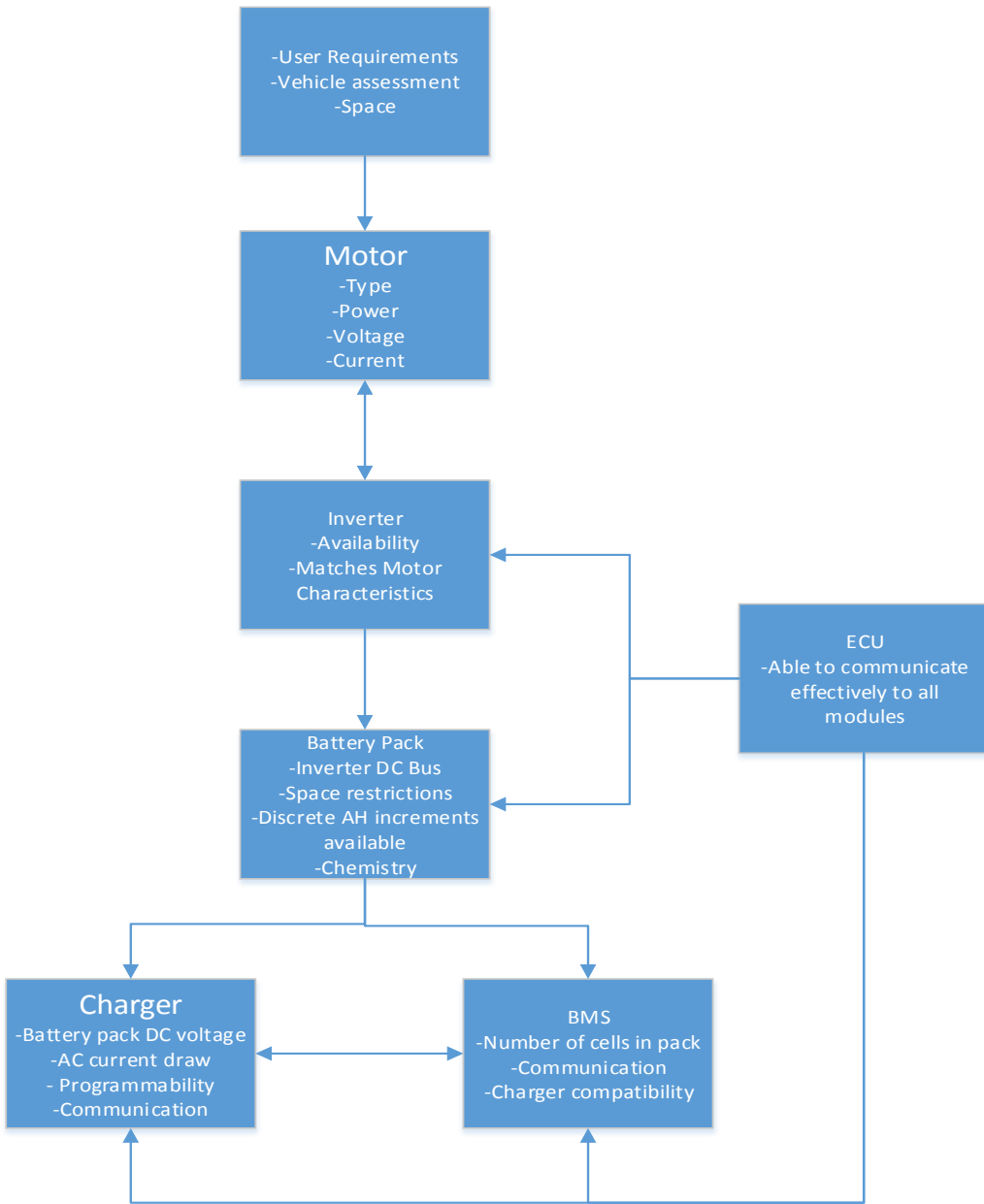


Figure 14 Product sourcing flow diagram

3.4.1.1. Motor Selection

A list of motors that would meet the user requirements is listed in table 1.

Motor Vendor	Type	Typology	Power kW _{peak}	Power kW _{cont}	DC bus Voltage (V _{dc,max})	DC Current (A _{dc,max})	Regen	Sealed	Availability
Netgain	HV11	DC series	200	-	288	1000	No	No	Easy
HPEV	2 x AC75	AC	125	18 ¹	144	538	Yes	-	Easy
Yasa	YASA-400	PMAC	165	-	700	-	Yes	Yes	Low
Remy	HVH250-115P	PMAC	300	-	700	600	Yes	IP67	Medium
UQM	PP100	PMAC	135	-	425	400	Yes	Yes	Medium
Siemens	1PV5135	Induction	100	-	300	400	Yes	IP67	Medium

¹Passive Air cooled

Table 1 Motor Selection

Where further weighting factors are defined below in order of importance to HiCEV:

1. Motor maximum power
 2. Continuous power
 3. Availability
 4. Compatibility with inverter systems
 5. Regenerative braking compatible
 6. Environmental Sealing
 7. DC Bus voltage
 8. Weight
 9. Cost
- The motor power requirements have been highlighted in above sections.
 - Availability is the ability to locate, purchase and ship component.
 - Compatibility with available inverter systems is an important aspect of integration and is defined by the matching of both HV electrical characteristics and LV sensor integration. HV power integration is not only characterized by magnitude of voltage and currents, but the waveform outputs.
 - Regenerative braking and environmental sealing ensuring it will be suited to the operation environment.
 - HVDC voltage - A higher bus voltage helps with system efficiency – as seen by the equations below:

$$V_{inverter} = V_{batt,total} - V_{sag}$$

Where:

$$V_{sag} = I_{draw} * (R_{batt,internal} + R_{Batt,connectors} + R_{cabling})$$

And:

$$P_{inverter} = P_{batt,total} - P_{losses,transmission}$$

Where:

$$P_{losses,transmission} = I_{draw}^2 * (R_{batt,internal} + R_{Batt,connectors} + R_{cabling})$$

Thus, for a higher current draw, compensation in battery voltage is required to account for the voltage sag associated with the resistances. To illustrate this two 150kW systems, both with 50mΩ total resistance (battery IR (internal resistance), interconnects and cabling) at 25°C are compared: First system is 1000A_{dc}, the other 50A_{dc} max current draw. For 150kW of power at the inverter input side, the first system has a power loss of 50kW during transmission (75% efficient) compared with 12.5kW loss from the 500A_{dc} system (92% efficient). Therefore the first system requires a bus voltage of 200V_{dc} compared with 325V_{dc} required for the latter system. The voltage drop through transmission from battery is linear and can be used to prove the calculated voltages above: first system has a sag of 50V_{dc}, the second being just 25V_{dc} (bringing the voltage at the inverter end to 150V_{dc} and 300V_{dc} respectively).

The last motor weighting factors were weight and cost. Most electric motors in the power range required are 60-100kg – a 40kg weight range which makes negligible difference in total vehicle weight.

From the table below three motor solutions that were chosen to investigate further were the UQM, Remy and the Siemens. Factors were multiplied as a ‘0’ indicated a missing aspect that was required in specifications.

	Power	Availability	Regenerative	DC Bus voltage	Ease of implementing	Total Score
Netgain	5	5	0	3	5	0
HPEV	3	5	4	1	2	120
Yasa	4	0	5	5	3	0
Remy	5	3	5	5	5	1875
UQM	3	3	5	4	5	900
Siemens	3	3	4	4	3	432

3.4.1.2. Inverter Selection

Similar to the motor selection, performance and availability are the primary factors for inverter selection. Manufacturers design inverters to specific motors, where the motor must first be characterized (flux, inductance, cogging torque and back-EMF). Several inverter manufacturers that were approached for the project provided this characterizing service, but time constraints associated with the logistics (shipping a motor from USA to AUS then back to NZ in one case) made this option impractical.

		Voltage			Current Max		Power		
		Min	Operating	Max voltage	Input	Motor	Peak	Cont.	Peak
		V	V	V	A _{dc}	Arms	kW	kW	Efficiency (%)
Azure	DMOC 645	120	400	450	507	414	118	53	97
UQM	PP 135	250	425	425	288	235	135	80	95
Rinehart	150DX	50	360	400	551	450	150	150	97
Tritium	Wavesculptor200	0	450	450	367	300	165	75	97
Scott	Scott 200	200	425	450	600	490	200	55	-

Able to interface with VCU?	CANbus		Operating Temp.		Mass	Rotor Position Sensor	Motor Typology Supported	Integrated Pre-charge
	2.0A	2.0B	Sealed	Cooling				
Y/N	11bit	29bit	IP	Glycol/Water	°C	°C	Kg	-
Y	Y	-	54	G/W	-40	55	14.7	BLDC/PMAC
-	Y	-	67	G/W	-	65	27.7	BLDC
Y	Y	Y	6K9K	G/W	-40	80	10.7	PMAC/BLDC/Induction
N	Y	-	65	G/W	-	-	8.5	BLDC/Induction
N	Y	-	-	G/W	-	-	14	BLDC/Induction

Table 2 Inverter Selection

The five choices for inverters are shown above. Table 2 has been broken into two as to fit it in, but is color coded in the row direction for each inverter. The potential motor and inverter combinations (at the time of sourcing) as shown below in figure 15:

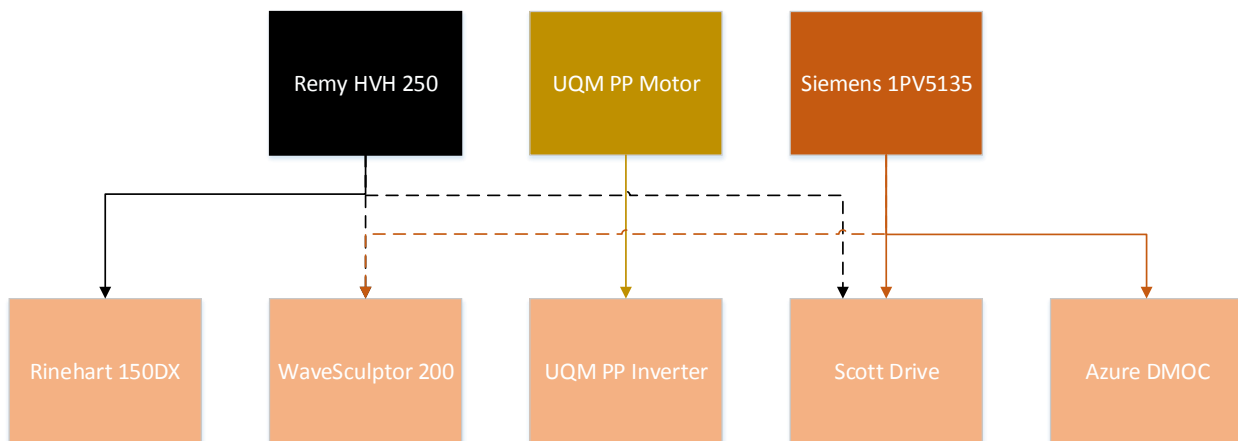


Figure 15 Motor Inverter Compatibility

Aside from power requirements, low voltage integration between motor and inverter is required to be considered. Motors use typically encoders, hall-effect or resolver position sensors to output rotor position information to the inverter, where waveform shape and frequency varies significantly with sensor technology. Remy has designed their motors with a resolver position sensor, whereas the Siemens motor uses an encoder. Without any changes to the DSP, this limits the possible inverters that can be used for each motor. Thermal sensors technology also varies between motors and is also a consideration in system integration.

The Remy and Rinehart combination of motor and inverter combination was selected from the above. Although the Scott Drive can provide higher current ($600\text{ A}_{\text{rms}}$ vs $450\text{ A}_{\text{rms}}$) than that of the Rinehart, it is not set up to interface with a resolver position sensor. The Remy was selected over the Siemens motor as the Siemens would not come with warranty, and was significantly lower power than the Remy (110kW vs 150kW). Although the UQM system was designed as a set combination, thus indicating reduced systems integration time, the Remy provides more power along with the potential to be coupled with a higher power inverter in the future.

The last aspect that made the Remy + Rinehart combination appealing was that the availability of these units, and essential downstream components (BMS, Charger, VCU) were all supplied by one supplier that had tested these systems prior which should ensure “seamless” integration.

3.4.2. Remaining Main Components

Downstream componentry associate with the main modules may be identified after the main components have been selected, indicated by figure 14 above. In this particular situation, the main modules that interfaced well with the motor/controller combination were able to be purchased through the same company.

3.4.2.1. Battery Pack Sizing

The advent of the Tesla model S is changing the public perceptions on EV ‘range anxiety’ with vehicles capable of traveling 320km on a charge. Unfortunately, achieving these ranges in a vehicle conversion is still difficult, as combustion vehicle chassis are not designed with battery holding capacity in mind.

The battery pack voltage is dictated by the maximum operating voltage of the inverter (360V_{dc}). Prismatic cells were chosen over pouch cells for three main reasons:

1. Availability
2. Enclosure Building
3. Swelling

At the time of souring, prismatic cells were easily attainable and relatively inexpensive when ordered in bulk. The enclosure of a prismatic cell is rectangular and brittle, which attributes to ease of implementation when designing an enclosure. Pouch cells require support from above increasing the complexity of an enclosure. Pouch cells are also prone to more rigorous swelling due to gaseous build up than prismatic. Due to manufacturing anomalies, cells will swell at different rates and can lead to rupture or break electronic displays if used to monitor the cells [40].

Knowing the inverter input voltage allows the specifics of the battery pack to be determined. The factors for sizing the battery pack are listed below in order of importance:

1. Volume (real estate).
2. Availability
3. Performance Characteristics
4. Ease of implementing
5. Repeatability

As Lithium batteries can be stacked in any orientation volume is the main concern when assessing the vehicle for available battery locations. Availability and Performance were weighted this way, as there is no choice between an attainable and lower performance product and a higher performance but unattainable product. Availability also includes correspondance, shipping and support.

The battery performance indicators of the narrowed down potential batteries are shown below. All the batteries are lithium chemistry with exception to the bottom two batterys (Trojan and Exide) that are 100Ah and 50Ah lead acid deep cycle respectively. It is quite clear that the performance of equivalent lead acid is far inferior, the author had no intention of using lead acid but included them in the table as a point of reference [41].

From here, the best performance battery looks to be the A123 M20, but the fact that it is a 20Ahr, means that to get into the 100Ahr region, parrallel connections are required in the order of 4-6 strings (a string being the number of batteries connected in series to obtain the required pack voltage). This has the effect of increasing both construction complexity in how to fit batteries in an enclosure it also increases the wiring complexity and chance of battery system failure by an order of magnitude.

This is where 'Ease of implementing' also becomes a factor in the component selection tradeoff – while still getting the required performance the vehicle requires, the larger capacity and volume cells can be more easily compiled into a pack and monitored by a BMS. For higher performance applications, the M20 battery may be the better selection, but to get a prototype implemented with desired performance, the large prismatic cells in the region of 100AH (to avoid complexity of parallel strings) are the better solution.

Winston batteries were easily accessible at the time of purchase, as it is the EV conversion battery of choice for the majority of vehicle conversions.

Manufacturer	Model	USD/Wh	Gravimetric Energy Density (Wh/kg)	Volumetric Energy Density (Wh/L)	Max Power Density by Weight (W/kg)	Burst Power Density by Volume (W/L)	Weight of 30 kWhr Pack
Winston	LYP90AHA	\$0.38	96.00	151.45	288.00	3029.01	312.50
	LYP100AHA	\$0.31	91.43	132.27	274.29	2645.32	328.13
Sinopoly	LFP90AHA	\$0.36	92.90	150.11	278.71	750.53	322.92
	LFP100AHA	\$0.36	103.23	166.79	309.68	833.93	290.63
CALB	SE60AHA	\$0.41	76.80	124.62	0.00	1246.19	390.63
	SE100AHA	\$0.41	100.00	154.29	0.00	1234.30	300.00
GBS	GBS-LFMP100AH	\$0.48	100.00	156.29	300.00	1562.88	300.00
A123	M20	\$0.29	112.68	233.48	563.38	4669.54	266.25
Trojan	T-1275+	\$0.14	35.68	80.63	35.68	483.76	840.91
Exide	ORB34DC-48	\$0.38	32.26	67.39	32.26	1010.83	930.00

The highest input operating bus voltage for the inverter is the ceiling limit for the battery pack, unless an expensive and impractical DCDC converter is utilised. Thus, $360V / 3.3V = 109$ Cells in series at a maximum charge voltage of 3.3 V per cell. The graph below shows manufacturers data for discharge under 'normal' temperature:

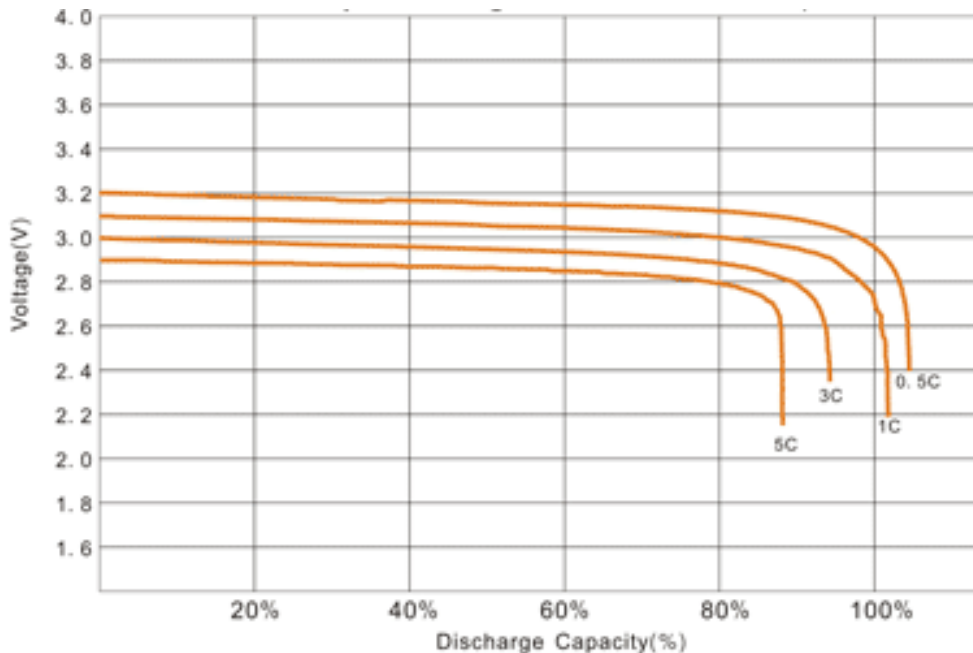


Figure 16 LYP Discharge curve at different C ratings [38]

The inverter has a maximum current draw of $450A_{dc}$, therefore the batteries must be capable of sustaining this output for at least 1 minute. The statistics are shown below:

Batteries			
Parameter	Units	Value	Notes
Winston WB-LYP100AHA			Winston battery datasheet
Nominal Capacity	(Ah)	100.00	
Operational Voltage	(V _{charged})	3.65	
Operational Voltage	(V _{discharged})	3.30	
Max Charge Current, ≤3CA	(A)	300.00	
Max Discharge Current, ≤3CA (Constant Current)	(A)	300.00	
Max Discharge Current, ≤20CA (Impulse Current)	(A)	2000.00	
Standard Charge/Discharge Current, 0.5CA	(A)	50.00	
Cycle Life at 80% DOD, ≥Times	(Cycle #)	3000.00	
Cycle Life at 70% DOD, ≥Times	(Cycle #)	5000.00	
Temperature			
Temp Durability Of Case	(°C)	200.00	
Operating Temp (charge)	(°C)	85 to -45	
Operating Temp (discharge)	(°C)	85 to -45	
Monthly Self-discharge Rate	(%)	3.00	
Weight	(kg)	3.00	

Hand Calculations

HV Power Setup

Operating Voltage	(V _{dc})	356.40	
Motor Voltage	(V _{rms, I-I})	252.01	
Max Motor Current	(A _{rms})	450.00	
Op Voltage (under load)	(V _{dc})	288.90	(internal resistance of HV connections = 150mΩ)
PF**		0.95	** Presumed PF
Efficiency	(%/100)	0.94	
Battery Pack	(kW)	130005.00	DC max power from batteries
Motor Power	(W)	116094.47	
Motor Power	(kW)	116.09	At the motor

Range Calculations

Battery Pack			
Number of cells (WB-LYP90AHA)	(#)	108.00	
Total kWh of pack	(kWh)	35.64	
Available kWh at 70% DoD	(kWh)	24.95	70% DoD = 5000 Cycle life
Available kWh at 80% DoD	(kWh)	28.51	80% DoD = 3000 Cycle Life
Power gained through range extension	(kWh)	2.50	3kW charger estimated output
New Available Pack Power	(kWh)	27.45	70% DoD
	(kWh)	31.01	80% DoD
Factoring Regen			
% Regen of total Pack Power	(%)	10.00	
Power regained through regen	(kWh)	2.74	70% DoD
	(kWh)	3.10	80% DoD
Total Potential Available Pack Power	(kWh)	30.19	(DoD + Regen + Range Extender)
	(kWh)	34.11	

Hand calculations can only provide limited accuracy. Computer simulation tools help provide an increased accuracy model of a system while in the early feasibility stages of a project to give more accurate predictions.

The vehicle simulator ADVISOR is used in industry and research to simulate ICE, Hybrid, Fuel Cell or BEV drivetrains and their performance for various drive cycles. ADVISOR is a GUI extension of Simulink and Matlab that models in Matlab code system components such as motors, gearboxes, and battery packs to emulate the physics of a vehicle. This vehicle can then be analyzed on various recorded driving patterns called drive cycles. In this way, different vehicle typologies can be tested against the same driving cycle to compare performance.

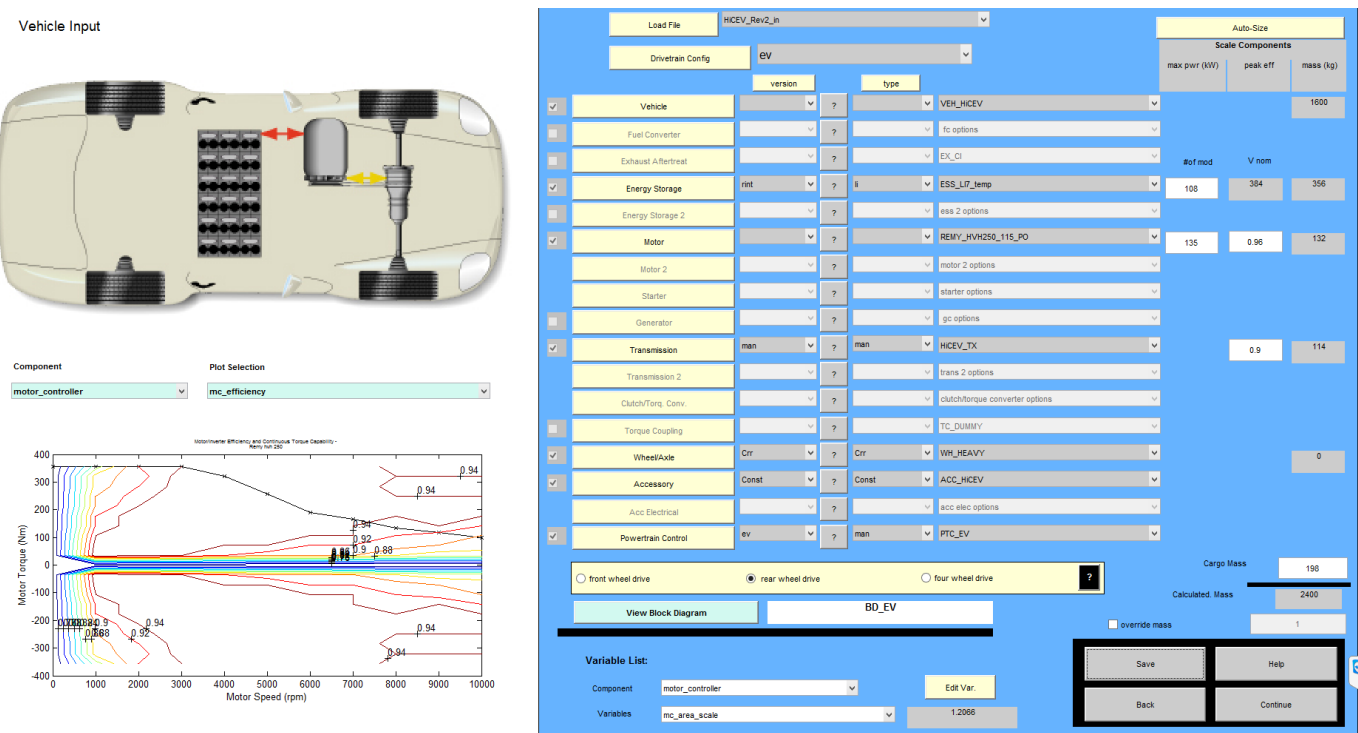


Figure 17 ADVISOR vehicle simulator

A basic model for HiCEV was created and modelled in Matlab. The figure below depicts the drive cycle manipulated to emulate possible farm driving. It can be noted that there is a large amount of fluctuation in vehicle speed (blue) and there is a constant road grade (α) incline of 200 feet ($\alpha = 1.5\%$) over the duration of 15 minutes (green). This drive cycle was manipulated from the NYCC (New York City Cycle) and was chosen for its general low speed (<40mph) and frequent stopping and starting – to simulate low speed off-road use.

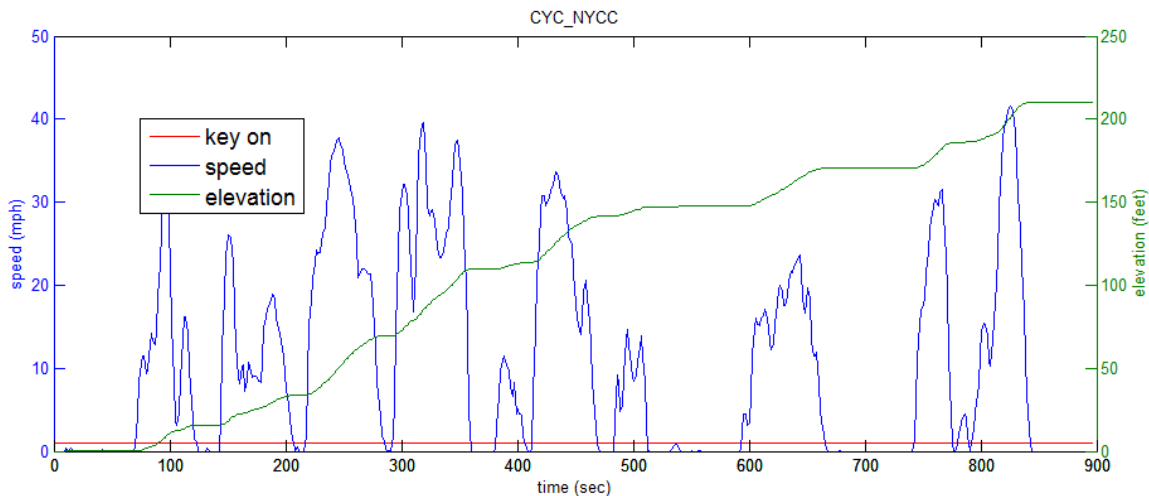


Figure 18 NYC Drive Cycle

As can be seen on the X-axis, this drive cycle is 900 seconds, 15 minutes in duration. Thus to get an hour of commuting, four of these cycles were used back to back, shown in figure 19:

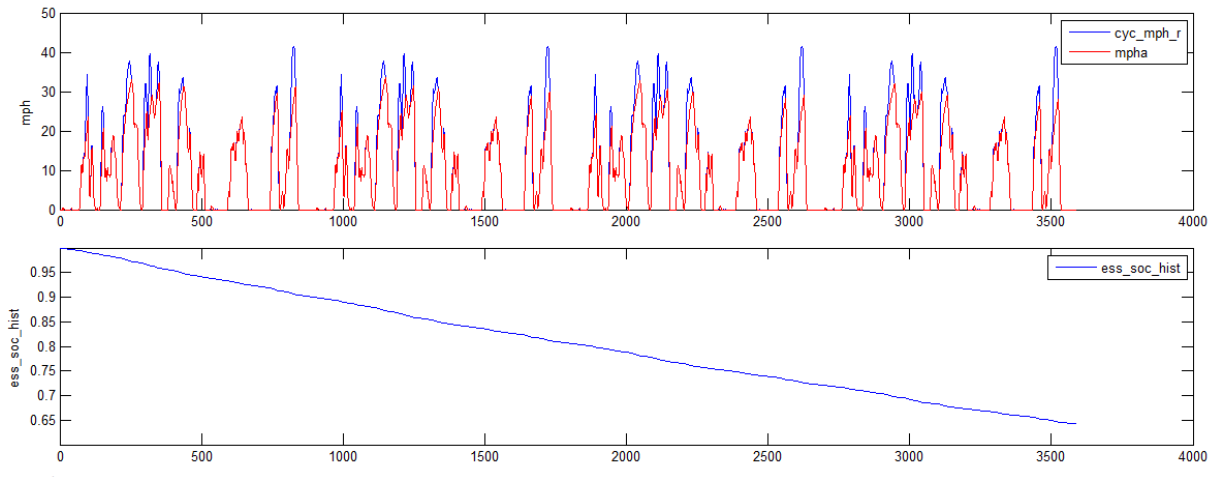


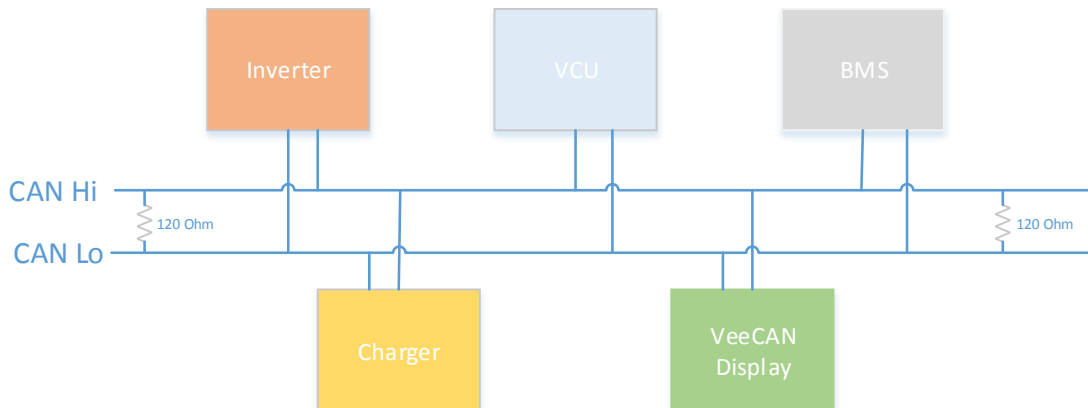
Figure 19 Multiple Drive Cycles

This simulation shows one hour of stopping and starting on constant incline gradient. The top plot shows the simulated ideal vehicle performance (driver dependent) in red against the drive cycle plot. The discrepancies in the two speed traces can be attributed due to acceleration required to reach the peak speeds quickly— to be expected from a farm truck on a semi urban drive cycle.

The top lower graph in figure 19 shows a linear change in state of charge (Δ SOC) of 35%, starting from maximum capacity over the 1 hour duration using the selected drivetrain and using the vehicle parameters from the EoM analysis.

3.4.2.2. Remaining main system modules

The main system modules were purchased from New Eagle Control Systems, a Michigan based company in USA. The motor and controller were a package, along with the auxiliary main modules that have compatibility for reduced system integration complexity. The main system modules communicate through CANbus as shown below:



The main modules seen here are the Vehicle Control Unit (VCU), Battery Management System (BMS), Battery Charger and the VCU Display. The easy integration comes through pre-configuring of CAN messages between modules to ensure effective communication. For example, the VCU has no access to CAN message configuration, but has been specifically set to talk to a discrete number of modules, which is selectable.

3.4.2.2.1. Electric Vehicle Control Module (EVCM)

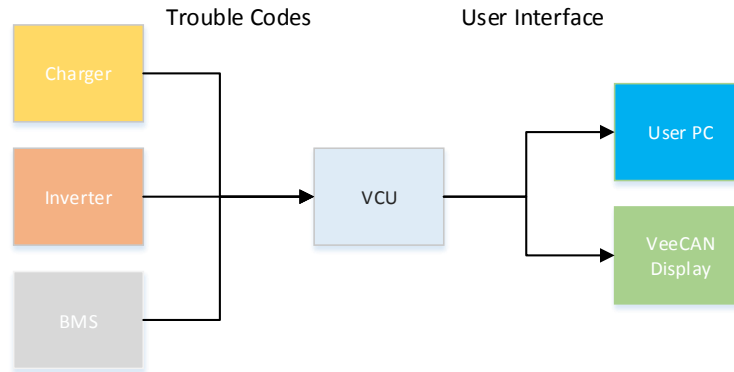
The system complexity increases with additional components. By having a centralized master control unit the number of units requiring parameter changes during refining can be reduced to initial configuration of each unit, then trouble shooting and programming one unit from then on out. This system was designed with the Electric Vehicle Control Module (EVCM) in mind to reduce the points of contact a user can or has to make, while also allowing detailed calibration of the vehicle performance parameters.

The EVCM uses the ECM-0554-112-0904-C/F engine control module from Woodward as a hardware base, which is then loaded with a Simulink based control software called MotoHawk by the New Eagle Controls team. The EVCM aims to centralize control in a system with many processor based modules, through analogue and digital I/O.



Figure 20 EVCM - Vehicle Controller

The EVCM in Figure 20 above shows the EVCM taking inputs in the form of driver, vehicle, user interface and energy storage and outputting control over relays, vehicle component control units and drivetrain components in the system. The EVCM controls vehicle aspects such as startup relay sequence and user torque requests while performing vehicle diagnostics, taking trouble codes from other modules centralizing troubleshooting. The trouble shooting messages flow diagram can be shown as:



Where the ‘VeeCAN’ is a small LCD screen with a graphical display, used primarily for the client to refer to – displaying basic diagnostic data, but mainly basic operating parameters such as coolant temp and pressure.

3.4.2.2.2. Battery Management System (BMS)

The Battery management system (BMS) that is compatible with the VCU unit is the 108 cell Orion BMS. The wiring diagram for this unit and the connections the BMS has with the user PC, the charger, current sensor, thermal systems and the battery pack itself, figure 21.

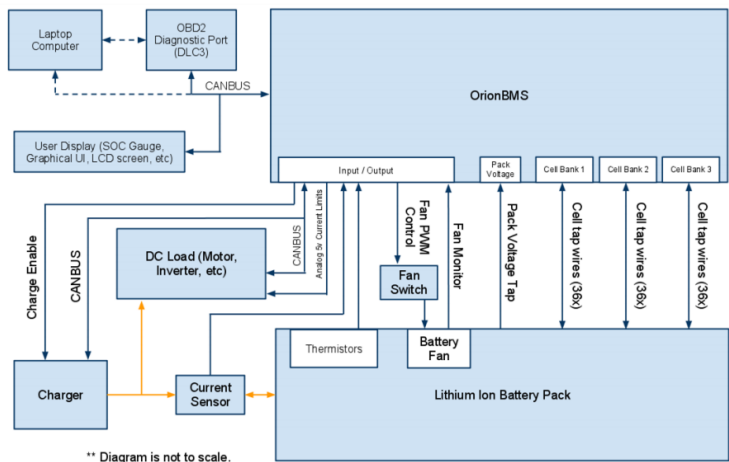


Figure 21 Orion BMS Layout [51]

The battery pack is the most expensive single part of an electric vehicle. The battery pack is made up of multiple cells, 108 in the case of this vehicle with each cell varying in capacity and voltage slightly (or sometimes noticeably) from neighboring cells due to unavoidable manufacturing imperfections. With this in mind, a pack is only as strong as the weakest cell, if a pack of cells is charged at a constant voltage equal to the multiple of the number of cells by the maximum cell voltage, a range of cell voltages will evolve at the high end of the charge cycle (last 10% of capacity). The highest of these voltages will be the weakest cell in the pack, thus resulting in overvoltage and damage to the cell if nothing prevents it from breaching the maximum voltage threshold. This is where the BMS helps by shunting power from the cell,

reducing the voltage of the weaker cells and enabling the stronger cells to still charge to their maximum voltage. This act is referred to as ‘top balancing’ as cells are being balanced at their top or max voltage threshold.

Winston Lithium Iron cells have a maximum voltage of approximately 4.0 V [38], where past this voltage breakdown of electrolyte starts to occur, bringing the formation of gases and thus swelling of enclosure (safety critical aspect), higher internal resistance (formation of lithium ‘shield’ on anode preventing ion transfer- leading to increased heat buildup during operation) and reduced capacity (ions have turned to gas). The BMS acts to *shift* energy from individual cells that will breach this top voltage during charging (i.e. wall charging or regenerative braking). This can be done a couple of ways- actively passing this energy to cells with a lower voltage (ideal scenario) thus losing minimal energy from the system, or through passive shunting of energy through resistive elements, dissipating as heat. The latter is most widely used as it is far easier to implement in practice and is still very effective. Passive energy shunting is diagrammatically shown below in figure 22.

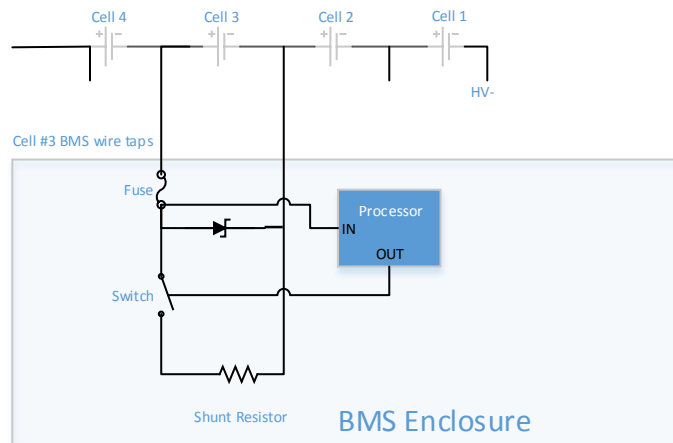


Figure 22: Cell Balancing

Only cell 3 is shown here being balanced (out of the 108), where the negative side of Cell 1 is the HV- of the battery pack. The tap comes into the BMS unit to an analogue input. This input uses the cell voltage as a reference, and commences shunting by activating a switching element which then bleeds the cell across the terminals. The Zener acts as an over voltage protection for the BMS inputs, whereby at 5.6V

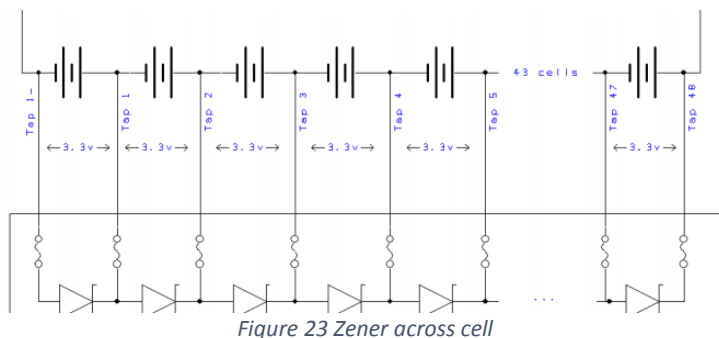


Figure 23 Zener across cell

the Zener conducts and the internal fuse blows. How the Zeners and fuses are configured with multiple cells is shown below:

The maximum shunt current for each cell is 200mA and the maximum heat dissipation is approximately 40 W from the BMS unit, thus giving a total of 55 cells (using a 3.5V threshold) that can be balanced simultaneously. Additionally this shunting current can initiate one of two ways: the cell voltage threshold (3.5V-3.65V) or difference between max cell voltage and min cell voltage.

The BMS calculates limits based on the thermal profile of the batteries. Internal resistance of a cell, and thus the output voltage of a cell changes with temperature. To monitor the cell temperature, 3 thermistors are utilized by the BMS to sense the temperature of the cells. Thermal breakdown of the cell's electrolyte occurs at around 60° C which forms gas that is vented if internal pressure breaches an engineered value. Rapid formation of gas can also cause cell rupture, thus for either scenario to be avoided, the temperature of the cells must be kept below this threshold. Thermistors must be attached to thermally conductive parts, figure 24, of the battery that are in contact with the cell electrolyte – even this will not be a perfect indication.

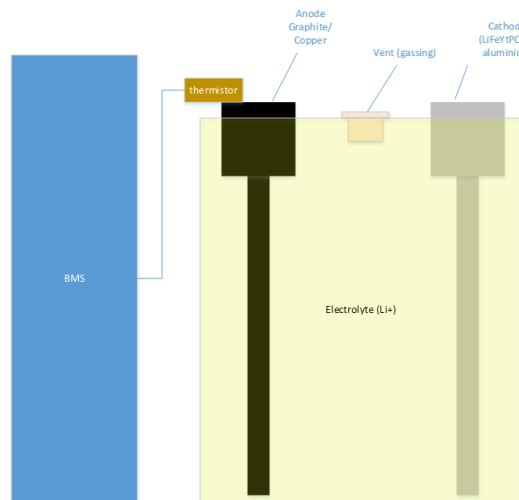


Figure 24 Thermistor Placement

3.4.2.2.3. Battery Charger

The compatibility between the BMS and the charger is important as both over-charging and under-charging of batteries must not occur, therefore effective communication between BMS and Charger is essential.

The chosen charger for the vehicle was the Eltek 3kW charger in an IP67 sealed rated enclosure. This charger must be controlled via the CANbus to operate. A diagram of how the BMS and the Charger integrate is displayed below:

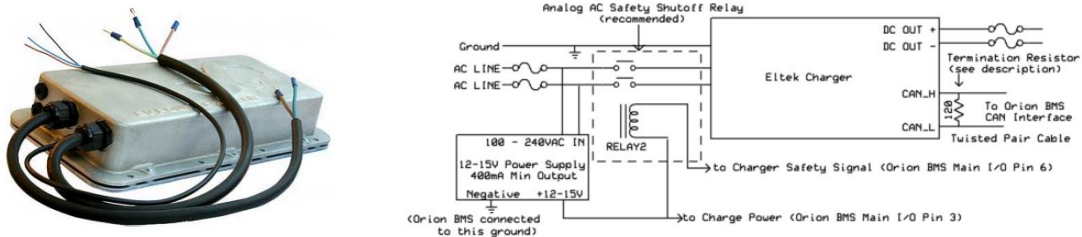


Figure 25 Interfacing with Eltek Chargers [52]

This charger meets the user requirements as follows:

- Availability
- Meets Environmental Constraints
 - IP 67 sealed
 - -40 to 40°C operating range
- Compatibility
 - Both with NZ AC input voltage (230Vac, 50Hz)
 - 3kW Capable, aligns with standard output
 - BMS CANbus communication
 - Spans required HV_{dc} range

The Eltek charger parameters below in table 3 meet the specifications required of the charger.

EV Power Charger 360/3000 HE IP67 G2	
Input Voltage	85-275 V _{ac} , 50Hz (230V _{ac} nominal)
Input Current	14 A _{rms}
Output Voltage Range	250-420 V _{dc}
Output Current	10 A _{dc}
Power Factor	0.99 (@ 50% load or higher)
Charge Control	CANbus
Ripple and Noise	<250 mV _{rms}
Efficiency	96%(@50% load) - 95%(@100% load)
Operating Temp	-40 to 60 °C
Storage Temp	-40 to 85 °C
Dimensions	60 x 355 x 167 mm
Weight	4.3 kg

Table 3 Eltek Charger Specs

3.5. Main Architectural Design

The physical design process regarding placement of components was important to effective system integration in HiCEV. Careful thought is required in how to use space effectively while maintaining the performance of the systems left in place (i.e. Brakes, 12V system, lights, steering, and chassis integrity).

With this in mind this section aims to detail the process of physical layout of components, from the general main component layout to the in depth mechanical and electrical connection designs.

3.5.1. Component Layout

The vehicle was stripped and measured as shown in figure 26. This allowed measurements to be taken as to how the systems would interface physically. Deciding where components are going to be placed is a significant design choice, although with some components, there is not much choice i.e. the motor has to be in line with the pre-existing driveshaft. At this point it is useful to break down the system dependencies, i.e. the requirements of successful integration.



Figure 26 HiCEV Stripped

After the vehicle was stripped, available space could be measured and a clearer understanding of how components would interface took place. Spatially, the vehicle can be broken down into three compartments; the engine bay, the cab and the deck (or rear), as depicted in figure 27:



Figure 27 Spatial view

A bird's eye approach is useful for seeing how the components will interface on a broad level.

The largest constraints facing the component layout are detailed in the diagram figure 28:

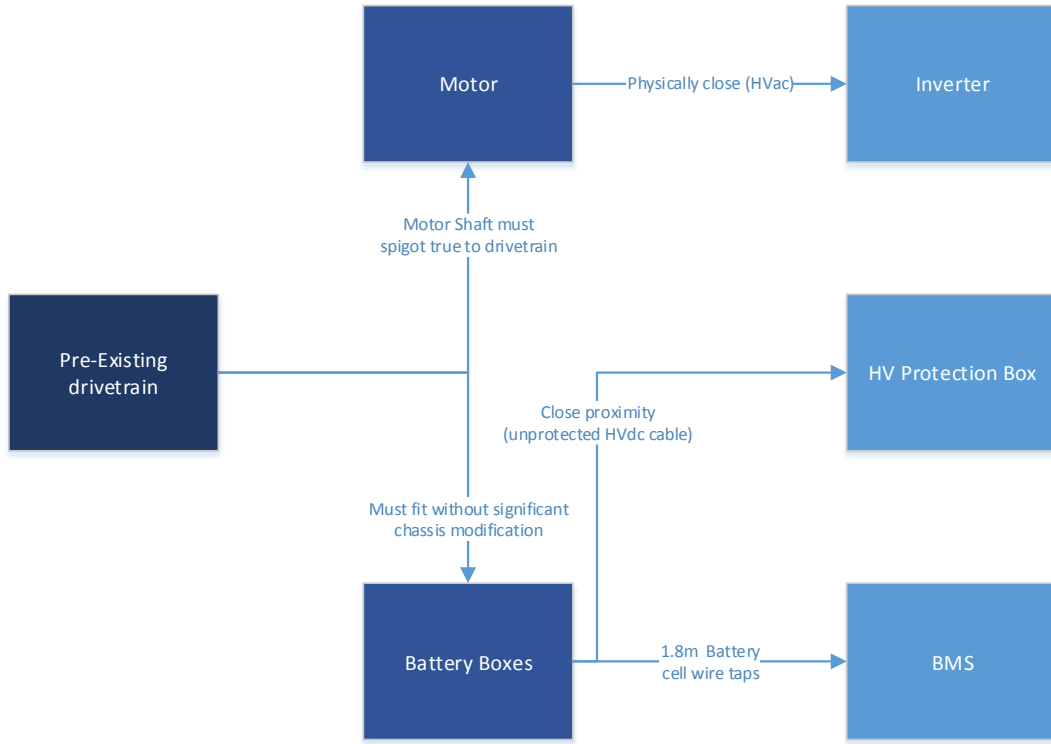


Figure 28 Main Constraints on Component Placement

The components and their downstream dependencies are depicted by the arrow directions. Main spatial dependencies stem primarily from the pre-existing drivetrain, and secondarily from the motor and the battery locations. The primary concerns for motor and battery boxes are alignment of the motor shaft with the driveshaft and supporting enough space for the batteries without cutting away structural chassis components respectively. Secondary dependencies consist of:

- Location of inverter in order to keep EMI (electro-magnetic interference) from HV_{ac} reasonably low
- location of HV protection box for adequate isolation and location of BMS so the wiring looms can reach every cell in the battery pack without requiring lengthening.

The choices of where to place the primary spatial concerns are shown superimposed over the vehicle chassis mechanical drawing shown in figure 29.

The location of the motor was dictated from the transmission input shaft which is shown in the drawing;

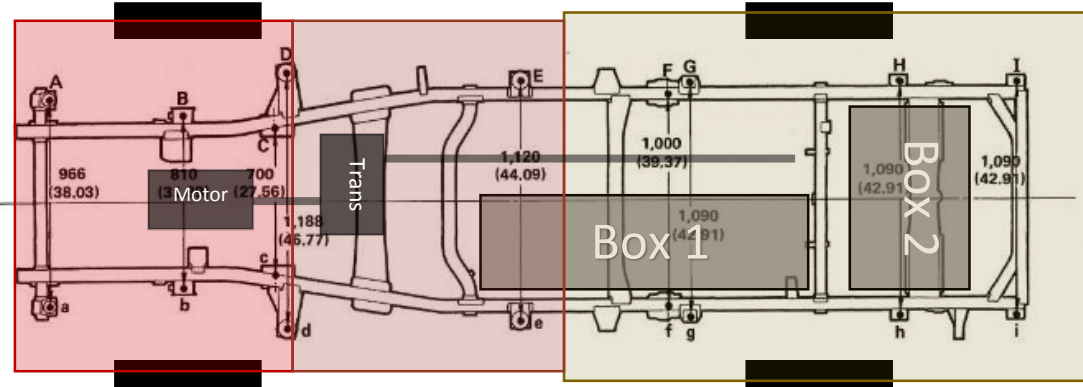


Figure 29 Battery Box placement

central, along the mid-line of the vehicle. The battery boxes require the maximum space allowable without affecting vehicle performance. The mass distribution and thus the center of gravity (COG), brakes and suspension is dependent on battery mass placement.

The station mechanic was crucial here in declaring safety distances from driveshaft and suspension. The boxes were designed to sit above the chassis rail to reduce the chance of impact from underneath. The rear lateral support that Box 2 interferes with was not classified as structural (it provided a place for the spare wheel to fasten) and therefore was removed.

3.5.2. Electrical Layout

The electrical layout was split into three categories: High Voltage Power, Low Voltage Power and Communications, a flow diagram of component interconnection is shown in figure [30]. High voltage is defined as anything in excess of $50V_{dc}$, where low voltage power focuses on the 12V vehicle auxiliary bus and communications is the combination of CANbus and Serial communication. An initial bird's eye approach of the electrical layout of the components spatially in the Appendix 7.1.

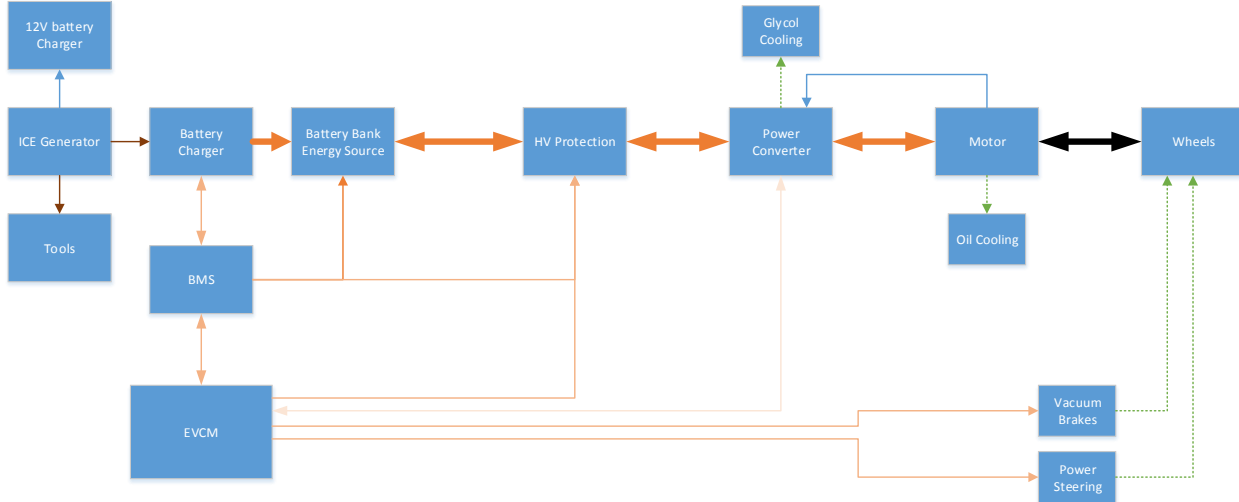


Figure 30 Electrical Power Flow

3.5.3. Mechanical Layout

Mechanical layout details the way devices physically connect to the vehicle. The specific connections of consequence are the motor shaft connection to the drive train and placement of the battery box.

3.5.3.1. Motor to drivetrain

Effective coupling of motor to the drivetrain is crucial for power transmission. The Remy motor has internal bearings that support the rotor. They are only designed to support the motor mass and gyroscopic forces on the rotor [42]. Therefore to couple the flywheel to the motor, an adapter shaft with separate bearings needed to be designed to take the radial and axial loading of the flywheel mass and the clutch engaging respectively. The basic initial idea behind this is depicted graphically in figure 31.

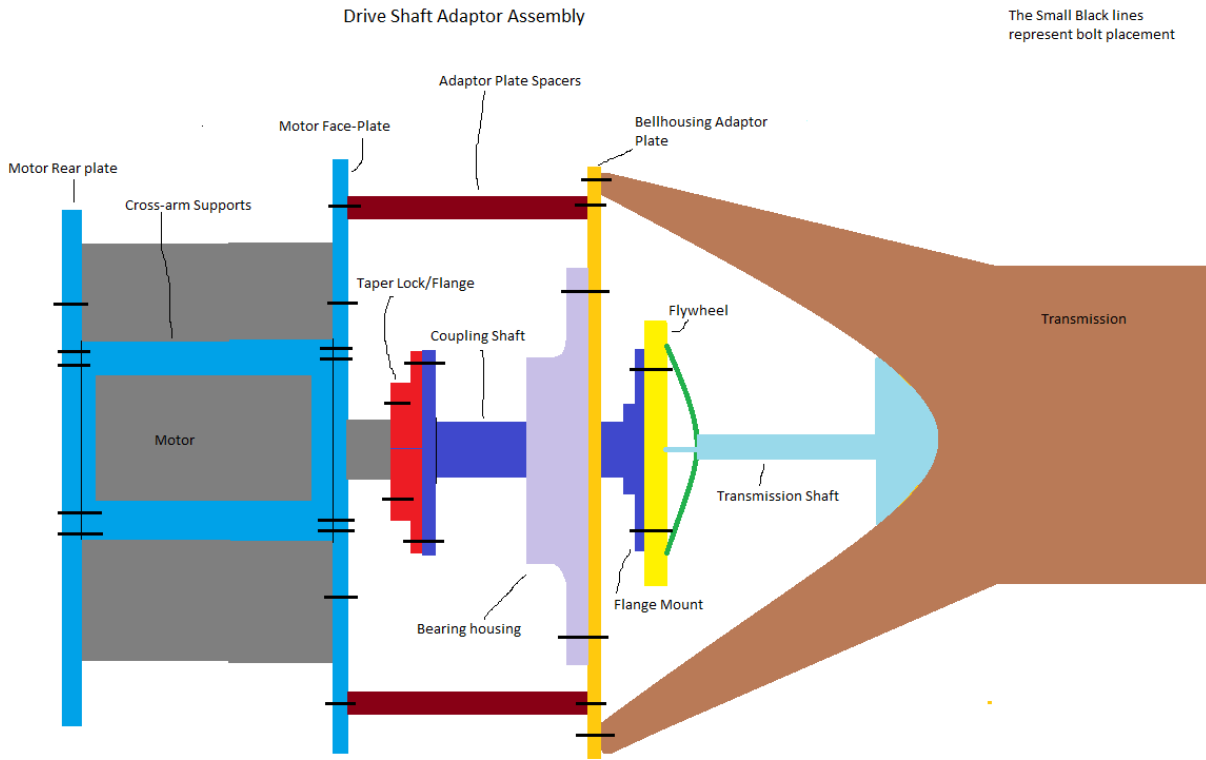


Figure 31 Cutaway of initial adapter shaft design

The figure shows how the motor could couple to the transmission and the various components required to fasten everything in place. Where the flywheel spigots to the left hand side, and the motor spline is inserted in the right hand side. The stress analysis that took place consisted of static radial forces due to the 15kg flywheel and the dynamic forces due to the motor torque transmission.

There two main aspects that are considered when undergoing shaft design and construction are: Stress analysis and reducing runout. Stress analysis aims to ensure the shaft will not fail during operation due to both static and dynamic forces. Runout is an alignment issue, the degree of which can be reduced but never completely removed.

A machinist specializing in driveshaft construction was consulted and provided the base design and a shaft diameter derived from empirical experience. This was stating a minimum driveshaft diameter of 50mm to transmit the required motor torque of 350Nm, using 4140 machining steel. This empirical derivation was checked against hand calculations to ensure the torsional yield stress generated by the motor on the shaft does not exceed the material yield. Thus forming the basis of the shaft analysis, where shear stress in a circular shaft can be described as:

$$T_{max} = \frac{\tau_{max} \cdot r}{J}$$

Where T is shear stress (MPa), τ (Nmm) is transmitted torque and r (mm) is the shaft radius and J (mm^4) is the polar moment of inertia. Where J is given as:

$$J = \frac{\pi \cdot D^4}{32}$$

Where D is the shaft diameter. Thus Table 5 gives the results:

Parameter	Value
D	50 mm
J	613592 mm ⁴
τ_{\max}	350000 Nmm
R	25 mm
T _{motor torque}	14.3MPa

Table 5 Shaft Parameters

Thus the motor produces a shear torsional stress of 14.3MPa. The yield strength of 4140 is in the order of 500MPa (atmospheric conditions), sufficiently high to negate torsional effects.

Radial forces are also considered, where the shaft acts as a cantilever from the motor if unsupported. Due to the mass of the flywheel, support must be employed on the shaft to eliminate loading the rotor bearings. Observing figure 32, shifting the point of support or fulcrum from position 1 to 2, the torque is reduced proportional to the difference in distance.

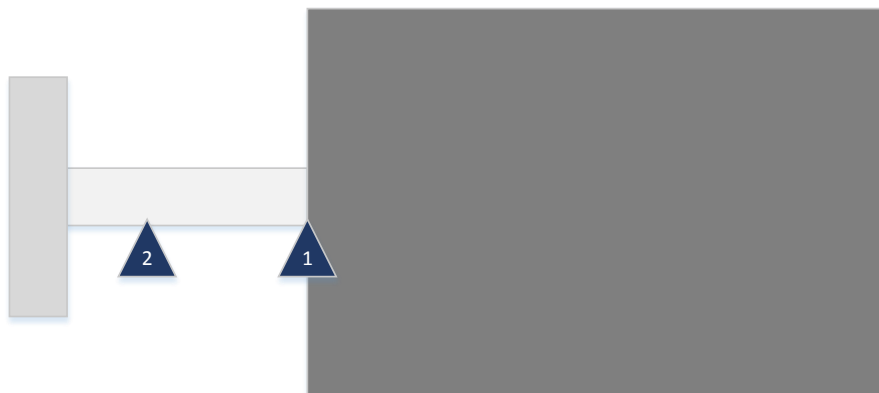


Figure 32 Shaft support

This support must be in the form of a bearing, since the shaft will be rotating. Thus the bearing is required to eliminate the radial loading. A second support bearing is utilized here at the motor end of the shaft. This ensures the pivoting of the shaft around the flywheel end bearing doesn't cause vertical radial loading on the rotor bearings, thus a different design is employed to that of figure 33

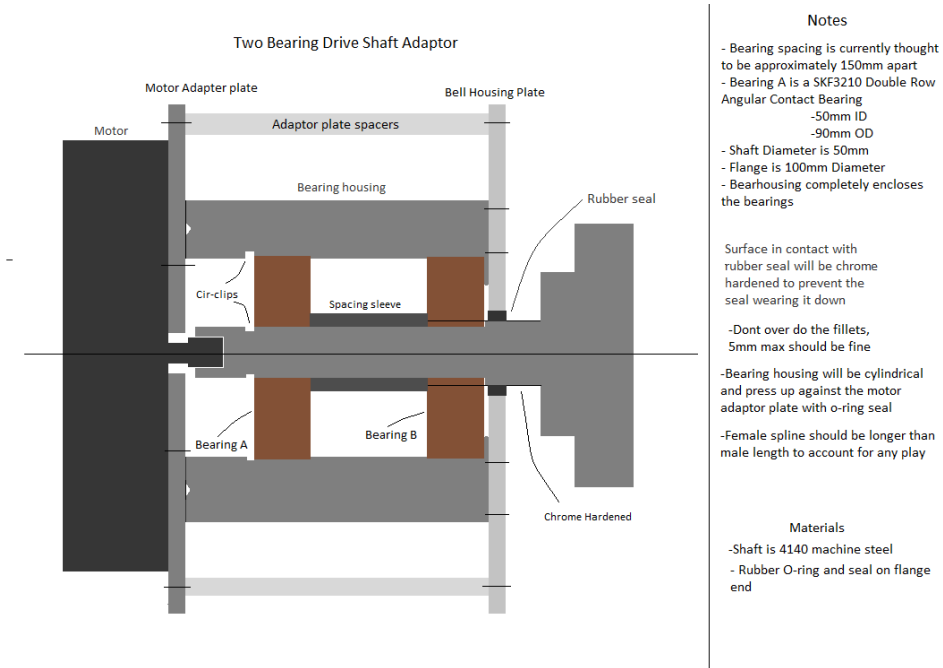


Figure 33 Secondary Adaptershaft Design

Runout occurs in every rotating system and increases bearing wear which can have a range of downstream effects, from impeded performance through to system failure. The motor bearings are the

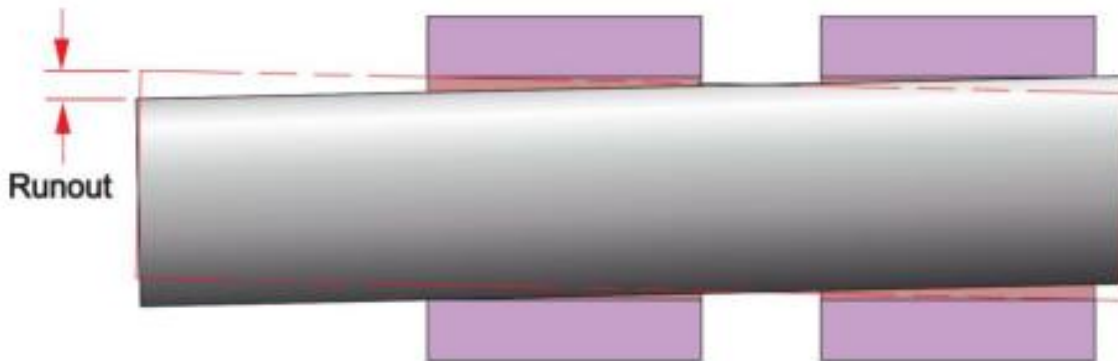


Figure 34 Shaft runout [53]

crucial parts here, as they cannot be easily accessed for maintenance. Runout of a system can be measured by dial indicator, but due to the inaccessibility of the system, estimates were employed.

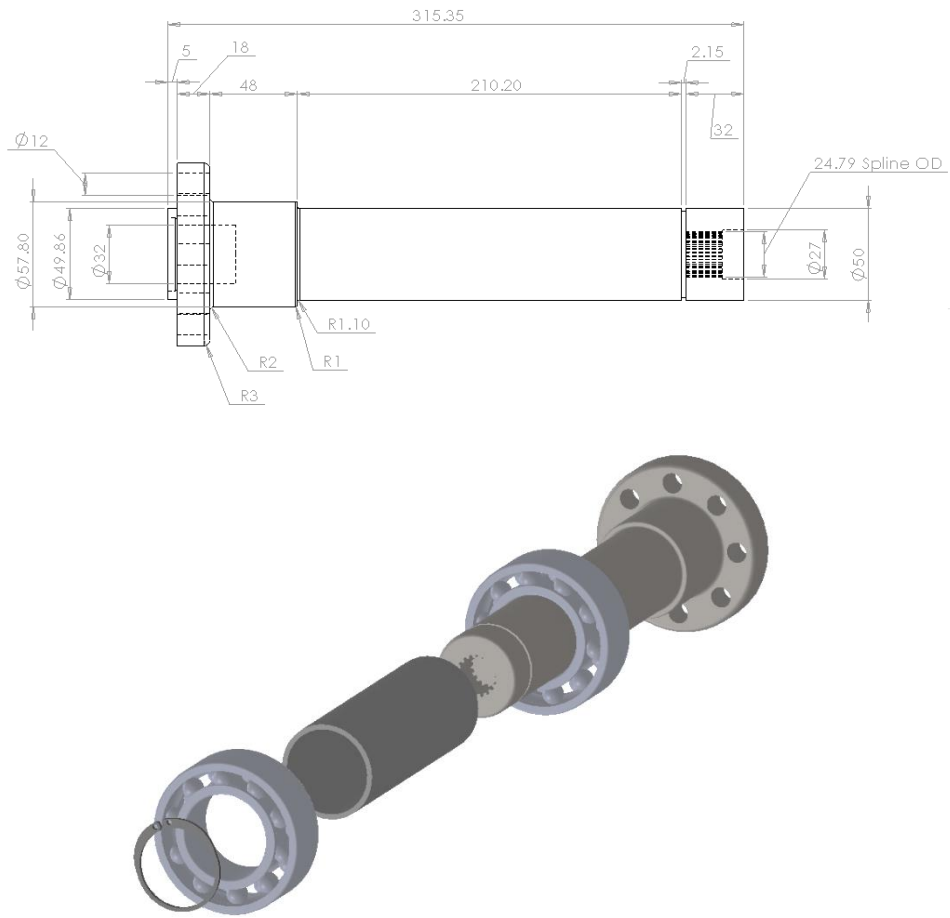


Figure 35 Final Adapter Shaft

The final shaft design was designed in CAD. The five main design constraints consisted of; Mechanical loading on the motor and shaft, the length of the shaft from motor to transmission, correct 24-tooth spline dimensions for motor connection, bearing placement and flywheel attachment. The final driveshaft is shown in figure 35 and the associated bearing housing in figure 36.

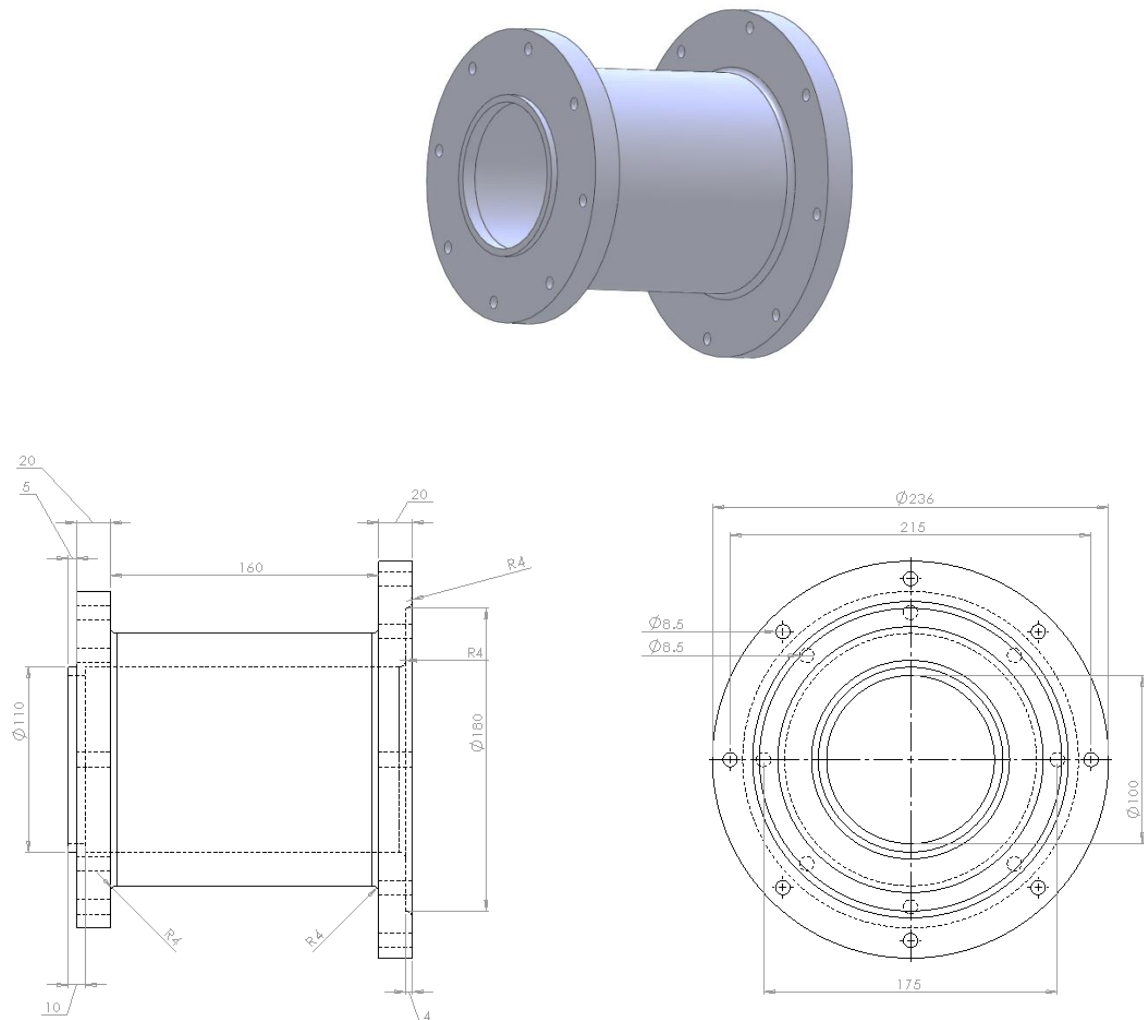


Figure 36 Bearing Housing

3.5.3.2. Battery Boxes

Battery placement impacts vehicle performance and systems integration. The battery weight is ideally situated as low as feasible on the vehicle, this helps with stability by making it more difficult to allow the vehicle center of gravity outside the vehicle basis of support (wheel base when all four wheels are on the ground). The 70 Series landcruiser has two chassis rails running the length of the vehicle. These rails give two major benefits for battery placement:

1. Secure place to fasten to
2. Provide impact protection
3. These chassis rails are shown below with the battery box layout superimposed:

Braking is also affected by vehicle mass distribution. By taking weight out of the front when removing the motor and putting back less than half that with the electric drivetrain, suspension and thus brakes will be less loaded in the front. To compensate for this, battery weight has been designed to be distributed over both axles, by having the majority of battery weight in the middle of the vehicle.

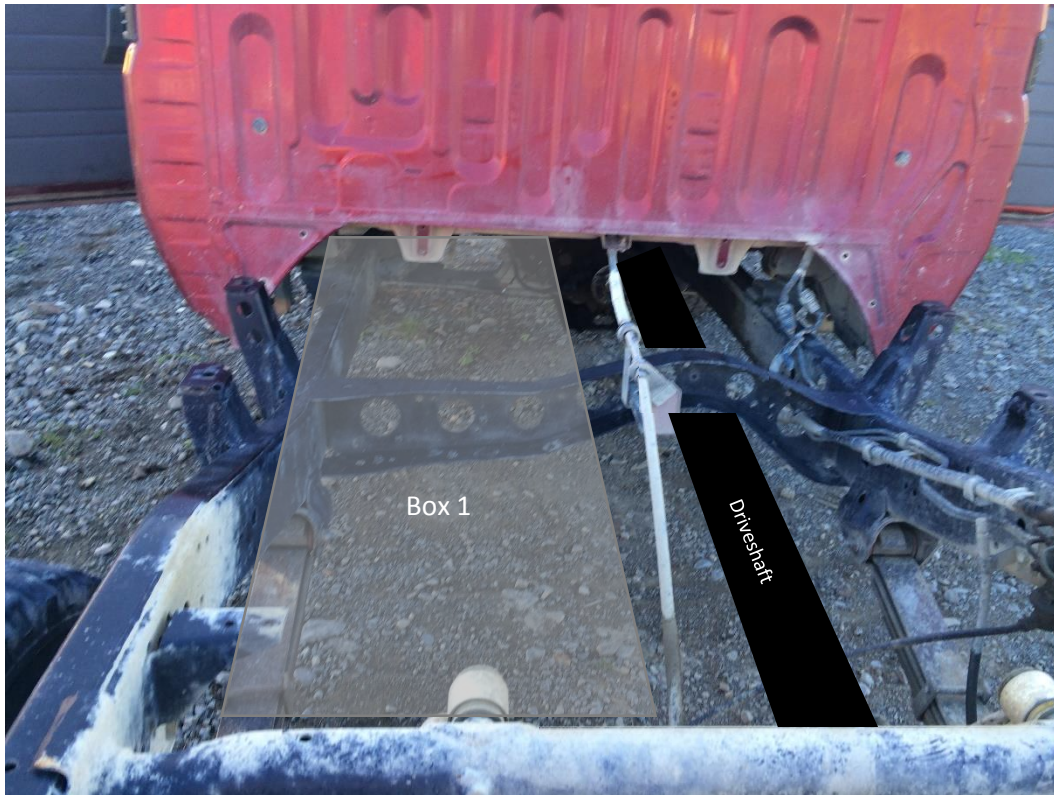


Figure 37 Battery Box location

Main battery box (box 1) placement is shown in the above Figure 37, where approximate clearances for chassis twist were taken into account to ensure the driveshaft did not impact against the box. From this sketch of dimensions in figure 38, a CAD drawing was constructed with more specific dimensions relating to placement orientation of the 108 x 100Ah Winston cells in Appendix 7.2

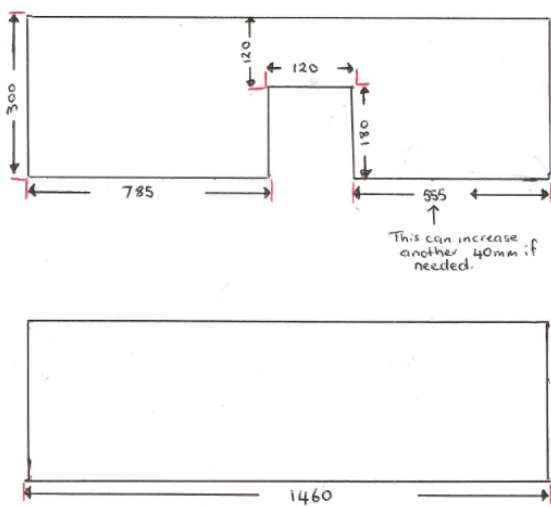


Figure 38 Hand measuring the available space

To keep the battery box bottom above the chassis rails, the total height of the battery boxes was found as 300mm through hand measurements. The battery sits at a height of 218mm, and with interconnects and HVDC cable also in the box, a total clearance of 19mm was calculated as shown in Table 6 below.

Battery Height Calculations

	Units	Value
Height of Battery	Mm	218
Braided Interconnects	Mm	15
Bolt Head Height	Mm	10
DC Cable thickness	Mm	20
Insulation thickness	mm	2
Aluminum Thickness	mm	6
Double floor	mm	10
BMS wiring?	-	
Top supports	mm	
Allowed Space	mm	300
Total Clearance	mm	19

Table 6 Battery box height calculations

3.1 Subsystem Development

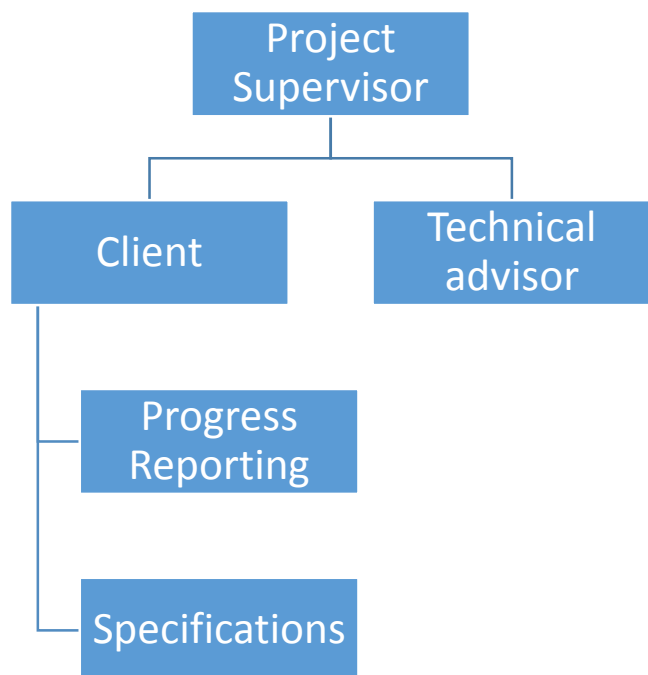
This area of vehicle development was largely worked upon by the two final year undergraduate engineering projects that ran during 2014 and 2015. The undergraduates were assigned individual accessory modules and guidance by the author. The modules that were developed are listed below:

2014

- Jack Stanton:
 - Motor Cooling
 - HV Cabin Heater
- Jonathan Sapson
 - Inverter Cooling System
 - Electric Power Steering
- Matt Barnham
 - Dash Instrument Cluster interface

2015

- Bram Humphris
 - Charger changeover switching unit
 - Inverter Calibration
 - Battery Testing
- Mitch Graham
 - Inverter Commissioning
 - HV Safety Box Fabrication
 - Battery Testing
- Devesh Sanjay
 - Charger implementation
 - General Wiring



3.1.1 Thermal Systems

There are three main thermal management systems on the vehicle associated with EV Components: Motor cooling, Inverter cooling and the Charger cooling. The BMS also has elements of cooling associated with it that will be discussed later, but it does not require an external thermal management system.

3.1.2 Motor Cooling

Oil cooled HVH motors have oil-cooled stators and rotors. In oil cooled versions of the motor, oil is fed into the cooling jacket and flows from there over the end turns in the sump. This flow path ensures additional cooling to both the rotor and stator allowing higher power outputs for longer durations than would be allowable without the rotor cooling path. Cooling reduces the negative impacts associated with the motor such as: winding insulation break down, bearing seals degradation and the rotor magnets do not de-magnetize as they approach the reaching Curie temperature point.

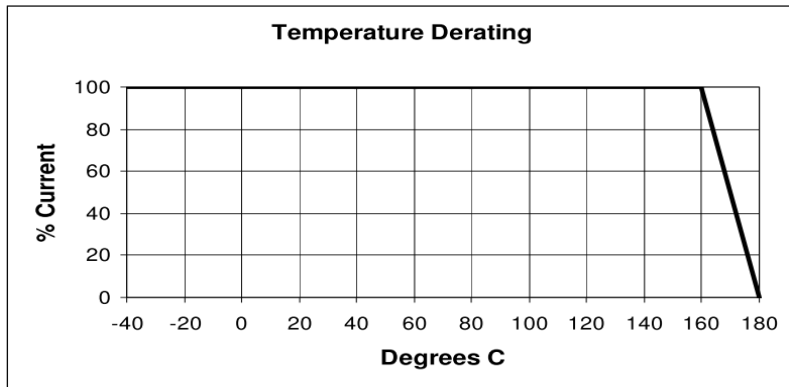


Figure 39 Motor Temperature Limits [42]S

Circulation of cooling fluid is a basic operating mode for the motor, a failsafe that is also built into the thermal system is current derating. This graph shows the de-rating that occurs to avoid demagnetization of the stator before reaching the Curie temperature. At 160°C the de-rating starts, and has a linear decline to 180°C where the inverter limits current to 0, figure 39. The permanent magnets in the HVH series motors are chosen for their high magnetic flux density and coercivity and are further protected from demagnetization by the motors' basic design. Temperature sensors are integrated into Remy motors, which signal the inverter to reduce current when pre-set thermal limits are approached

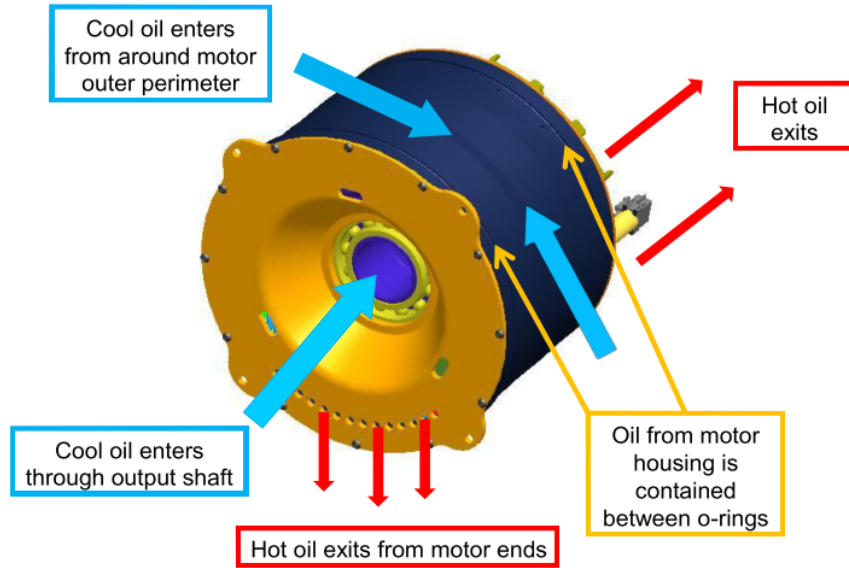


Figure 40 Motor Coolant pathway [42]

The bearings are also lubricated by the coolant oil. The motor application manual states that a filter is mandatory oil cooled Remy motors and to use only approved oils to avoid insulation break down and other negative effects. The cooling requirements are given below:

- Fluid: (ATF) Dexron VI
- Flow rate: 5-15 L/min
- Fill point: op level > 100 mm below shaft center

The application manual gives a basic schematic figure 41 which details pump and heat exchanger configuration. The motor is configured as a 'dry sump' which means that oil is stored externally from the motor in a reservoir. A more accurate cooling schematic is shown below with components required figure 42.

Example cooling circuit

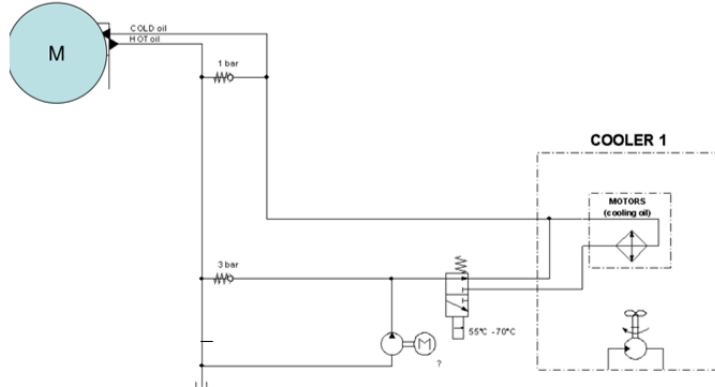


Figure 41 Example Cooling schematic [42]

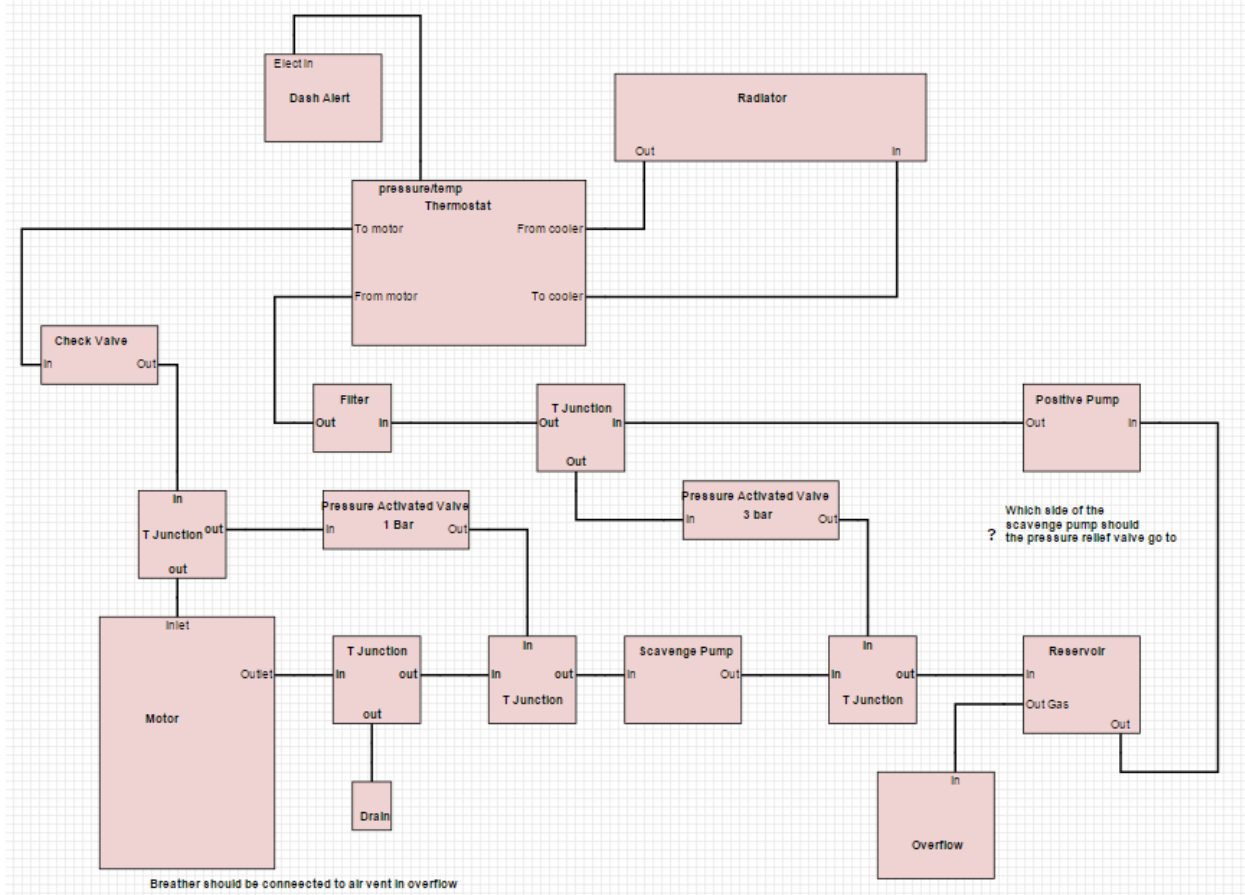


Figure 42 Cooling schematic created

These components are based off the application manual requirements example circuit below where the check valves provide protection against excessive accumulation of pressure. The 1 bar check valve in particular gives the limiting pressure differential across the motor to avoid damaging rotor bearing seals.

If sufficient accumulation of oil is built up in the motor, fluid can get into the airgap between the stator and rotor. The presence of oil in the airgap gives rise to additional heat losses due to friction and thus is to be avoided through design at all possible. The scavenge pump ensures that oil is removed from the motor housing, and in principle has to have higher flow than that of the positive pressure inlet pump to ensure oil accumulation is avoided. The cooling circuit in figure 42 above addresses this issue by using identical pumps for scavenge and positive pressure, but placing an oil filter after the positive pressure pump to ensure a pressure drop, and thus lower flow is experienced on the inlet side of the motor.

The sizing of the heat exchanger is important as to ensure adequate heat can be dissipated form the system. Using the nominal heat dissipation (15kW) and thermal transmittance $U = 600 \text{ W/m}^2\text{K}$ and the values in table 43 gives the surface area of 1.02m^2 .

$$A = \frac{q}{(U \cdot dT)}$$

Parameter	Value
Peak Power	130kW
Min Efficiency	78%
Max Heat Dissipation	28.6kW
Assumption, nominal dissipation	15kW
U	600W/m ² .K
Oil Temp	70°C
Air Temp	35°C
Area	1.02m ²

Figure 43 Cooling sized by Jack

These cooling calculations and sizing's were completed by Jack Stanton, but were crucial to getting HiCEV to a moving state.

3.1.3 Inverter Cooling

The Rinehart inverter electronics are encased in a CNC aluminum billet, which acts as an excellent passive heat exchanger in itself. To enable such a small footprint, additional active cooling is also required. The inverter cooling is a much easier concept than the motor. The glycol/water heat exchanger cooling requirements are given below in table 7 [43]

Coolant Type	50/50 mix ethylene glycol (antifreeze) / water or propylene glycol / water; with Aluminum corrosion inhibitor additive
Coolant Temperature	-30°C to +80°C full power Operation -40.. -30; +80.. +100°C with derated output
Coolant Flow Rate	8 – 12 LPM (2 – 3 GPM)
Pressure Drop	PM100, < 0.3 bar (4.4 psi) @ 8 LPM
Port Size	PM100 and PM150, AN-6

Table 7 Inverter Cooling

The cooling circuit diagram is shown in figure 44. The check valves have not been properly implemented across the motor or across the inverter, but are vital in avoiding over pressure situations.

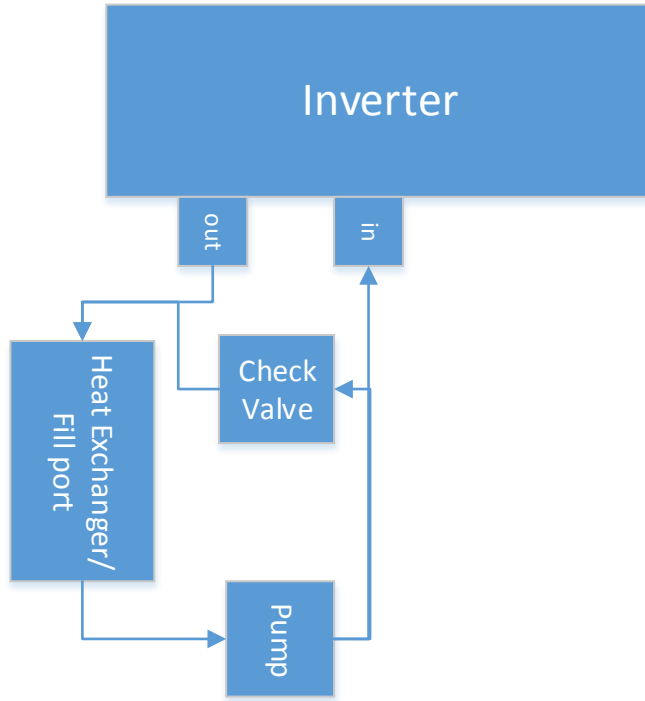


Figure 44 Inverter Cooling Circuit

Table 8 Inverter Cooling Circuit

Where the check valve is rated at 1 bar (14 PSI) cracking pressure. The heat exchanger can double as a fill port, thus reducing the number of components in the cooling loop. Sizing the heat exchanger is much the same as the process as the motor exchanger above, using the figures in table 9 a maximum heat dissipation of 3.9kW was derived and a minimum surface area $A_{\text{Heat Ex, Inverter}}$ of 0.186m².

Parameter	Value
Peak Power (Inverter)	130 kW
Efficiency	97 %
Max Heat Dissipation	3.9 kW
T _{ambient}	35 °C
T _{coolant}	70 °C
dT	35 °C
U	600 W/m ² .K
$A_{\text{Heat Ex, Inverter}}$	0.186 m ²

Table 9 Inverter Cooling parameters

3.1.4 Charger Cooling

Charger Cooling was completed by Devesh, and consists of a passive air cooled heatsink.

3.1.5 Power Steering

Power steering was completed by Jono, and implements an electric Holden Astra power steering pump. The current configuration is such that the $12V_{dc}$ bus is pulled low due to current draw at low speed turning from the power steering pump, which breaches the $9V_{min}$ operating region of the EVCM, so the vehicle loses power.

3.1.6 Dash Cluster

Dash cluster driver board was made by Matt to drive the cluster gauges from CANbus vehicle information, and still requires work to interface to the CANbus system.

3.1.7 Change Over switching unit

The changeover switching unit was developed by Bram and allows the charger to switch between an onboard generator source implemented as a range extender and the wall socket power. This is a break-before-make arrangement to avoid sourcing from two places. This circuitry has RCBO to trip if mains voltage leaks to chassis GND.

4.0 Testing and Commissioning

This section was the most time and energy intensive part of the project.

It has been structured so that the details of software used on each module are incorporated into each module's section. This is opposed to giving the software components their own section as the author feels that the focus could be easily diverted away from the data and vehicle performance.

4.1 Main Modules

The system of HiCEV are comprised of six main modules: Motor, Inverter, Batteries, BMS, Charger and EVCM. It is around these components that sub-systems form. Based on the prototyping specifications a final system was determined in table 10 below.

HiCEV Main Modules		
Module	Type	Vendor
Motor	Remy HVH250-115-PO	New Eagle -Remy Inc
Inverter	Rinehart 150DX	New Eagle – Rinehart Motion Systems
Batteries	108 x 100Ah Winston Battery	Winston Battery
BMS	Orion 108 Cell BMS	New Eagle – Orion BMS
Charger	Eltek 360/3000 IP67	New Eagle – Eltek Valere
EVCM	ECM-5554-112-0904-C/F	New Eagle – New Eagle/Woodward

Table 10 Final main modules

This can be visualized by figure 45 below that shows the main modules centralized and their sub-system dependencies surrounding them. To simplify the diagram, both the interconnectedness of modules through the CAN network and the mechanical fastening have been omitted.



Figure 45 Main modules and subsystems

Note that the number of subsystems depicted above for each module does not necessarily relate to the complexity of implementation.

4.2 Calibration

4.2.1 Electric Vehicle Control Module (EVCM)

The Electric Vehicle Management System (EVCM) used in HiCEV is the equivalent of an Engine Control Unit (ECU) in a combustion vehicle. The EVCM, by New Eagle, utilizes the ECM-5554-112-0904-C/F ECM hardware package made by Woodward from the Woodward MotoHawk Control Solution product line. The software on the EVCM is called MotoTune and is created from MotoHawk, a Simulink based program. The EVCM is the central control unit for the vehicle, and as such is linked to most components via CAN but also controls the 12V power to modules through external relays.

How the EVCM oversees the control of modules is shown below in figure 46; where the blue connections represent 12V power control, green represents CANbus flow, and black represents analog information.

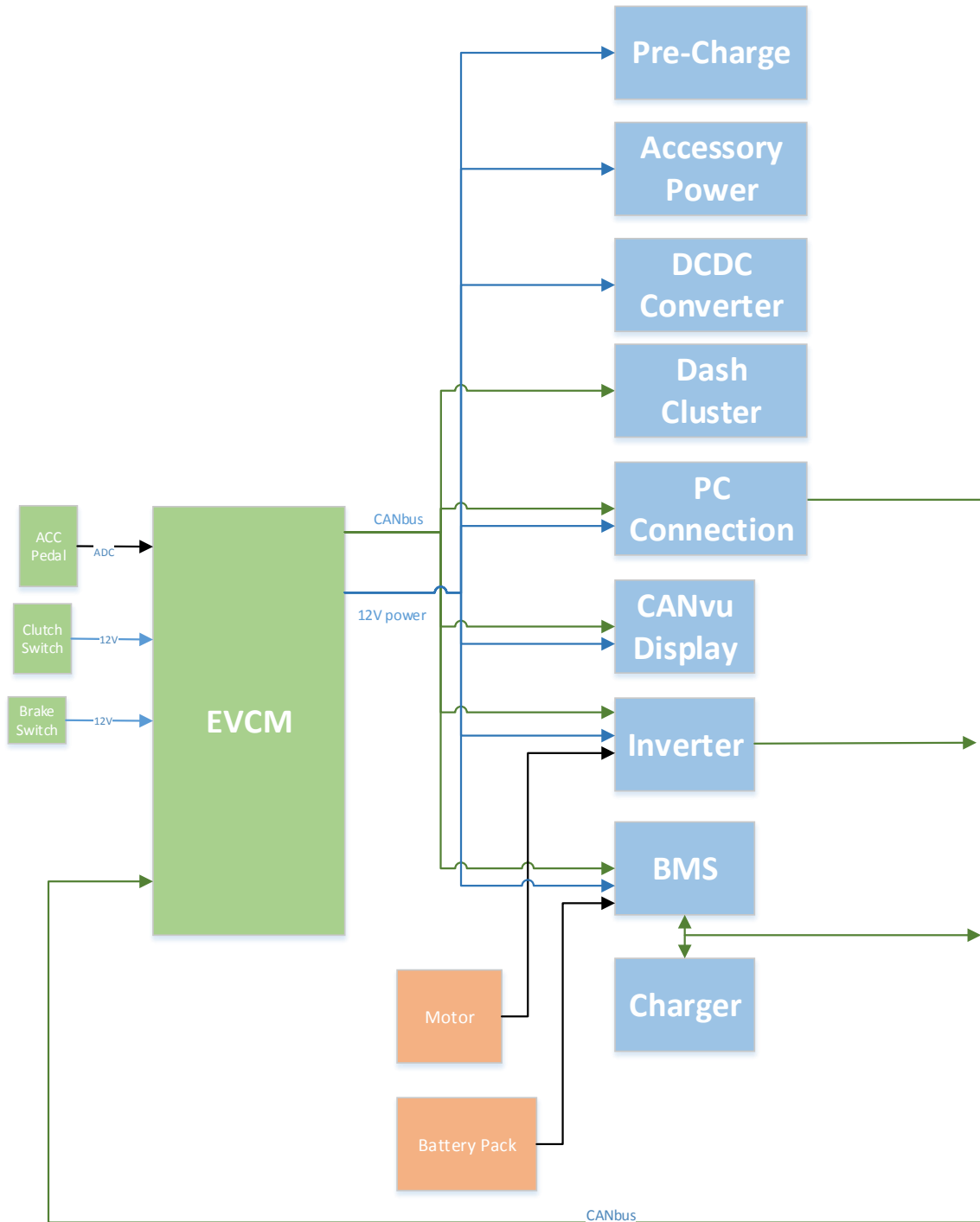


Figure 46 EVCM Control

The motor and battery pack are included here, as the motor feeds the inverter data such as rotor position from the resolver sensor and temperature which is used by the EVCM to calculate important information such as vehicle speed and current derating on torque requests. Similarly, battery information such as cell voltage, state of charge and temperature are processed by the BMS and utilised by the EVCM control system to operate the vehicle within safe limits. Also worth noting is that only four of the six modules that utilise CANbus feed information into the EVCM, whereas five of the six modules are controlled by the CANbus transmissions from the EVCM. That is, the BMS controls the charger directly during the charge cycle, but the EVCM can see the charging data.

4.2.1.1. EVCM Hardware, Control and Implementation

The EVCM is supplied by Woodward, then programmed through MotoHawk at New Eagle Control to perform various tasks in different industries. The EVCM is the electric vehicle controller version based on this common hardware platform.

ECM-5554-112-0904C/F Hardware

The hardware platform for the EVCM is the Woodward ECM-5554-112-0904C/F engine control module. From the modules name, it is implementing a Freescale 5554 micro-processor, 112 available pins in table 11:

PARAMETERS	
Microprocessor	Freescale MPC5554, 80MHZ
Memory	2MB Flash 64K RAM 32K Cache 32K EEPROM
Calibratable memory	2 x 256K RAM
Operating Voltage	9-16V _{dc} 24V _{dc} (Jump start) 4.5V _{dc} (crank)
Operating Temperature	-40 to 105 Deg C
Input Types	33 Analog 4 Oxygen Sensor (Not Required) 3 Speed 2 Knock Sensor (Not Required) 1 Emergency Stop
Output Types	14 Low Side Driver (LSO) 8 Injector 8 Electronic Spark 1 Tachometer 1 Digital Output 1 Main Power Relay Driver 2 H-Bridge Outputs
Communications	3 x CAN 2.0B Channels 1 x RS-485 Channel

Table 11 Woodward Vechicle Contol Specs [44]

The ‘C’ and ‘F’ in the product name denotes **Calibratable** and **Flash** versions of the controller respectively. Flash versions are pre-loaded from supplier with desired engine characteristics but retains

base level client-programmability for production applications. The calibratable version allows increased programming flexibility which includes field calibration and therefore is more suited for prototyping applications such as HiCEV.

Three sealed ‘pockets’ are built into the EVCM to provide the pinouts to the three Molex connectors A, B and C which are also color coordinated as black, brown and grey respectively. Figure 48 shows how the connectors are configured:

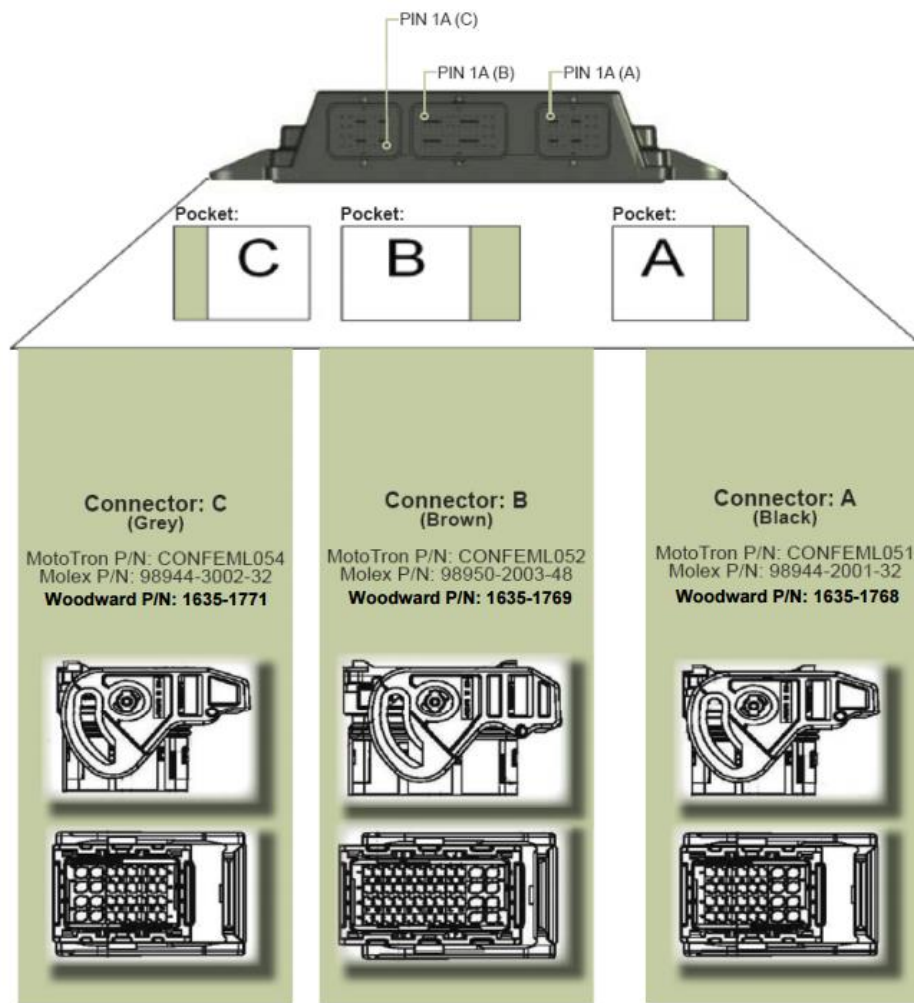


Figure 47 EVCM Pinout

Control

The EVCM allows for standard vehicle inputs such as brake and accelerator pedal to implement vehicle startup and control. Vehicle startup involves moving through a stepwise process to allow safe transition from a zero power state to operating mode. The steps are listed below in order:

1. EVCM Sense 12V and enable other components power through relay control

2. HV Sense
 - a. Pre-Charge Sequence
 - b. Close Main Contactor (Make-before-Break logic)
3. Foot Brake Sense – Inverter enable over CANbus
4. Vehicle ON

The key switch 12V ignition circuit has been retained, with modifications to the components engaged at ACC and IGN 12 Sources. A pre-charge sequence whereby the internal HVDC bus capacitors in the inverter requires a minimum three RC time constants [43] to charge. This part of the startup sequence is important as pre-charging prevents high inrush currents to the capacitors

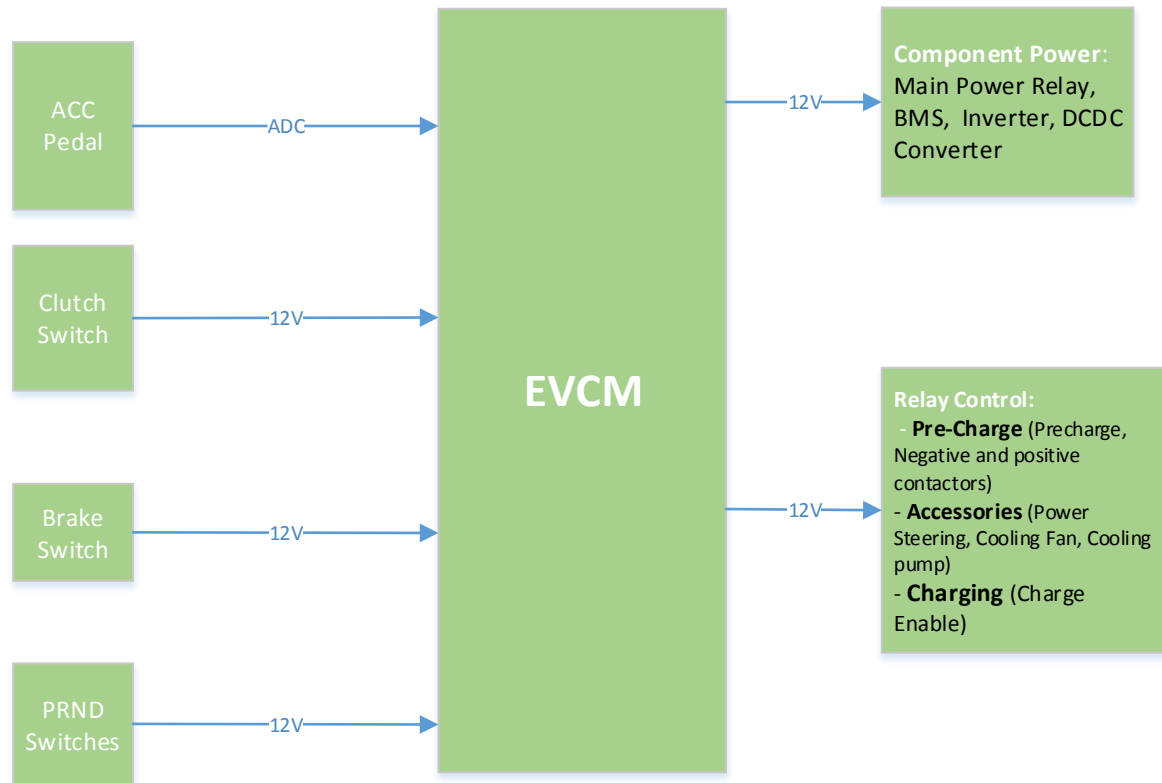


Table 12 EVCM Control Flow

Torque Requests

HiCEV can either be setup so that the inverter has torque requests sent directly to it, or sent over the CANbus by a central control unit – the EVCM. The EVCM allows the extreme end of customization in terms of vehicle torque mapping - based on parameters such as user pedal inputs, vehicle speed, temperature of modules and battery state of charge.

These EVCM aspects that control the inverter power flow to the motor are shown in Figure 48. The pedal inputs are all ADC controlled, where the accelerator pedal is an ADC controlled value, based on a

dual position sensing (for redundancy) using both a 5V and 2.5V analog input. The brake and clutch switch are both 12V switch signals (also ADC threshold controlled).

The module parameters such as vehicle speed (which is derived from the motor speed), motor temperature, inverter temperature, battery state of charge and battery temperature are used to scale the torque request to avoid component degradation.

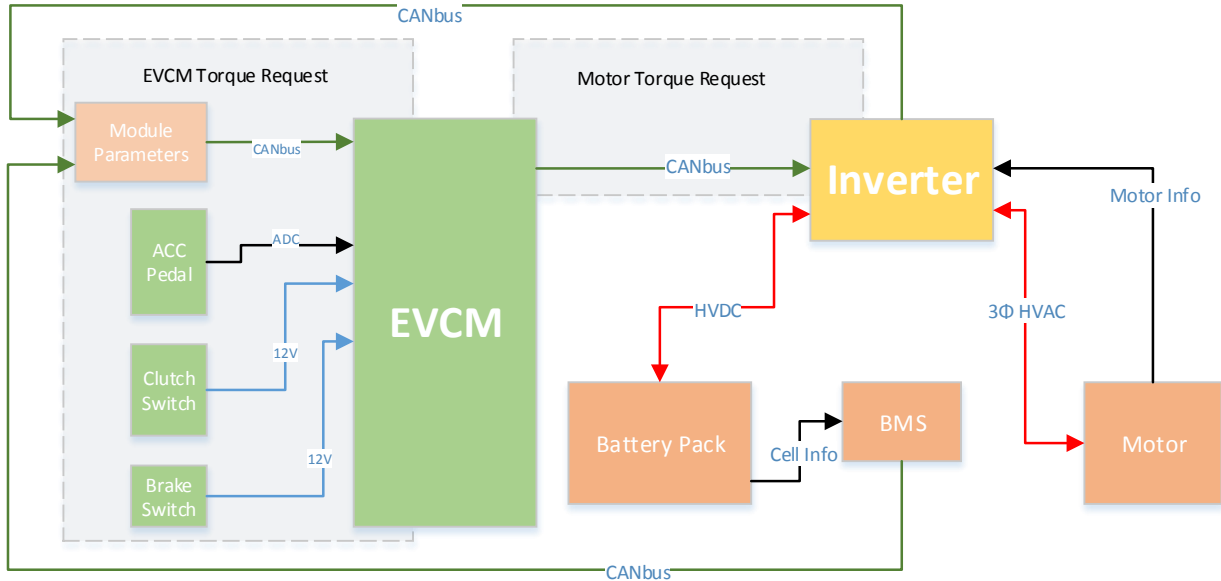


Figure 48 EVCM Torque request

The motor torque request (τ_m) is sent over CANbus to the inverter, thus controlling the flow of current both to the motor from the batteries (Motoring) and to the batteries from the motor (Regenerative Braking), denoted by the bi-directional red arrows. Also shown in the figure is the inputs to the EVCM, these directly affect the torque request, and the relationship is shown as:

$$\tau_m = \begin{cases} (k_{scale}) \cdot \tau_{evcm}(\theta_{AP}, \omega_m) & \text{if } \theta_{AP} > 0 \quad (\text{Motoring}) \\ - (k_{scale}) \cdot [\tau_{evcm}(\omega_m) + \tau_{BP}(\omega_m) \cdot k_{BP}] & \text{if } \theta_{AP} = 0 \quad (\text{Regen braking}) \end{cases}$$

Where scaling factor k_{scale} is the product of the clutch switch position and the torque derating factor:

$$k_{scale} = k_{CS} \cdot k_{DR}(T, SOC)$$

Where clutch switch setting k_{CS} is:

$$k_{CS} = \begin{cases} 1 & (\text{Clutch switch disengaged}) \\ 0 & (\text{Clutch engaged}) \end{cases}$$

Derating k_{DR} due to module temperatures and battery SOC is:

$$k_{DR} = k_m(T) \cdot k_i(T) \cdot k_{batt}(T, SOC)$$

And state of brake pedal k_{BP} is:

$$k_{BP} = \begin{cases} 1 & (\text{Brake engaged}) \\ 0 & (\text{Brake disengaged}) \end{cases}$$

What can also be derived from the above is that the torque request during motoring mode is based on accelerator pedal position θ_{ap} and motor speed ω_m which is then scaled by $k_{CS} \cdot k_{DR}$. Clutch switch position is important as the motor should not be allowed to accelerate/decelerate unloaded. That is, during motoring, mode k_{CS} helps reduce the chance of damage to the motor - during operation - from impulse unloaded acceleration. The threat is potent damage to bearings and rotor damage due to high centrifugal forces. Furthermore if the clutch pedal is engaged (decoupling the motor from the drivetrain) during operation the only energy source from rotational inertia contributing to regenerative braking is that of the motor's rotor, adapter shaft and flywheel.

$$E_{rotational,kinetic} = \frac{1}{2} \cdot I_{total} \cdot \omega_{motor}^2$$

Where I_{total} is:

$$I_{total} = I_{Rotor} + I_{Shaft} + I_{flywheel}$$

Which is calculated in the table below:

Part	Mass (kg)	Radius (m)	Inertia (kg.m^2)
Rotor	-	-	0.086
Shaft	~5	0.025	0.003125
Flywheel	~15	0.2	0.6
Total			~0.7

Therefore maximum rotational energy (at 5000 rpm) from the motor-to-flywheel assembly is approximately:

$$E_{rotational,kinetic} \cong \frac{1}{2} \cdot (0.7) \cdot (500)^2 = 87\text{kJ}$$

$$t \cong \frac{E_{rotational}}{P_{regen}} \cong \frac{87}{30} \cong 2.9 \text{ seconds}$$

With the drivetrain still be spinning at ~ 5000 RPM, the difference in speeds between the motor assembly and the drivetrain could cause shock impulse loading to the motor and deterioration of the clutch. The assumption of constant regen power is not a reality though, as the regen torque request is scaled by motor speed- which can be mapped through the EVCM to reduce/negate the power draw at low speeds.

Regenerative braking engages when the accelerator enters the calibratable zero range ADC value in MotoTune, which is proportional to $\tau_{evcm} = 0$. The motor torque request τ_m is the sum of τ_{evcm} and the brake pedal torque τ_{BP} both of which are solely a function of motor speed. The activation of the brake pedal switch ($k_{BP} = 1$) allows the additional torque from τ_{BP} while also activating the standard friction brakes simultaneously.

The regen torque request set to zero in the inverter gui is shown in figure 49, whereby the limits set in the inverter, trump the EVCM torque request. I.e., to attain a torque request, first the RMS needs to be setup correctly.

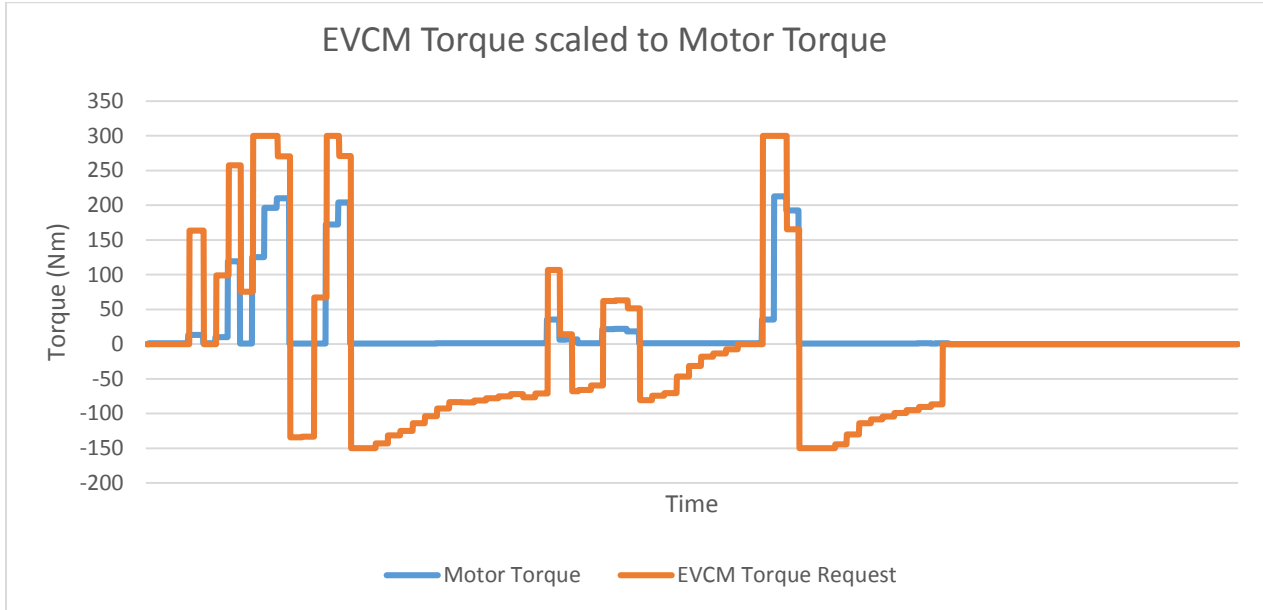


Figure 49 Zero Regen

Also, an example of the effect of the break torque multipliers is given below in figure 50. In the test, the motor speed has been accelerated to 5000RPM then left to ramp down slowly. At ~1100RPM, the speed multiplier starts reducing to zero (blue line in the top graph) which corresponds to an abrupt hold in the motor regen braking torque in the graph beneath.

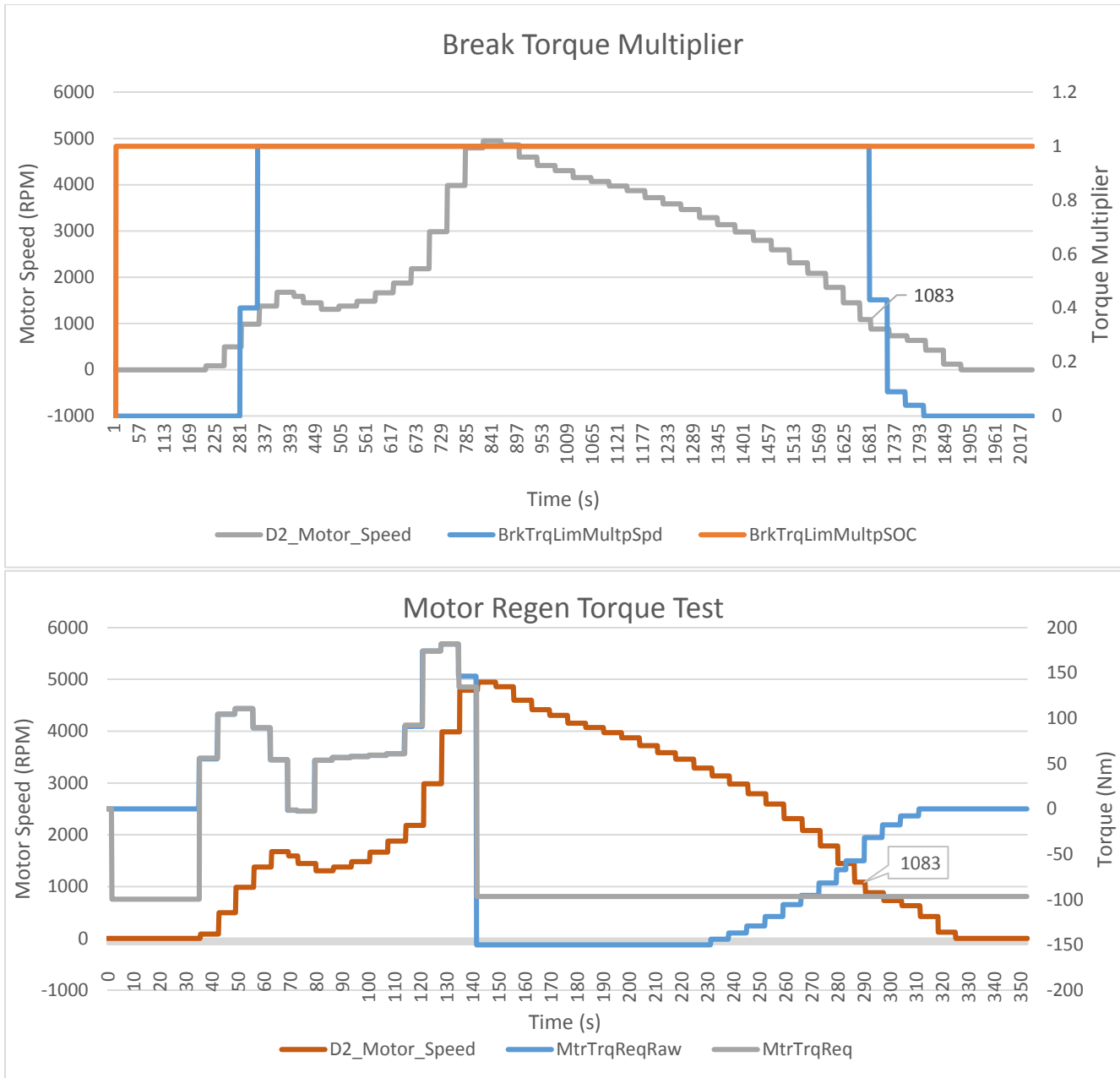


Figure 50 Motor Regen torque Multiplier

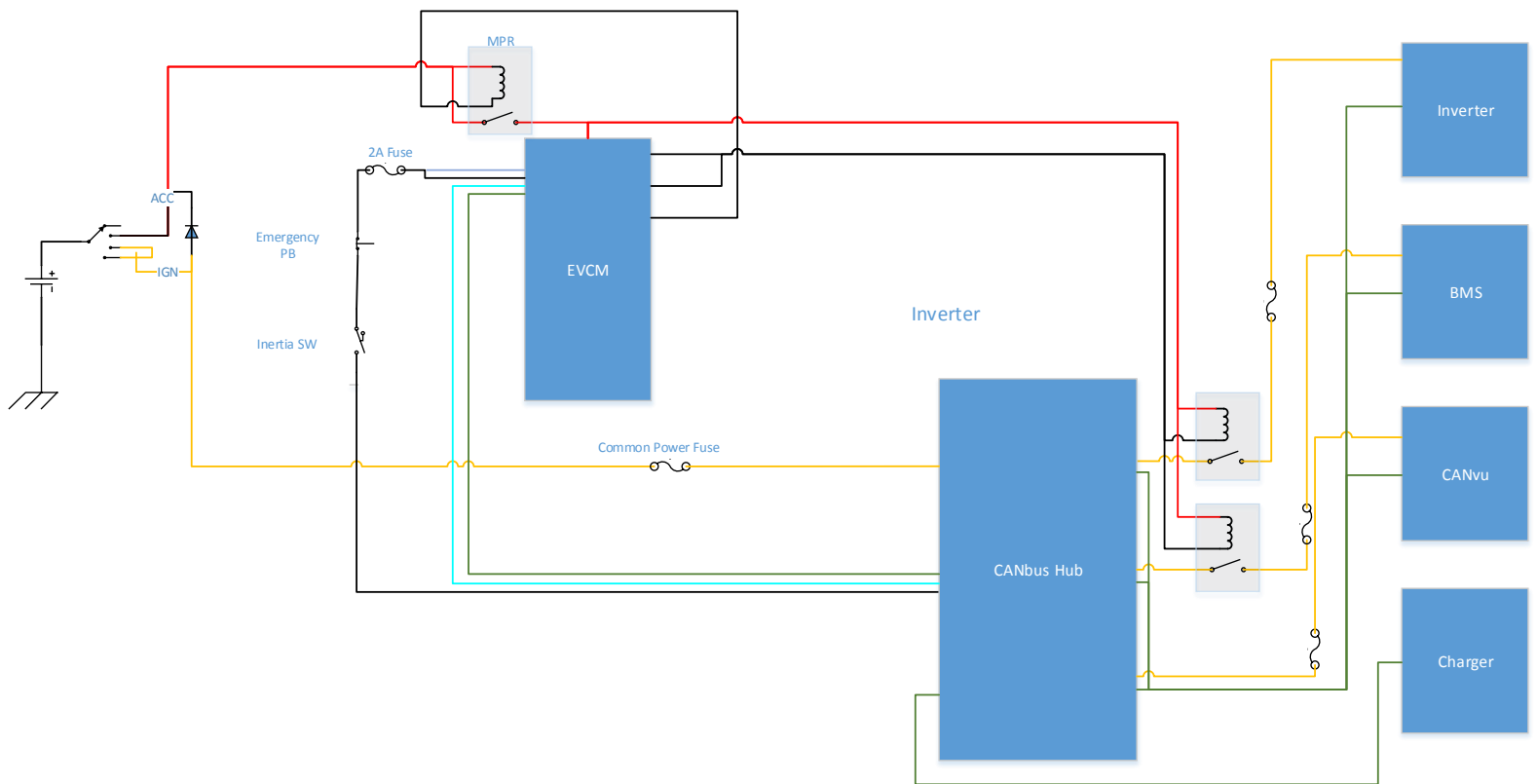
Physical Wiring

Construction of the physical wiring requires extensive connection analysis to ensure loom reliability and longevity. There are two main steps to laying the loom:

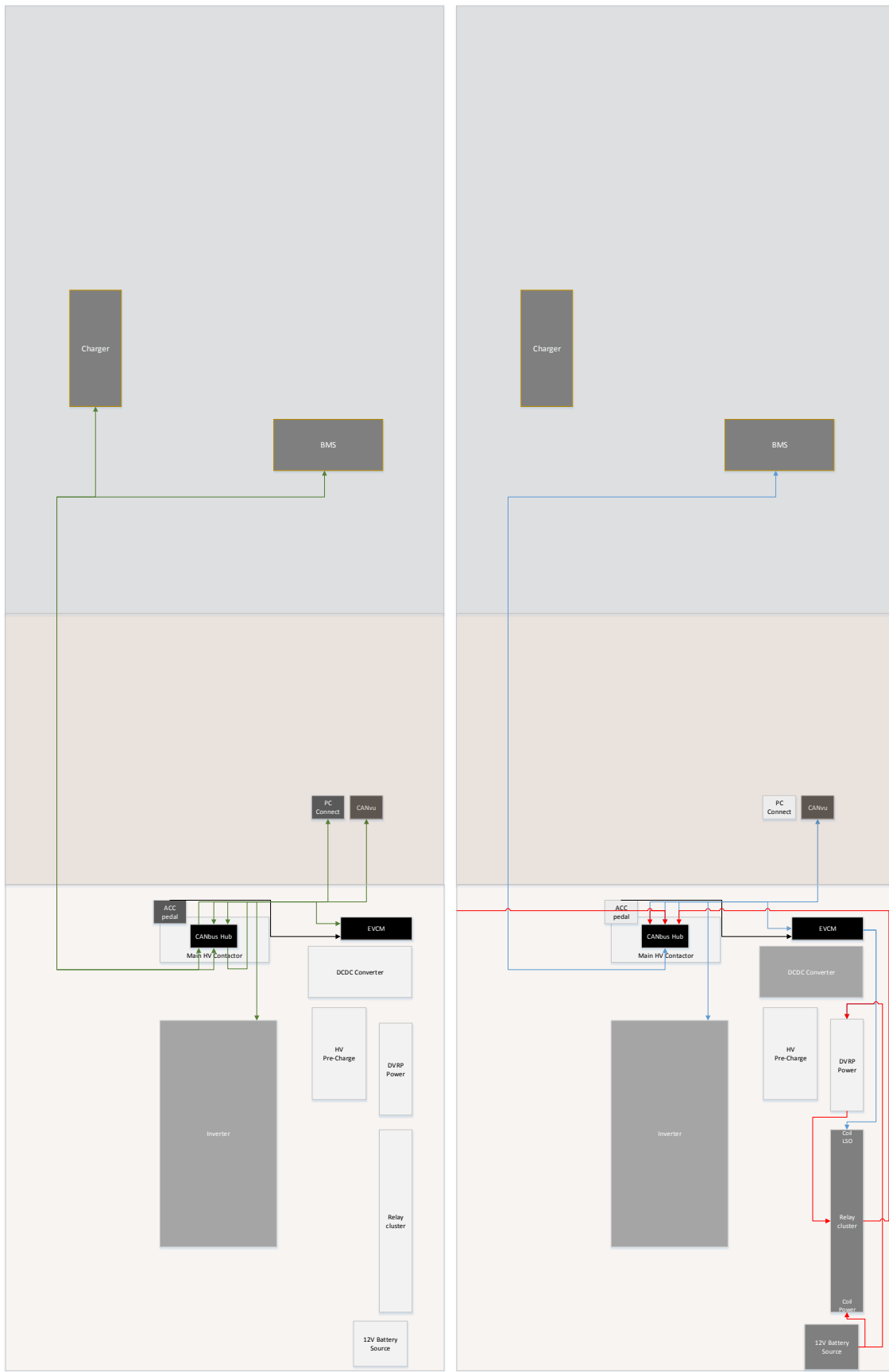
1. Gather wiring diagrams for all components that are being connected

- a. Connector information
 - i. Plug
 - ii. Connector
 - iii. Wire Seal
 - b. Determining current carrying capacity of the wires
 - i. Size wire AWG appropriately
2. Determine final location of components
- a. Determine distance between components
 - b. Route cable liberally before cutting to size for loom

The wiring of the SmartCraft connectors is given below. The EVCM uses the SmartCraft to control 12V power to modules and ensure a common ground exists for CANbus is given below. The ignition circuit is also shown here.



The physical layout of these 12V systems is given below, where the CANbus routing is on the left hand side, and the 12V power is on the right.



4.1.1.1.2 MotoTune Software

The controls solutions can be made in the MotoHawk environment using Simulink models as a ‘higher up’ level of programming and is suited for rapid prototyping. The diagram below shows the dependencies of the software:

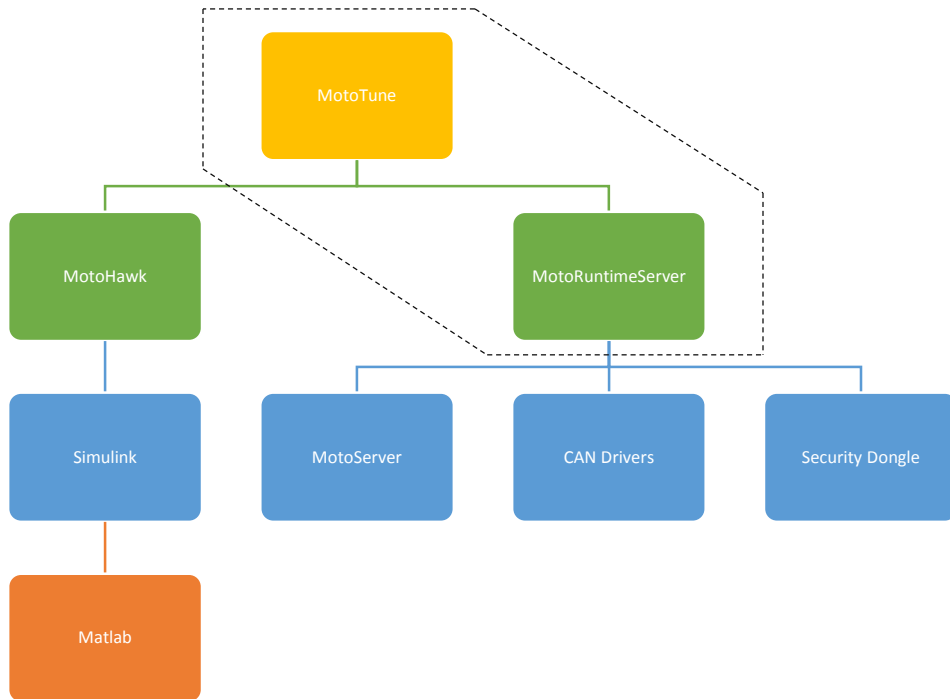


Figure 51 MotoTune Software Hierarchy

The depth of MotoHawk was beyond the project scope of design and commissioning, as this falls into the realm of refining control system models at a Simulink level and therefore is a project in itself. The program that is the user interface with EVCM is MotoTune.

MotoTune Software is a calibration tool that allows the user to measure and control various vehicle parameters in real time or offline. MotoTune also provides data logging, monitoring the CANbus and returns an excel format spreadsheet of the desired values.

There is a steep initial learning curve with how to operate MotoTune with respect to:

- Many variables that can be altered
 - locating the desired variable
 - The effects the variables have on the system
- Using the scrolling marquee error codes for troubleshooting

Once these aspects are understood, MotoTune becomes a useful centralized tool for refining vehicle performance, trouble shooting and viewing system data.

One of the most important aspects of MotoTune is that it allows the user to set variable limits and implement de-rating schemes to avoid component failure. This helps increase the life cycle of the main modules as it is adding a layer of protection against system failure. These safety aspects that are monitored include low voltage rail, high voltage rail, module temperature and HV current draw.

In summary, MotoTune allows the user to:

- Monitoring and analysis of main modules from one unit
- Data logging and Refining of system variables for desired performance
- Safety derating and threshold setting for system longevity

4.2.2 Eltek Charger Calibration

The Eltek Charger is shipped with a base calibration – which must be altered to more easily integrate with HiCEV's systems. The two main parameters that required an update were the charge current and the CANbus speed. Default current draw from mains was 15A at 230V_{ac,rms} which would blow fuses on the standard 10A wall socket supply. CANbus default speed was set to 500 kBit/s and if kept this way, HiCEV would have two separate CANbus's, one at 250 and on at 500 kBit/s. Thus these parameters required changing, which turned out to be more difficult than expected.

There are two ways to program the Eltek charger, the ‘clean’ or the ‘messy’ way. The clean way consists of downloading the graphic user interface (GUI) EV Powercharger Tools, connecting the charger to 230V_{ac} and using the IXXAT USB-to CAN hardware to connect and program parameters. However, there are always hurdles in projects such as these, and the hardware was not supplied with the module.

Available CAN hardware consisted of the Kvaser Leaf light which came with the EVCM – which unfortunately does not interface with the GUI which relies on the IXXAT drivers, not Kvaser. This leaves the ‘messy’ way using the CAN database document associated with the charger, also not supplied. By this means, the Kvaser Hardware and CANbus environment ‘Kvaser CAN kingdom’ became the substitute for the EV Powercharger GUI and IXXAT hardware.

To be able to program the charger, a heartbeat ‘Charger Control’ CAN signal must be sent every 1000ms [44] to keep the charger in a ‘Ready’ state, this concept is shown in the state flow diagram in figure 52. In this ready state, the charger can then progress to either charge state or programming state.

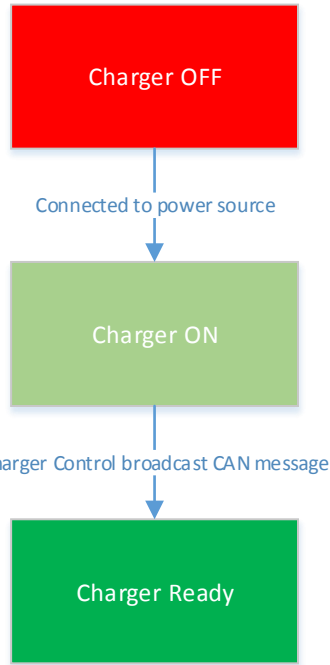


Figure 52 Charger State Diagram

The ‘Charger Control’ message broadcasts the following information: Charger Enable, Charger Power Reference, Maximum DC Voltage and Maximum DC current. This is shown in the following format:

	Bit 7 (MSB)	Bit 6	Bit 5	Bit 4	Bit 3	Bit 2	Bit 1	Bit 0 (LSB)
Byte 7				RESERVED				
Byte 6					CHARGER_MAXDCCURRLIMIT_MSB			
Byte 5					CHARGER_MAXDCCURRLIMIT_LSB			
Byte 4					CHARGER_MAXDCVOLTLIMIT_MSB			
Byte 3					CHARGER_MAXDCVOLTLIMIT_LSB			
Byte 2					CHARGER_POWER_REFERENCE_MSB			
Byte 1					CHARGER_POWER_REFERENCE_LSB			
Byte 0					CHARGER_ENABLE			

Figure 53 Charger Control Message Layout

Breaking this down further- the signal description and hexadecimal value (HEX) to physical conversion is displayed below:

Signal	Description	Min	Max	Data Conversion
CHARGER_ENABLE	Turns the charger on or off (PFC and DC/DC on/off)	0	1	Physical = (HEX)
CHARGER_POWER_REFERENCE	Power reference demand in percent of maximum power	0.0%	100%	Physical = (HEX/10) %
CHARGER_MAXDCVOLTLIMIT	Maximum charger DC voltage	0.0V	6553.5V	Physical = (HEX/10) V
CHARGER_MAXDCCURRLIMIT	Maximum charger DC current	0.0A	6553.5A	Physical = (HEX/10) A

Table 13 Charger Message Parameters

To obtain *write* access rights to change parameter values, the ‘Charger Configuration’ message must be broadcast over CANbus. A ‘Configuration Response’ is then sent by the charger to acknowledge changes that are made. This process is shown below in figure 54.

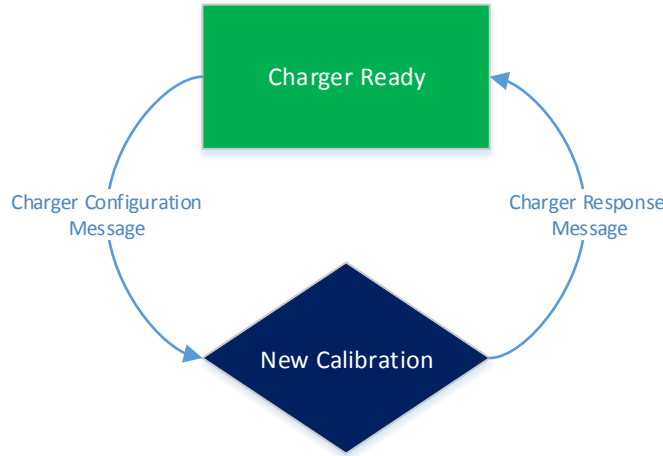


Figure 54 Charger Configuration and Response

Where the ‘Charger Configuration’ message is shown below, and only one parameter can be changed during a programming cycle:

Byte 7 (MSB)	Bit 6	Bit 5	Bit 4	Bit 3	Bit 2	Bit 1	Bit 0 (LSB)
Byte 6				CHARGER_CONFIGURATIONDATA			
Byte 5				CHARGER_CONFIGURATIONDATA			
Byte 4				CHARGER_CONFIGURATIONDATA			
Byte 3				CHARGER_CONFIGURATIONDATA			
Byte 2				CHARGER_CONFIGURATIONDATA			
Byte 1				CHARGER_CONFIGURATIONDATA			
Byte 0				CHARGER_CONFIGURATIONPARAM			RESERVED
							CHARGER_RW

And the general format for this message is shown as:

Signal	Description	Min	Max	Data conversion
CHARGER_RW	Charger read/write configuration	0	1	0=Read, 1=Write
CHARGER_CONFIGURATIONPARAM	Configuration parameter	0	255	Physical = (HEX)
CHARGER_CONFIGURATIONDATA	Configuration data	NA	NA	NA

The EV Powercharger CAN protocol then gives the specific ‘Charger Configuration’ Message for each parameter. For CANbus speed changes, the format is:

Write operation:

Byte 7 (MSB)	Bit 6	Bit 5	Bit 4	Bit 3	Bit 2	Bit 1	Bit 0 (LSB)
Byte 2				CHARGER_CANSPEED			
Byte 1				0			
Byte 0				RESERVED			1

Where CHARGER_CANSPEED can be set as any one of the following values;

- 0 = 125Kbit
- 1 = 250Kbit
- 2 = 500Kbit (Default)
- 3 = 1000Kbit

And the ‘Charger Configuration’ message for maximum AC current draw is given as:

Write operation:

Byte 7 (MSB)	Bit 6	Bit 5	Bit 4	Bit 3	Bit 2	Bit 1	Bit 0 (LSB)
Byte 3				CHARGER_MAXACCURRENT_MSB			
Byte 2				CHARGER_MAXACCURRENT_LSB			
Byte 1				23			
Byte 0				RESERVED			1

Where CHARGER_MAXACCURRENT can be set between 10 to 16A and this physical value is = (HEX/10) A.

The heartbeat ‘Charger Control’ message is required to keep the controller active during programming- which posed the major obstacle. Kvaser CANking allows the user to send messages individually or as a group of messages at the rate the CANbus is configured to. Sending multiple messages automatically is achieved by first configuring and sending individual messages in the correct order. These messages are then saved as historic messages in the ‘History List’ which can be sent as a ‘one shot’ timed transmission as shown in example figure 55 below:

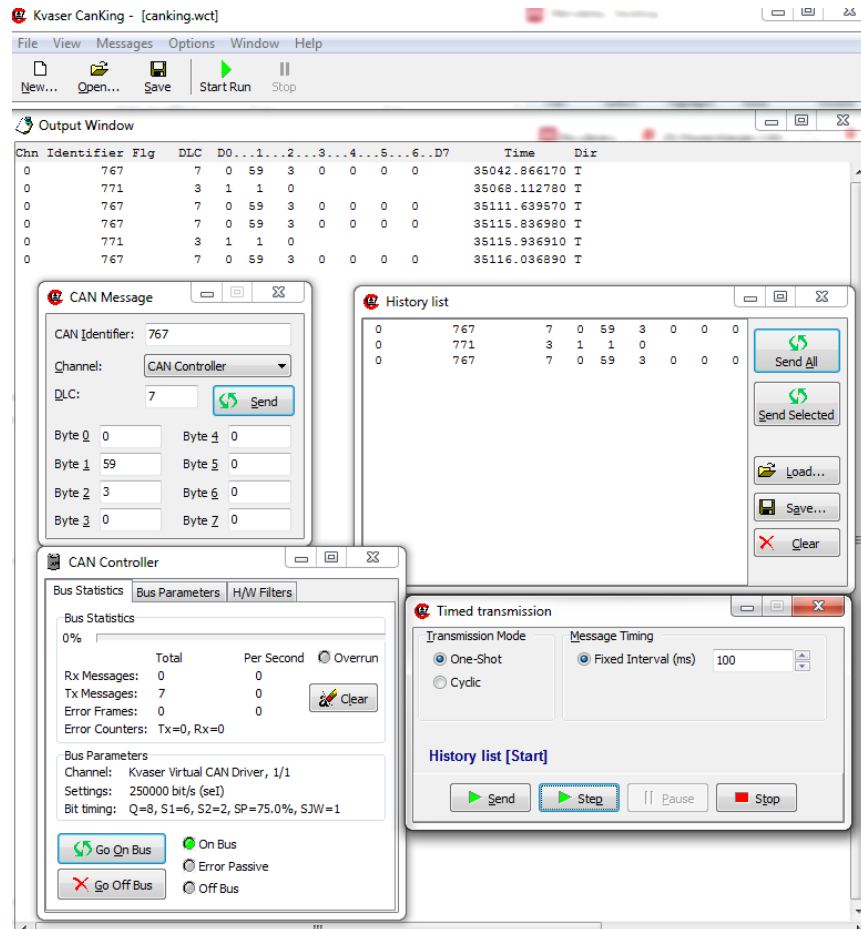


Figure 55 Kvaser CANking

Where the ‘Output Window’ displays information relating to the messages sent; ID Flag, DLC, Data bits and most importantly here: Time. The ‘CAN Controller’ allows the user to setup the bus parameters (i.e. Channel, Speed and whether the PC is on or off the bus) and the ‘CAN Message’ window allows the formation of individual CAN messages. Six messages were sent in total in the output window- first the individual three messages (Charger Control -> Charger Configuration -> Charger Control), followed by those same three messages sent via the ‘Send All’ in the History list. The idea behind sending the ‘Charger Control’ message twice was that the first message enables the charger and the second keeps the charger active while the parameters are being programmed. In the EV Power Charger GUI, this heartbeat message would be sent automatically. The ‘Time’ stamp in the Output indicates when the message was sent, and it can be seen that the first three messages have a delay of between 20-40 seconds as the messages were individually written, but only 100ms (set in the ‘Timed Transmission’ window) for the last three, a short enough time difference in the heartbeat ‘Charger Control’ (Message

ID= 767) message transmission to keep the charger ‘Ready’. It is worth noting that the charger was not on the bus at the point of transmission, as the ‘Charger Response’ message would have been broadcast onto the bus by the charger.

4.2.3 BMS Calibration

Battery management systems exist due to the nature of imperfections and repeatability. It is impossible to make batteries with *exactly* the same characteristics, and thus manufacturing defects or slight variations (I.e. materials used or process control variations) result in variations in battery profiles. The BMS compensates for these discrepancies during manufacturing to ensure the pack has reduced exposure to threshold limits which could cause damage or failure of the batteries and associated systems. Many different battery chemistries are available, each with different voltage and capacity profiles – thus the BMS must be setup for the specific LiFeYtPO₄ chemistry of the Winston batteries to ensure correct parameters and thresholds are in place.

Since the EVCM controls the load, the BMS primary functions are reduced to monitoring cell parameters and controlling the charging of the batteries and cell balancing associated with this.

As with the charger, the Orion BMS is programmed over CANbus and associated Orion GUI. The ‘CANapter’ hardware connects the PC to BMS, where the BMS also requires a 12V power source for programming and operation.

For an accelerated setup, the BMS has a ‘profile wizard’ that allows the user to select not only the general system settings such as CANbus speed, relays, thermistors and cooling fans that are configured but also battery type to be monitored from a database of pre-characterized batteries from a variety of vendors. Although the Winston batteries being used are not within this database (at the time of calibration), the Sinopoly and CALB chemistries are very similar (all three are LiFePO₄) so are suitable for a base calibration profile. Choosing a battery from the database loads information such as:

1. Cell Settings
 - a. Maximum and Minimum cell voltage threshold
 - b. Cell resistance profile
2. Charge and discharge current limits
3. State of Charge drift points

These default settings for the Sinopoly 100Ah battery as displayed below in table 14

Settings	Descriptor	Value	Unit
Cell Voltage	Maximum	3.75	V
	Minimum	2.8	V
Cell Voltage while charging	Maximum	3.8	V
Cell Balancing Thresholds	Start balancing if above	3.5	V
Charge Current	Max. Continuous Charge	200	A

	Max. Amperage while Charging	33	A
Derating	Reduce if Temp. >	40	°C
	By	10	A/°C
	Reduce if Temp. <	20	°C
	By	10	A/°C
	Never reduce below (for Temp alone)	0	A
	Reduce if SOC >	95	%
	By	20	A/(%SOC)
Discharge Current	Max. Continuous Discharge	300	A
Derating	Reduce if Temp. >	40	°C
	By	15	A/°C
	Reduce if Temp. <	25	°C
	By	7	A/°C
	Never reduce below (for Temp alone)	0	A
	Reduce if SOC <	10	%
	By	20	A/(%SOC)
Cell Resistance (per cell)	At -20° C	6.53	mOhm
	At 0 °C	3.60	mOhm
	At 25°C	1.27	mOhm
	At 40°C	0.59	mOhm

Table 14 Cell Settings

The system settings were set as per Table 15 below:

Settings	Descriptor	Value	Units
Current Sensor	LEM S/24	500	A
	Multi-Purpose I/P Function	Keep-Awake	-
	Multi-Purpose O/P Function	Err Signal Output	
	Invert Multi_purpose Output Polarity	No	
	Pack Amp Hours	100	Ah
	Current Sensor Polarity inverted	No	-
	Always on Power Not Used	Yes	-
Charger Safety Relay	Activated?	Yes	-
	Trip if pack current exceeds CCL by	30	%
	Max time relay stays on	600	min
Charge Enable Relay	Activated?	No	-
Discharge Enable	Activated?	No	-
Thermal Settings	Active Thermistors	2,3,4	-
	Intake Air Thermistor	None	-
	Enable Fan Control Circuit	No	
Fault Settings	Isolation Fault Detection Circuit	Ignore	-
	Fault when 'Charge' AND 'Ready' power on	Yes	-
	Fatal error if $ V_{packsensor} - \sum V_{celltaps} >$	101	V

Table 15 General Settings (Orion BMS)

From the profile wizard, the cell resistance profile is loaded based on testing done at Orion. The resistivity map compared to temperature of a cell can be seen in figure 56, which is used to compensate for changes in the cells internal resistance and thus output.

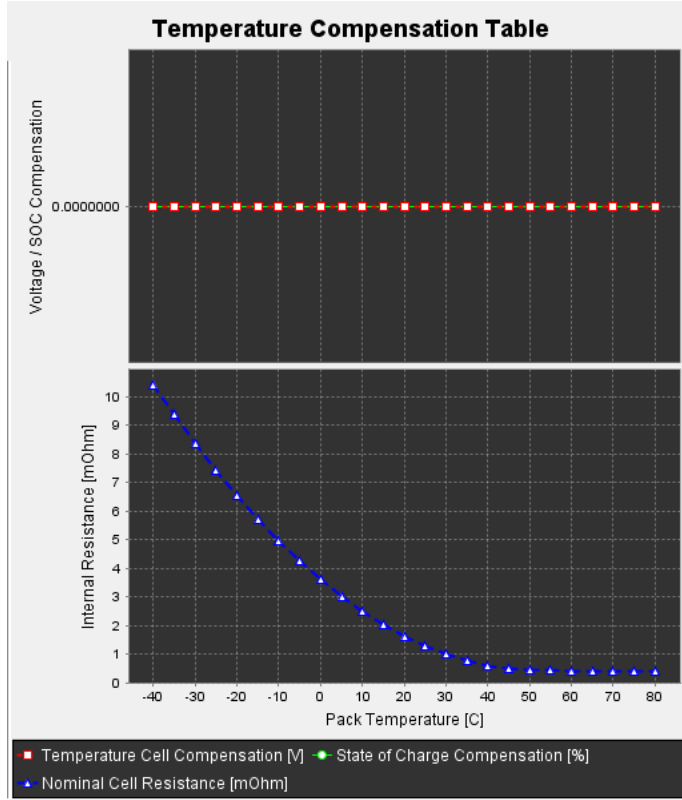


Figure 56 Cell Temperature Compensation

4.2.4 Rinehart 150 DX inverter Settings

The inverter converts the DC battery power to useable AC motor power. As Highlighted in the prototype specifications, it has a maximum rating of 150kW at 360Vdc. Rinehart supports the customer with a large amount of documentation including a software user manual and calibration document – thus only an overview of the calibration is required, with the settings that were programmed. Also provided is a general ‘road-map’ to completion for the inverter supplied by Rinehart, which has been adapted for HiCEV in figure 57 to show sections relevant to either calibration or commissioning. To prepare the PC for connecting to the inverter the following downloads are required:

1. Tools
 - a. C2Proog
 - b. RMS GUI
2. Files
 - a. RMS GUI Library File
 - b. Latest Firmware files
 - c. Documentation

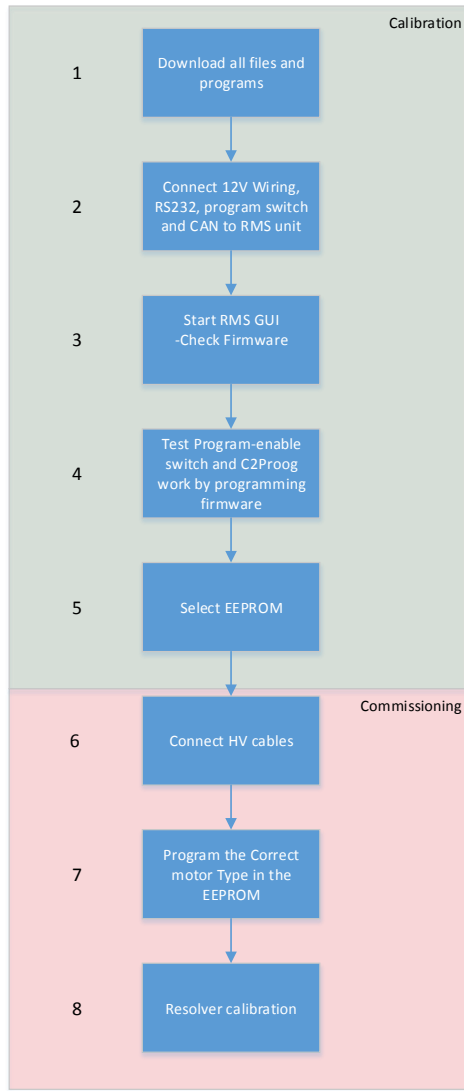


Figure 57 Inverter Calibration steps

Connecting to the inverter requires connecting the 12V power, RS232 and program enable switch at a bare minimum. The wiring diagram in Appendix 7.3 and the inverter loom mapping table in Appendix 7.4 gives the inverter pinout connections and the Rinehart suggested connectors, the inverter loom in figure 58 was created based off this information.

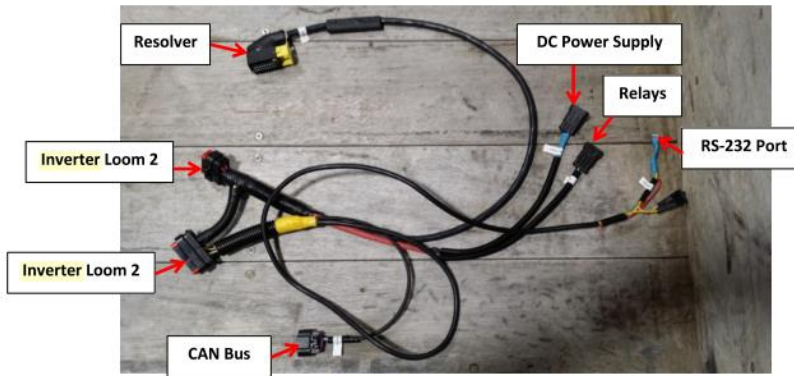


Figure 58 inverter wiring loom - final sizing

There are seven plugs in total; 2x Inverter connectors, SmartCraft (CANbus and 12V power), Resolver, DC Power Supply (for bench programming) and SCI (RS232). The loom shown is the final loom lengths, as during programming the lengths were an excessive length then reduced once the component approximate lengths had been measured.

The 150DX differs from the EVCM, Eltek and the BMS as SCI (RS232) is used to program the module, whereas CAN is used for control and feedback during operation. This is highlighted in figure 59 below where the two PC utility tools are also shown; C2Proog and the RMS GUI are both broadcast over RS232.

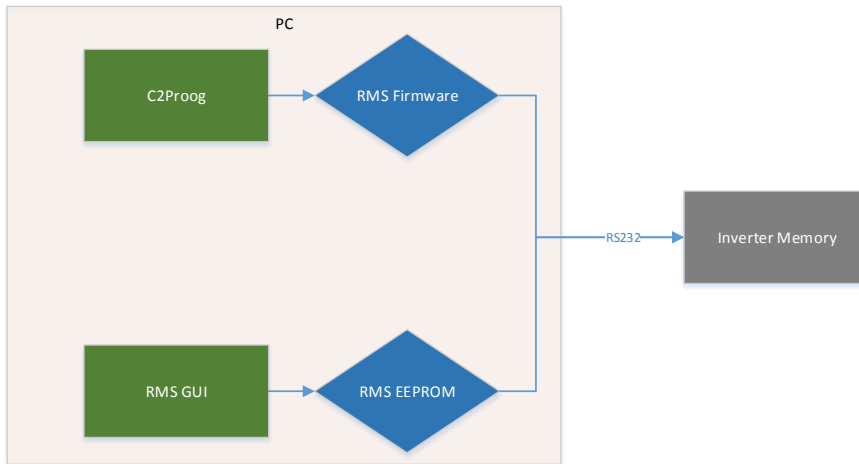


Figure 59 Firmware and EEPROM programming inverter over SCI

C2Proog updates the inverter firmware of the inverter in hex file format. The release of new firmware depends on New Requests, Change requests and system bugs. An example of this is a new request for motor parameters for a motor not previously integrated with the inverter.

The RMS GUI is required to setup the correct inverter parameters, which is loaded into the inverter EEPROM. A snapshot of the RMS GUI EEPROM values is given in figure 60, where Motor_Type_EEPROM = 36 represents the Remy HVH 250 115-PO motor and both Gamma_Adjust_EEPROM and Resolver_PWM_Delay_EEPROM_(Counts) are set during the resolver calibration.

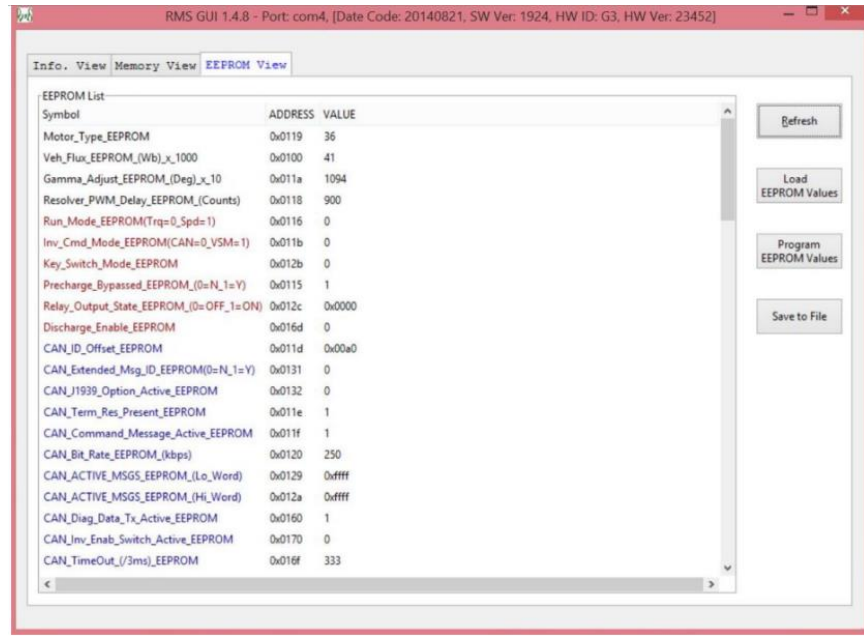


Figure 60 Snapshot of RMS GUI EEPROM parameters

Worth noting is that Inv_Cmd_Mode_EEPROM(CAN=0_VSM=1) is set to '0' representing the EVCM controlling the inverter though CAN and CAN_Bit_Rate_EEPROM is set to 250 kbps. Also, although the EVCM provides the platform for programming parameters, if the thresholds are not set more liberally in the inverter EEPROM than the EVCM, the inverter EEPROM values become the limiting thresholds. The below values in Table 16 from the inverter EEPROM are essential to vehicle performance as it was discovered that regenerative braking was not working as the Regen_Torque_Limit_EEPROM was set to '0', even though it was programmed higher at the EVCM.

Parameter	EEPROM Value	Physical Value	Unit
IQ_Limit_EEPROM_(Amps)_x_10	5300	530	A
ID_Limit_EEPROM_(Amps)_x_10	5300	530	A
DC_Volt_Limit_EEPROM_(V)_x_10	3900	390	V
DC_UnderVolt_Limit_EEPROM_(V)_x_10	2500	250	V
Motor_Torque_Limit_EEPROM_(Nm)_x_10	3300	330	Nm
Regen_Torque_Limit_EEPROM_(Nm)_x_10	2000	200	Nm

Table 16 Inverter EEPROM – HV Power

The current limiting parameters; IQ_Limit_EEPROM_(Amps)_x_10 and ID_Limit_EEPROM_(Amps)_x_10 represent the quadrature and direct current limits respectively, indicative of the 3 phasor currents (through inverse Clarke transform, on the assumption that the scaling '2/3' is used) current magnitude.

The DC voltage limits are based on limitations of the inverter and the battery pack. The upper voltage limit (DC_Volt_Limit_EEPROM_(V)_x_10) is dictate both by the inverter upper voltage limit of $400V_{dc}$

while operating and the battery cell voltage limits of 3.65V per cell while charging (regenerative braking). Thus, a voltage of 390V_{dc} provides a margin of 10V_{dc} on the inverter limits while allowing a 0.4Vdc margin per cell. The lower voltage limit of 250V_{dc} is dictated primary by the battery cell resistance, and the associated voltage sag at maximum discharge current. At 80% depth of discharge, the average cell voltage will be 3.2V_{dc} unloaded, thus gives the lower limit of pack voltage of 345.6V_{dc}. This entails that a discharge current of 450A_{dc} will ‘sag’ the DC bus voltage to 250V_{dc} if the internal resistance per cell is equal to approximately 2mΩ, which according to the BMS cell resistance profile is at temperatures above 15°C.

Both the motor and generation torque limits (Motor_Torque_Limit_EEPROM_(Nm)_x_10 and Regen_Torque_Limit_EEPROM_(Nm)_x_10 respectively) are based on the Remy HVH250 motor performance curves and the motor constant. From the motor performance curves in Appendix 7.5 the maximum torque is 425Nm at a current of 600A_{rms} giving a motor constant of approximately 0.71 Nm/A, thus for a current of 450A_{rms}, developed torque is 320Nm. Thus a torque of 330 Nm max allows the user to calibrate up to the maximum allowable torque in the EVCM, with a 10Nm buffer for safety. The regenerative braking was set to 200Nm to start, this parameter may have to be altered to allow for more breaking depending on the customer’s drive profile and how they want the breaking to feel.

4.3 Commissioning (Systems integration)

The physical commissioning of HiCEV maintains the modular approach, but with increased focus on the module subsystems. Effective systems integration relies on robust and effective subsystems, as communication errors cause incorrect operation, leaking coolant reduces thermal capability of a module or high voltage on the vehicle chassis represents poses a safety hazard. To commission each module, the subsystems are first mapped at a fundamental level in a top down approach, before being tested and assessed.

4.3.1 Motor Mechanical Development

The motor commissioning can be broken down into four subsystems, all of which are mechanical based as the electrical aspects are the focus of the inverter. These subsystems included the adapter shaft assembly, adapter plate, motor cradle and the motor cooling. The system reliance flow diagram is shown in figure 61 below:

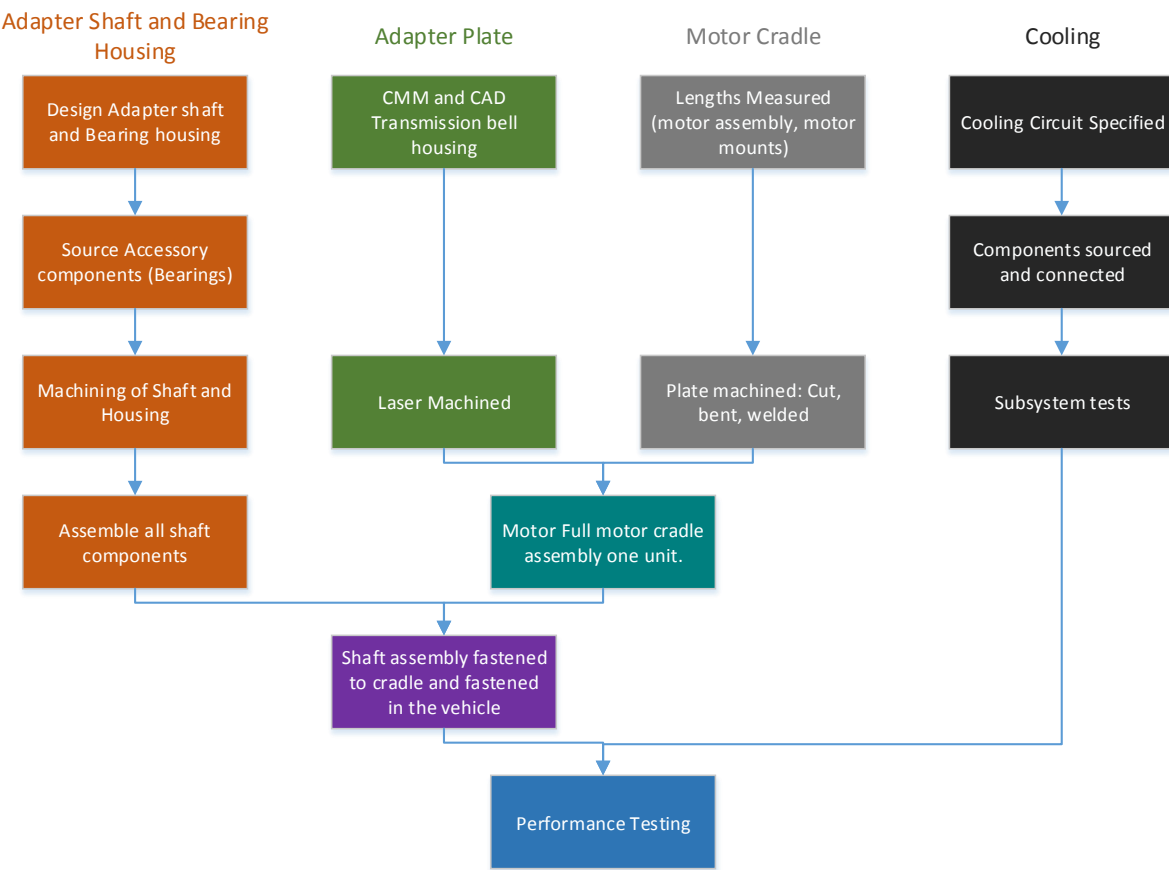


Figure 61 Mechanical breakdown of motor requirements

The adapter shaft was machined by a third party and assembled in house. The prototyping of the adapter shaft dictates that the shaft was to be machined from a piece of round solid 4140 machine steel. Two pictures below in figure 62 show the machining of the shaft and final assembly post

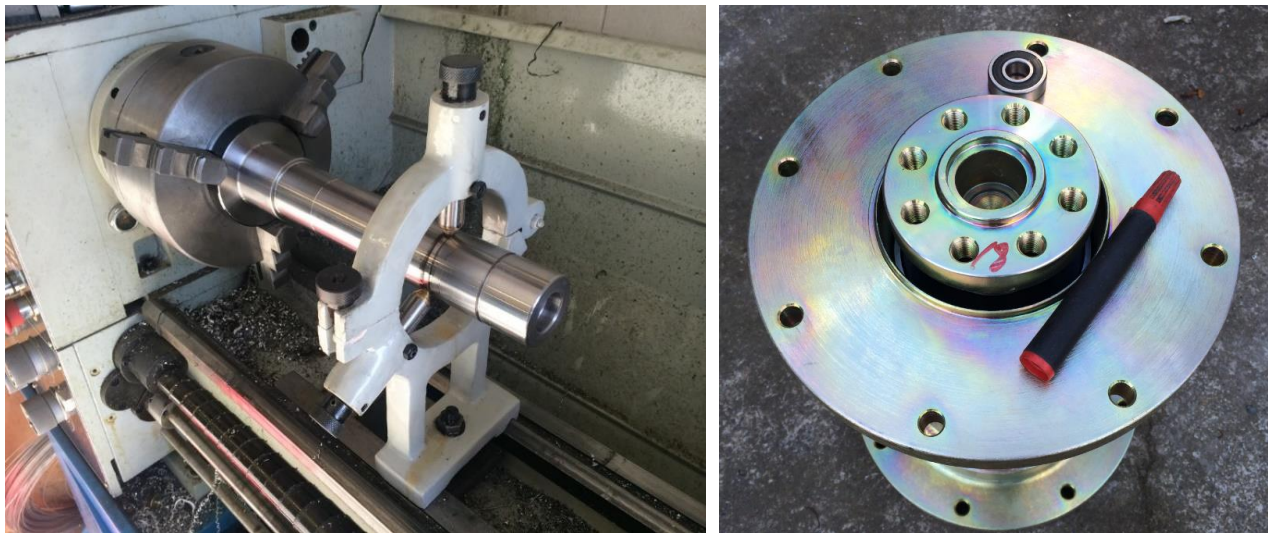


Figure 62 Adapter shaft machined

anodizing.

Notable features of the shaft are the spigot ridge on the adapter shaft which is concentric with the flywheel, and the recess in the end of the adapter shaft which supports the run-out bearing which supports the end of the transmission shaft. The runout bearing (shown sitting on the bearing housing above) also allows the transmission shaft to move at a different speed to the motor when the clutch is disengaged.

A metal gasket from the original engine to bellhousing was utilized to create the bellhousing adapter plate in figure 63. A CMM profile of the gasket provided the hole pattern for a CAD file to be constructed accurately. This was of importance due to the accuracy required to align the adapter shaft to prevent 'run out'. The center hole in the gasket is assumed (due to the difficulties associated with implementing a dial indicator in an enclosed space) to be concentric with the transmission output shaft. The transmission in



Figure 63 Bellhousing adapter plate

Figure 63 also displays how the adapter plate fastens to the transmission and the single aligning stud protruding through the bellhousing plate. The motor cradle is welded to the adapter plate and has a twofold purpose; to reduce the cantilever loading though supporting the motor from the rear and to also support the entire transmission though motor assembly from the pre-existing motor mounts.

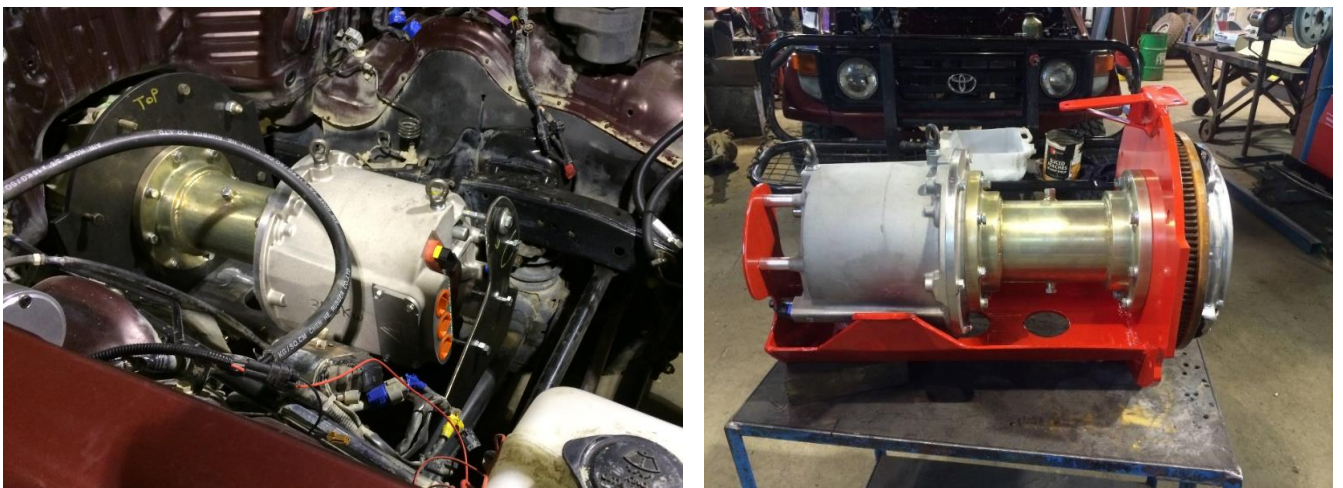


Figure 64 Motor Placement

The motor with lifting eyebolts in figure 64 above shows positioning of the motor, which was subsequently removed and giving a red powder-coat coloring to prevent rust.

4.3.2 Inverter

The inverter can be broken down to four base commissioning subsystem aspects; mechanical, low voltage, high voltage and cooling. These subsystems and dependencies are shown below in figure 65 to indicate the integration required to initiate performance testing of the inverter. Additionally, the red highlighted section indicates the focus aspects with interfacing the motor with the inverter physically.

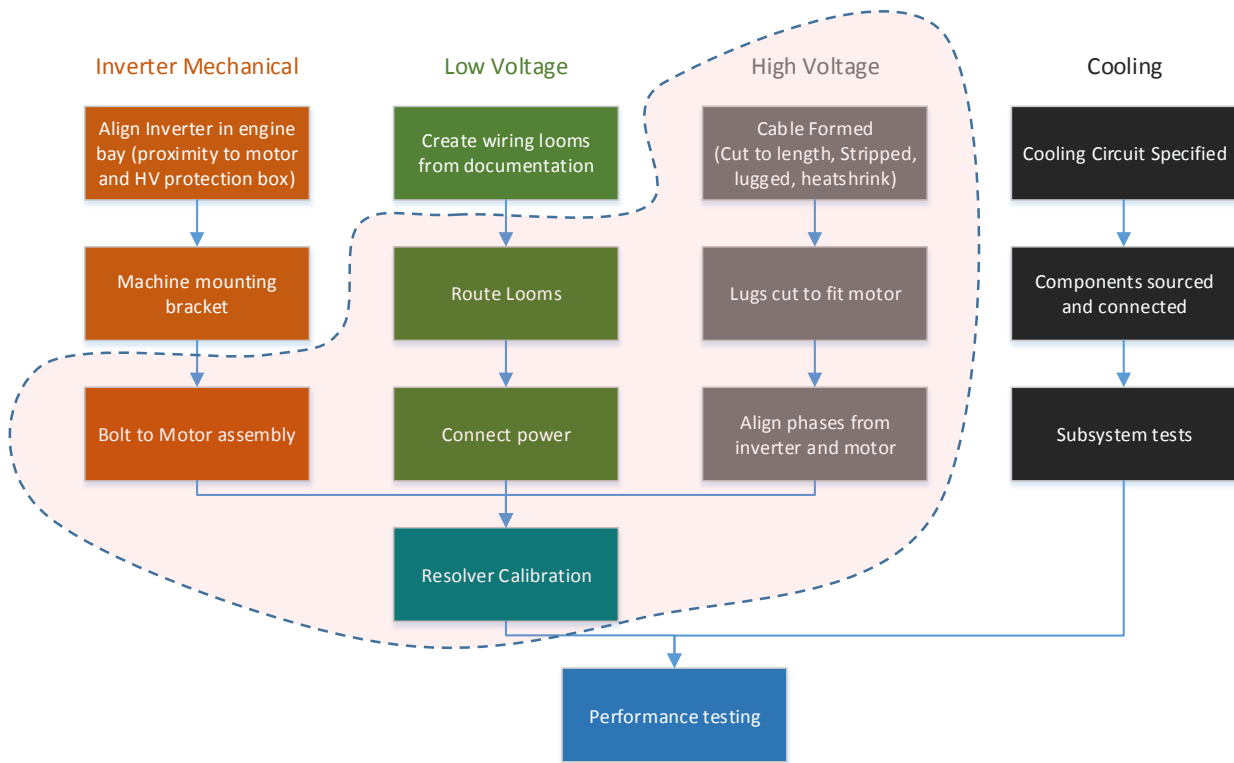


Figure 65 Inverter subsystems

4.3.2.1 Interfacing with Remy HVH 250-115 PO

The selected motor for the driving force of HiCEV is the Remy HVH 250-115PO. This three phase oil cooled motor utilizes a 5 rare earth magnetic pole pair rotor. The low voltage connection provides analog rotor position and internal temperature information to the inverter. Accurate rotor position information is required by the inverter DSP to implement effective switching.

4.3.2.2 Resolver

To effectively implement the output motor ac waveform, the inverter switching requires feedback in the form of the rotor position. Remy utilized the resolver as a position sensor which employs a coil which is supplied with a single frequency sin wave from an external source (the inverter). Another two coils are arranged to be 90 electrical degrees out of phases with one another (equivalent to Sine and Cosine) which is transmitted to the inverter decoding circuitry (arctangent function) to determine rotor position [42] the arrangement of which can be seen in figure 69. These connections are prone to cross talk due to the nature of induced waveforms and Remy claims to have implemented a strategy in the motor internals to reduce the effects. Thus, to maintain a high level of accuracy through faraday shielding of crosstalk on signal lines, twisted pair shielded cabling were utilized to connect between motor resolver and inverter. The way the twisted pairs were arranged is shown in figure 70 with the pinouts of each module on resolver end and inverter end, where the reference wiring diagram is shown in Appendix 7.3.

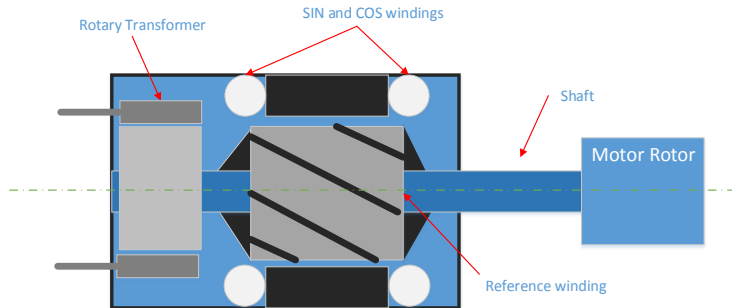


Figure 66 Example of brushless resolver

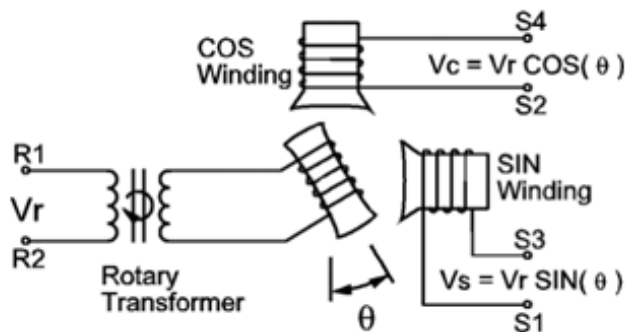


Figure 67 Electrical Circuit for rotary transformer resolver

It is assumed that a rotary transformer is utilized in the resolver to provide brushless operation, the concept is shown in figure 70.

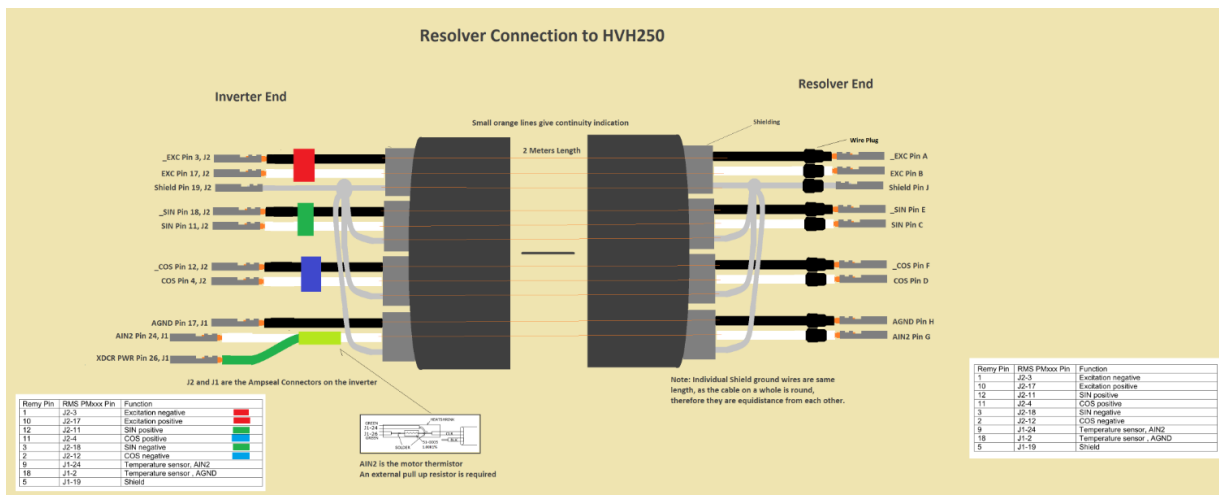


Figure 68Wiring from resolver to inverter

The calibration of the resolver is twofold; calibrate the inverter resolver delay from the resolver circuitry (Resolver Delay) and adjust the offset between resolver and magnetic field of the motor (Gamma Adjust). The aim of calibrating the resolver delay is to read the peak values of the SIN and COS position

waveforms, and thus maximizing the amplitude for the font end analog to digital converter to the DSP [45].

The inverter resolver calibration took place in-situ on the farm. At the time of calibration, the battery pack had not yet been placed in the vehicle and as such required an external aide to create rotation of the motor shaft. A tractor was utilized to tow HiCEV while the motor was mechanically connected to the drivetrain while parameters were read from the RMS GUI, shown in figure 72. The motor was allowed to spin at speeds up to 4000 RPM during testing, allowing a B-EMF to be generated in the region of 100Vac (based on a B-EMF co-efficient of $25.9 \text{ V}_{\text{rms, line-line}}/\text{krpm}$ [remy application manual]) on the HVAC connections to the inverter. The HVDC terminals were isolated during this calibration, a proportional voltage is generated across the terminals equivalent to $\text{V}_{\text{rms, line-line}} = 0.785 \cdot \text{V}_{\text{DC}}$ or 130Vdc. The parameter DC_UnderVolt_Thres_EEPROM was set to '0' in the RMS GUI to avoid the inverter producing an error code with not battery voltage present on the HVDC terminals during these calibrations.



Figure 69 Resolver Test Setup

Resolver Delay

The initial calibrate the resolver delay, the motor requires cogging-torque discrete increments of rotation. To achieve the smallest increment possible, the vehicle was placed into 2nd gear and pushed by hand while monitoring the RMS GUI. The maximum value of COS resolver waveform ($\text{Cos_corr(V)} \times 100$) was found at a resolver delay (Resolver_Delay_Command) of 900 which was then programmed into non-volatile memory (Resolver_PWM_Delay_EEPROM_(Counts)).

Resolver Direction

Direction of the resolver was verified to ensure that the resolver feedback correctly conveyed forward motion of the vehicle. Rolling the vehicle forward increases *electrical* angle of the motor (Gamma_Resolver_DEG_x_10) from 0 to 3600 then reset to 0 in the forward direction. Additionally, feedback speed parameter (Feedback_Speed_(RPM)) indicates a positive value in forwards direction and negative in reverse.

Physical wiring of motor phase connections also affect the motor direction. To verify correct phase connections, motor B-EMF is observed by the inverter at a speed of 4000 RPM ($\text{V}_{\text{BEMF}} = 100\text{V}_{\text{rms, line-line}}$) where polarity of the voltage feedback speed from the B-EMF matches the direction of the resolver.

Gamma Adjust

Due to manufacturing tolerances, the resolver rotational position is not always in the same place or aligned with the motor magnetic field. Similarly to resolver direction calibration, a sufficient B-EMF (and thus motor speed) is required by the internal voltage sensors in the inverter to determine the alignment.

The angle between the B-EMF and the resolver (Delta_Resolver_In_Fil_(DEG)_x_10) is required to be a constant value of $\Theta_{\Delta} = 90 \pm 2^\circ$ (900 in the RMS GUI) when rotating in the forward direction. The difference between the current delta angle and 90° is used to alter the current calibration angle between resolver and motor BEMF (Gamma_Adjust_(Deg)_x_10). An increase in calibration angle gives a decrease in resolver angle, thus if the resolver angle is higher than desired ($\Theta_{\Delta} > 90^\circ$), the calibration angle is increased to converge on 90° .

$$\Theta_{\gamma+1} = \Theta_{\gamma} - (90 - \Theta_{\Delta})$$

Thus the new resolver

$$\Theta_{\Delta+1} = \Theta_{\Delta} - \Theta_{\gamma+1}$$

This is an iterative process to converge on $\Theta_{\Delta+1} = 90^\circ$ whereby the final calibration angle $\Theta_{\gamma+1}$ is programmed ($\Theta_{\gamma e} = \Theta_{\gamma+1}$) into the EEPROM (GAMMA_Adjust_EEPROM_(Deg)_x_10). This yielded a calibration angle of $\Theta_{\gamma e} = 109.4^\circ$ or similarly, GAMMA_Adjust_EEPROM_(Deg)_x_10 = 1094.

[4.3.2.3 HV Safety Circuit](#)

Health and safety must be at the forefront of design, eliminating hazards where possible and failing that- mitigation. There are two major consequence scenarios; economic damage to property and damage to people. High voltage is the most obvious risk associated with an electric vehicle, it is has the highest presence in operating or working on the vehicle in terms of exposure. High voltage is required for vehicle operation, thus mitigation techniques to reduce consequence have been employed. These are explored below:

1. Visual indicators of HV
 - a. Orange insulation is used primary possible
 - b. Orange conduit is used as a substitute where cabling of certain sizes are not readily available with orange insulation
 - c. Appropriate signage
2. Safety Electronics
 - a. Mandatory fusing on all HV circuits
 - b. HV rated relays and switches
 - i. Dual Pole Isolation
 - c. Sealed enclosures to eliminate exposed HV surfaces and connectors
 - d. HV sensors on the BMS and inverter
3. Proximity
 - a. Ensuring HV cabling lengths are kept short
 - b. The two HVDC poles from the battery pack are kept apart to reduce chance of shorting during common cable failure
 - c. Accessibility of HV electronics
 - d. *Cable guarding HV cables under the vehicle*

Safety Electronics

The main battery fuse specifications are shown in the

Battery Characteristics			Bussman Fuse			
Op Voltage (Vdc)	Resistance (mOhm)	Short Circuit Current (A)	K Factor	I^2t	$K^* I^2t (A.s^2)$	t (ms)
360	100	3500	0.61	149000	90890	7

The HV safety wiring schematic is shown below in figure 70, where the physical HV Battery saftey box is shown in figure 71.

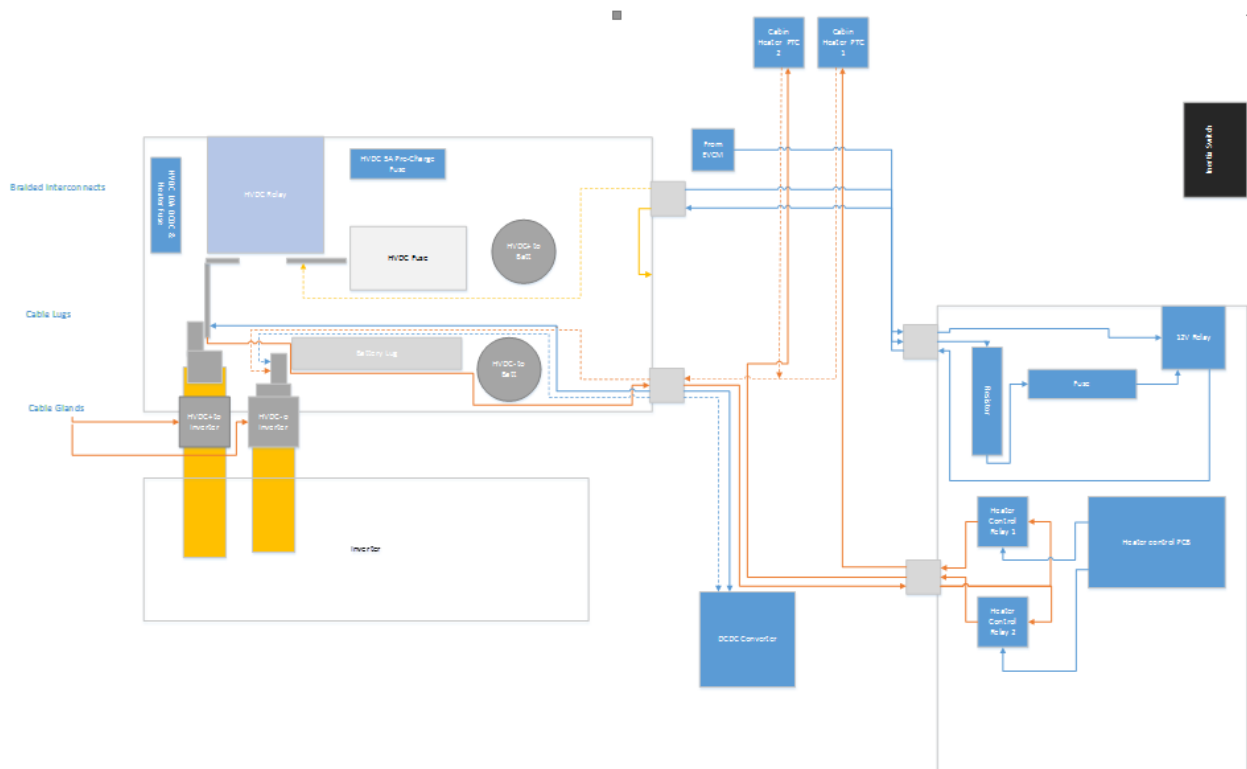


Figure 70 HV Safety Wiring

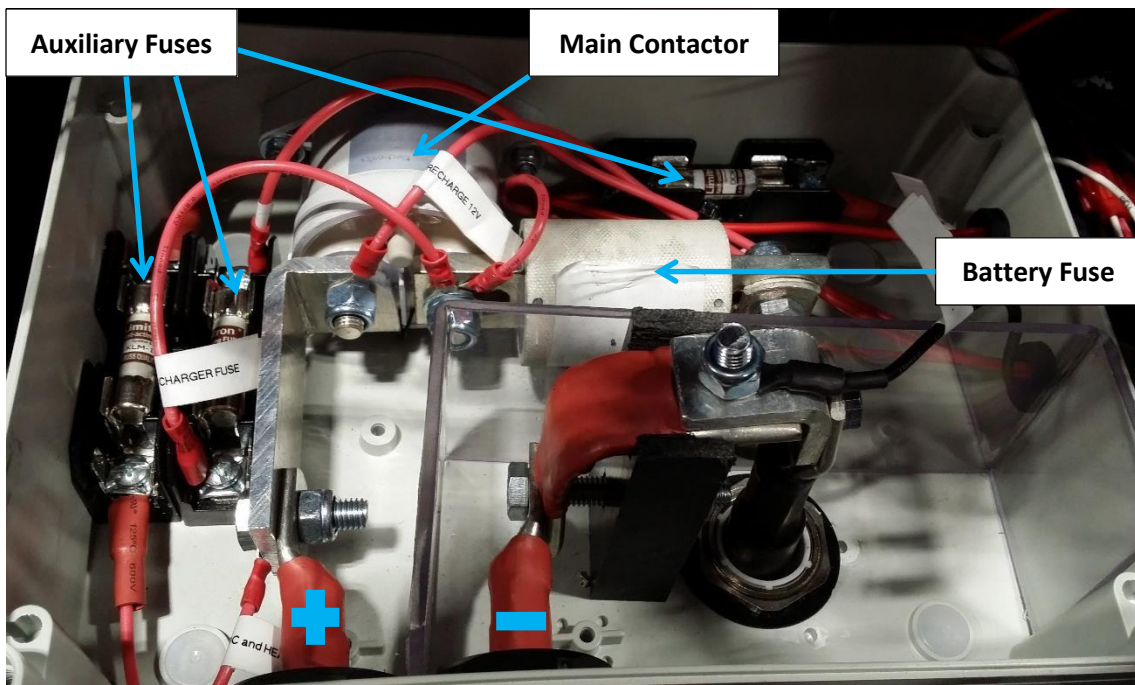


Figure 71 Physical HV Main Safety

The HV Safety Circuit consisted of the Pre-charge circuitry and the HV Main battery protection circuitry. The pre-charge circuit is shown below in figure 73 and the physical wiring the the safety elements in the HV circuit is shown in figure 74.

Pre-charge

Parameter	Value	Unit	Description
R	600	ohm	
C	500	uF	
taw	0.3	s	
#Constants	3	#	Number of constants
t	0.9	s	3 time constants
exp(-t/taw)	0.049787		
Vo	340	V	
V(t)	323.0724	V	
	95.02129	%	% of max voltage
Energy	26.09394	J	Energy in Cap
Q	0.161536	C	Charge
Fc	0.530516	Hz	Cut-off Freq

Figure 72 Pre-Charge component validation

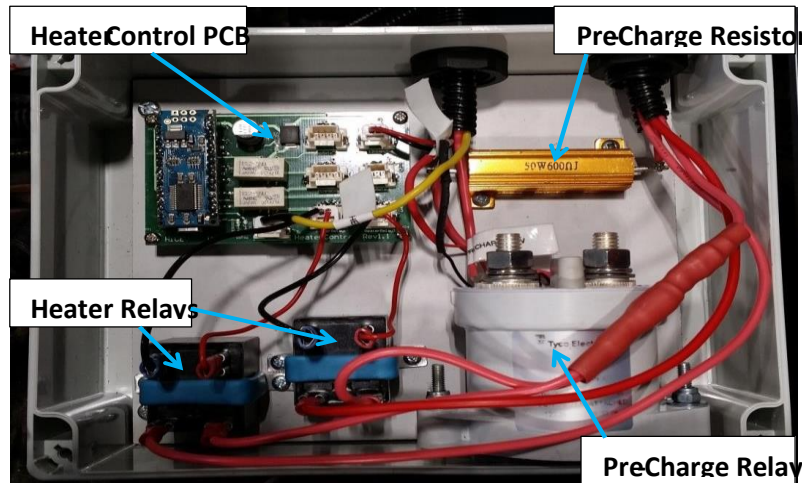


Figure 73Physical Pre-Charge Circuit

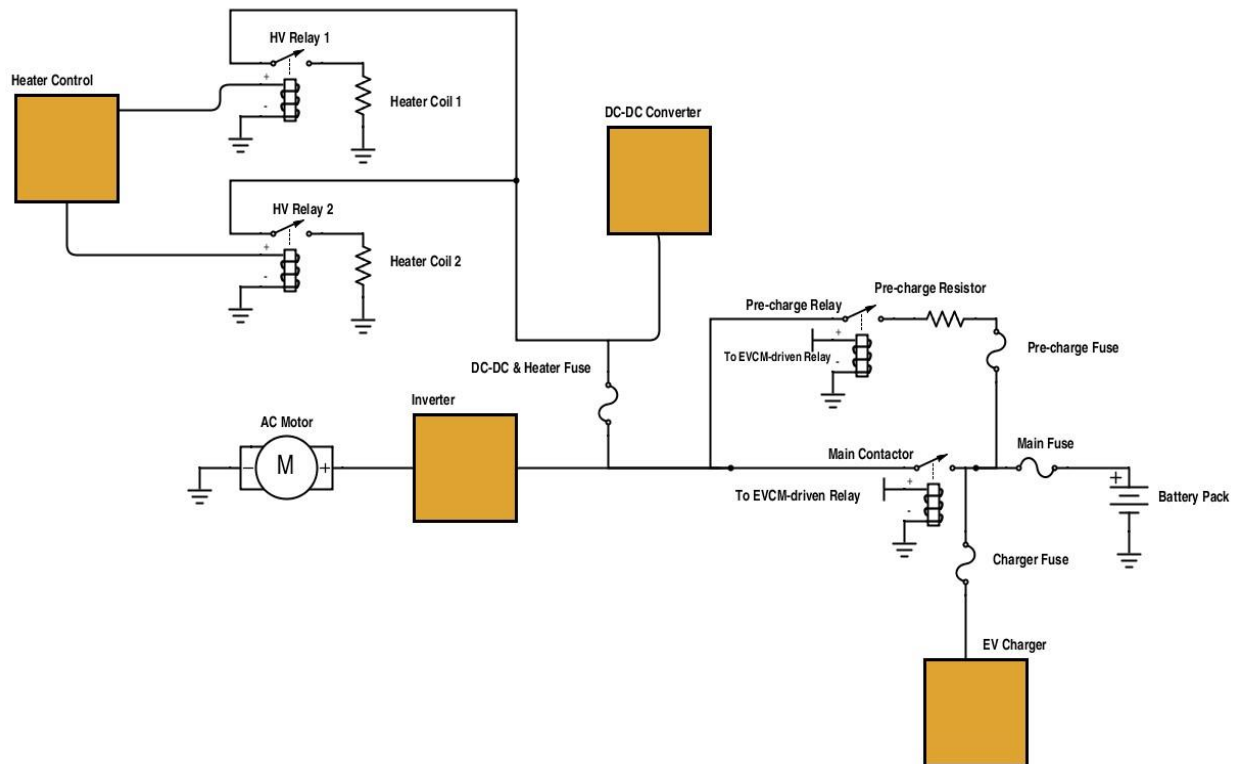


Figure 74MainBattery Saftey Circuit

HV AC Cabling

There are two main electrical aspects that are the forefront of considerations when sizing power cable: the ampacity (Ampere-Capacity) and the insulation rating. Ampacity refers to the magnitude of and RMS current a conductor in a cable can carry before incurring damage to the insulator [46]. Dependencies on ampacity include:

- Insulation temperature rating
- Electrical resistance of conductor
- AC Frequency
- Thermal conductivity of insulation
- Ambient temperature
- Humidity

Insulation ratings refers to both electrical and environmental ratings such as;

- Dielectric breakdown
- Resistance to corrosive substances
- Ozone resistance
- Weathering resistance
- Flame retardant

As a result, 95mm² Radox screened battery cable was sourced for the inverter connections which has the following properties:

Parameter	Value	Unit
Voltage Rating	600	Vac
Temperature Rating	-55 to 150	°C
Conductor cross section	95	mm ²
Ampacity	200A at 75°C	[47]
Conductor - ISO 6722		
Conductor - DIN EN 13602		
General – ISO 6722 class D, thin wall (Appendix 7.6)		
General – LV216		

Figure 75 HV Cable Specifications

Where Appendix 7.6 gives the specifications for ISO 6722 Class D, which covers thermal capacities, exposure to weathering and common automotive fluids [48]

With regards to the electrical specifications, the insulation needs to not undergo dielectric breakdown from the carrying voltage. If this is adhered to, the current carrying capability of the wire (ampacity) should be as large as possible to reduce the voltage drop per unit length along the cable. The ampacity of the cable is essentially related to the diameter of the power carrying core and the material (usually copper or aluminum). The diameter of the cable should be as large as possible to reduce the resistance and thus heat dissipation per unit length of the cable, but there may be constraints such as; maximum cable gland OD fittings on the HV modules, bend radius for space between modules or cost.

The Meger test results conducted by the undergraduate students are given below in table , showing cable insulation is in working condition.

Cable Section	Insulation Resistance
Battery to Protection DC+	>1000MΩ
Battery to Protection DC-	>1000MΩ
Protection to Inverter DC+	>1000MΩ
Protection to Inverter DC-	>1000MΩ
Inverter to Motor A	>1000MΩ
Inverter to Motor B	>1000MΩ
Inverter to Motor C	>1000MΩ

Figure 76 Meger test results on HV Cable

In figure 68 below is the megger test completed by each cable and the HV Motor leads that had to have



Figure 77HV Cable meger tests and Motor Connections

modifications to the lugs to fit on the motor connections.

Figure diagram expands on the physical HV diagrams above and shows the HV routing though to the battery boxes also.

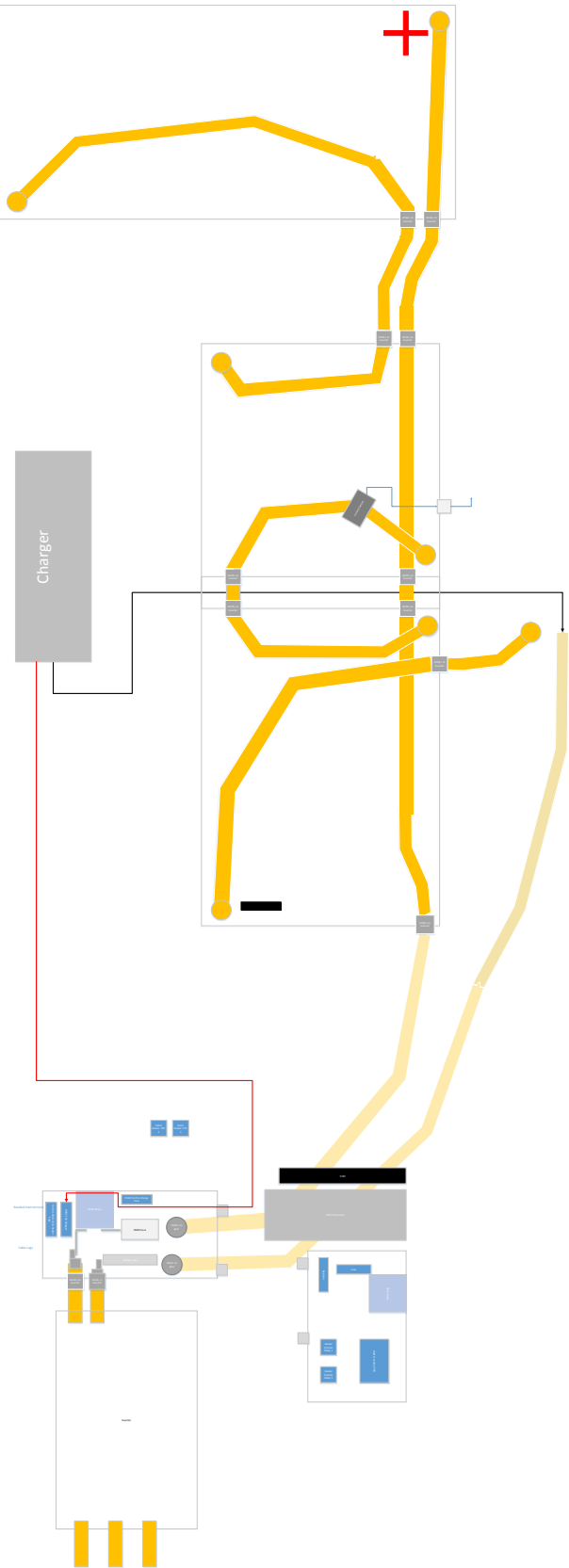


Figure 78 HV Battery cable wiring

4.3.3 CANbus

CANbus was created from twisted pair cable with grounds of each module all connected via the shielding to provide a common reference ground for all transceivers.

4.3.3.1 CANbus Database

A database of CAN messages was compiled for HiCEV and is shown below in table 17:

Message ID		DLC	Speed	Origin	Destination	Endian	Definitions	Timeout Threshold
Hex	Dec	(ms)						Sec (= Tx speed x 2)
A0	160	8	100	Inverter	VCM	Little	Temperatures #1 - IGBT's, Gate driver	0.2
A1	161	8	100	Inverter	VCM	Little	Temperatures #2 - Control Board, RTD's	0.2
A2	162	8	100	Inverter	VCM	Little	Temperatures #3 RTDS, Motor / Torque Shudder	0.2
A3	163	8	10	Inverter	VCM	Little	Analog Input Voltages	0.02
A4	164	8	10	Inverter	VCM	Little	Digital Input Status	0.02
A5	165	8	10	Inverter	VCM	Little	Motor Position Information	0.02
A6	166	8	10	Inverter	VCM	Little	HV Voltage information	0.02
A7	167	8	10	Inverter	VCM	Little	Flux Information (Control and feedback)	0.02
A8	168	8	10	Inverter	VCM	Little	Internal Reference Voltages	0.02
A9	169	8	100	Inverter	VCM	Little	Internal States	0.2
AA	170	8	100	Inverter	VCM	Little	Fault Codes	0.2
AB	171	8	10	Inverter	VCM	Little		0.02
AC	172	8	10	Inverter	VCM	Little	Torque and Timer Information	0.02

							Modulation Index / Flux Weakening	
AD	173	8	10	Inverter	VCM	Little	Output	0.02
AE	174	8	100	Inverter	VCM	Little	Firmware Information	0.2
AF	175						Diagnostic Data	
							Command Message: Inverter Lockout	
C0	192	8	20	VCM	Inverter	Little	Enable	0.04
							Write/Read a Parameter (Byte 2 = 1/0 respectively)	
C1	193			PC	Inverter			
							Response message from this	
C2	194			Inverter	PC			
101	257	8	45	BMS	VCM	Big		0.09
102	258	8	45	BMS	VCM	Big		0.09
103	259	6	20	BMS	VCM	Big		0.04
104	260	8	450	BMS	VCM	Big		0.9
106	262	1	90	BMS	VCM	Big		0.18

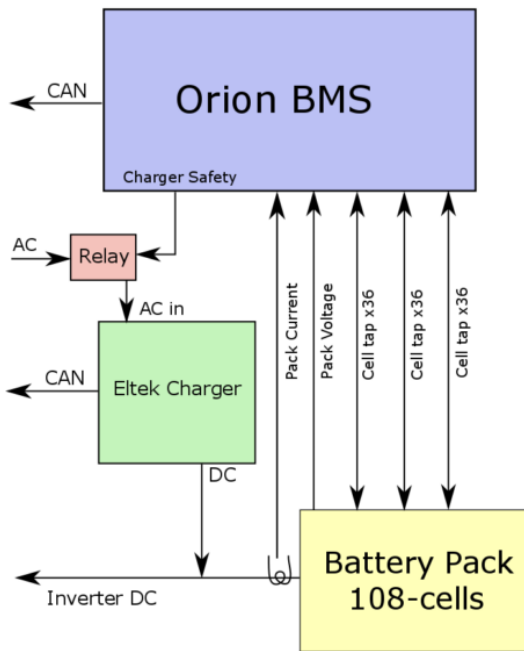
Table 17 CANbus Message Database

4.3.4 Battery Pack

The battery pack state of charge was unknown before putting it in the vehicle, as the cells hold a constant voltage over 80% of the operating region. Tests were conducted to test charger and BMS would charge the batteries before were placed in the vehicle.

BMS

The test layout was such that, a resistive load was put across the bank while monitoring the current manually by means of current clamps to compare against the BMS readout



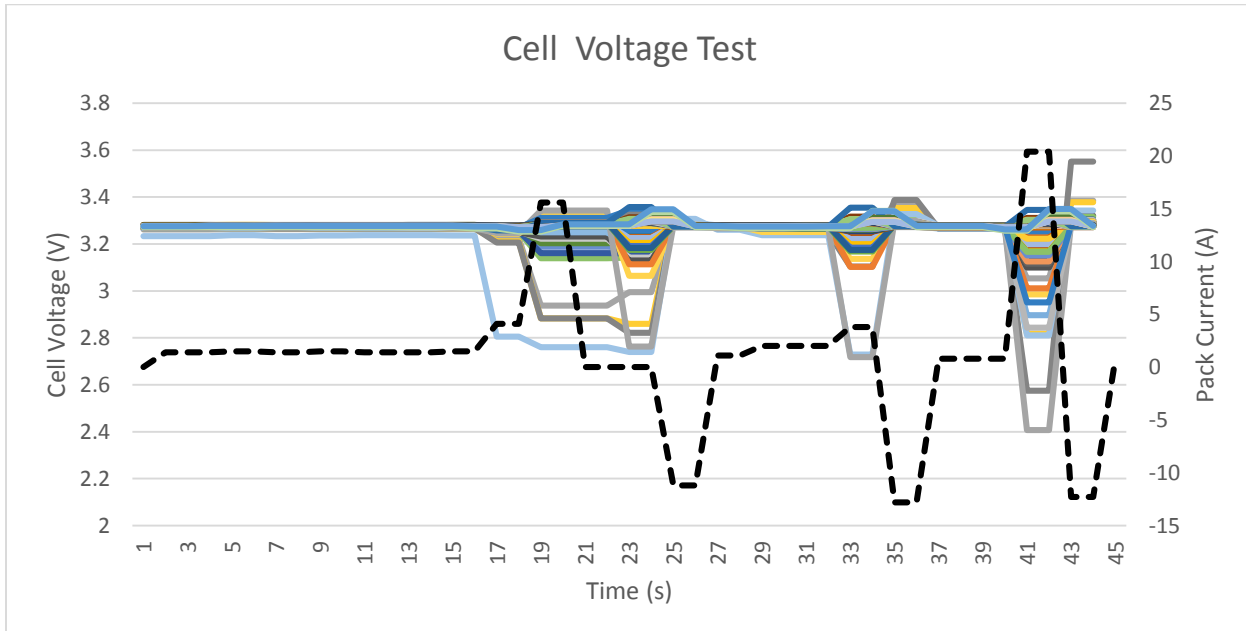
Batteries

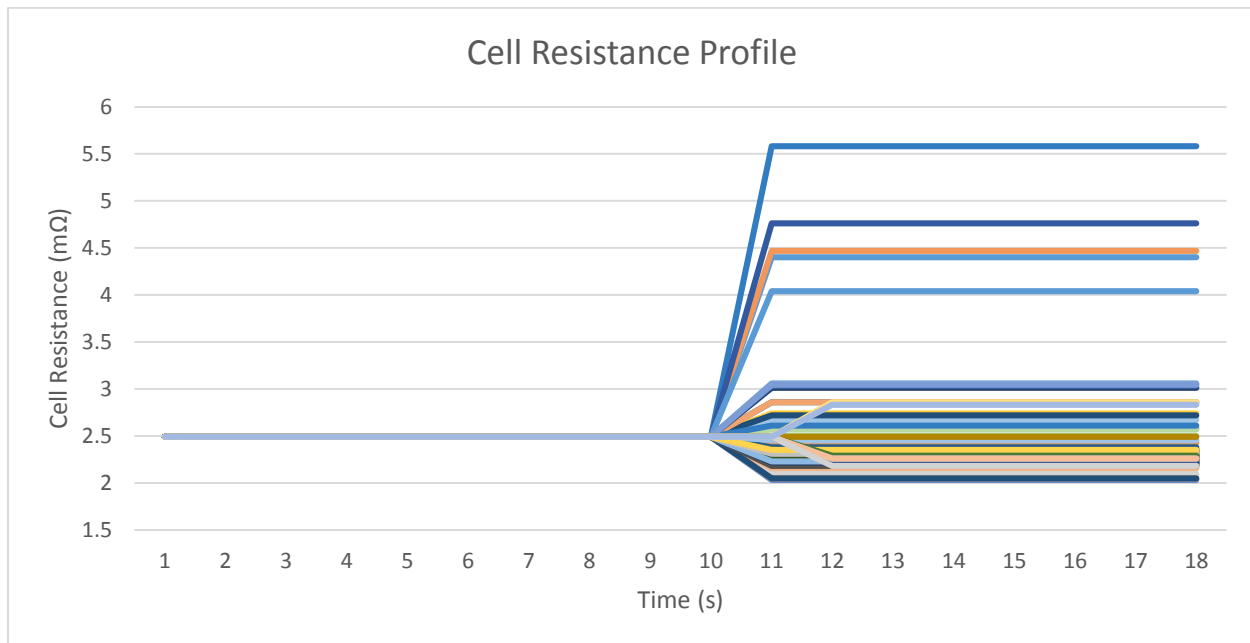
The battery pack consists of sections; batteries, enclosure and layout, connectors and BMS connections. Prototype specifying outlined the chosen battery pack as 108 Winston 100Ahr Lithium Ion batteries, and the enclosure as a 3mm aluminum box with detachable lid. Before the batteries were placed in the vehicle, since accessibility in and out of the vehicle is limited (about a day long process to remove the battery batteries, cabling and the enclosure) testing to ensure the BMS and charger interfaced correctly to both charge and monitor the batteries effectively was crucial.



4.3.4.1 Initial BMS Setup

The initial BMS tap connections were loose and resulted in the variations in voltage and resistance as shown below in the voltage test and the corresponding resistance profile spread. Tightening the taps would usually bring the resistance down to the $15\text{m}\Omega$ operating region.





4.3.5 Vehicle Analysis

Two drive scenarios were explored with the aim of proving that retaining the gearbox has performance benefits over a directly coupled shaft. The gear selected to conduct the comparison was third, where either Fourth or third gear could have been selected to simulate the directly coupled drive due to the ease of changing the rear differential ratio. The speedometer was out of service so a GPS system was utilized to indicate that the vehicle was traveling 100 km/hr. at which point the accelerator was abruptly released to indicate the target had been met (current tends to 0).

To allow for a valid comparison between the two drive scenarios, the following tests were conducted with the following conditions:

- The same driver used in both tests
- A common starting position
- Relatively even surface tar seal that was safe to use
- On the same day (Same weather conditions)
- Rear-wheel driven (not in 4WD)
- 100% Accelerator input

The rate increase of current is limited by the EVCM to 100 As^{-1} during testing. The directly coupled

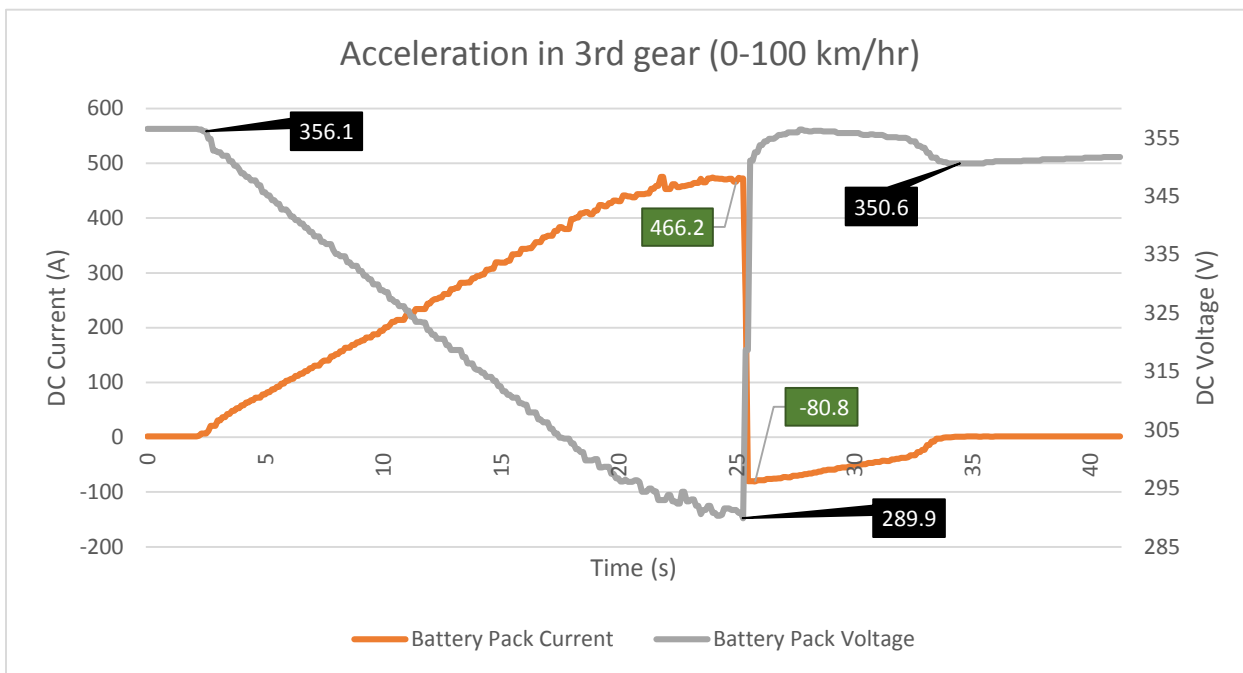


Figure 79 Acceleration in 3rd gear (EVCM)

simulation is shown in figure 78 where 100 km/hr is reached in ~ 23 seconds (25-2).

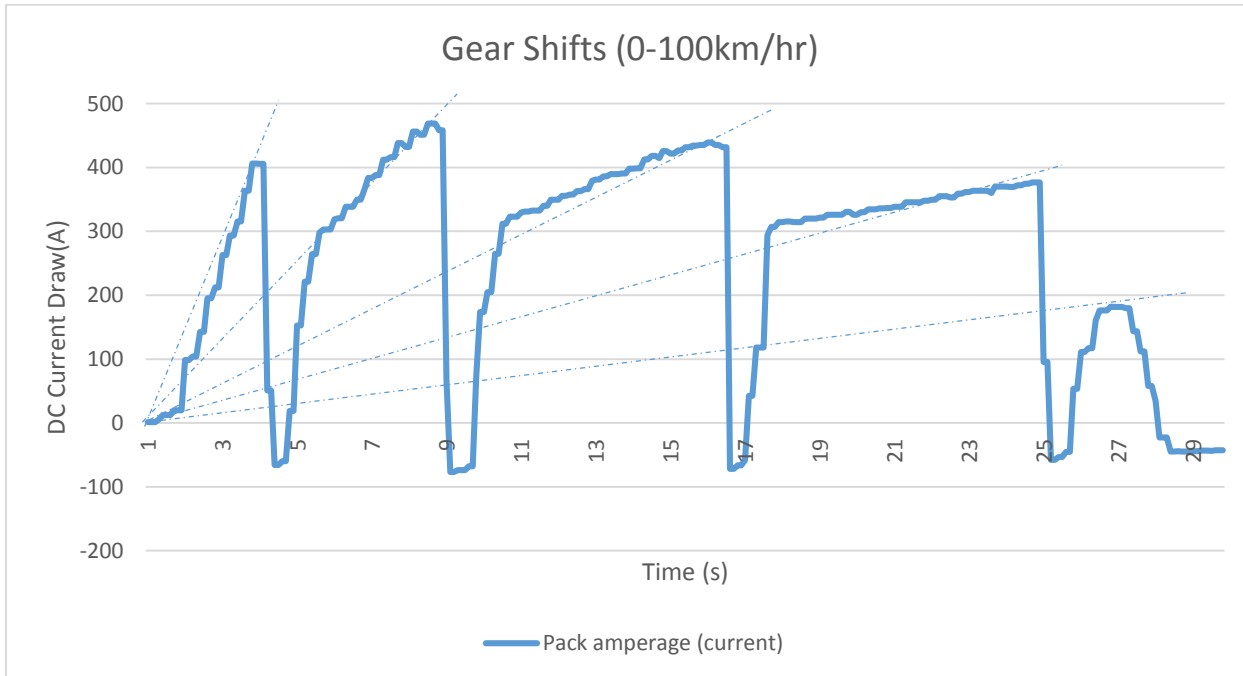


Figure 80 Gear Shifts 0-100

Shifting gears in the above figure 79 takes between 1.4-1.7 seconds, which gives approximately 6 seconds lost to shifting. Accelerating stopped at 25 seconds at the end of 4th gear, which is 2 seconds slower than fixed gear. Although the gear shifting is slower getting to 100 km/hr, the torques that are able to be developed with the low gearing allow the gear shifting scenario to attain 435A in 3rd gear 3 seconds faster than the fixed gear. Reducing the time from 0-100 km/hr could be done by implementing the clutch switch so regenerative braking doesn't occur during shifting, relaxing the thresholds of rate limiting on the battery current, reducing vehicle weight from the deck boards, a bash panel lining the engine bay to decrease the drag force, decreasing the shifting times, shifting to third and staying there or putting the vehicle in 4WD to reduce slip. Implementing the above changes, will increase the likelihood of attaining the <12s to accelerate from 0-60mph performance standard.

Additional energy and power information can be taken from figure 78 Peak power draw is ~135kW and uses 1.6MJ of energy (1.3% of SOC) ($J=(V_{av} * I_{av}/2)*22$) $V_{av} * I_{av} = 75\text{kW}$. The current regenerative breaking settings ~6% energy was recaptured (~100kj = $356\text{Vdc} * 40\text{A} * 7\text{sec}$).

The total dc system resistance is (@point 18) ($R_{tot} = 356-300/400 = 140\text{m}\Omega = \sim 1.25\text{m}\Omega$ per cell)

Towing a tractor simulated towing a 2 tonne trailer, which is standard for the work vehicles. To tow the Tractor at 10 km/hr in first gear, the battery current required is 50A_{dc} which gives a required power of 17.650 kW which gives an average operation time of approximately 2 hours. Switching to second gear at 25 second point reduces the current draw to 40A and thus an average power draw to 14kW or a 2.5 hour run time. An assumption made in these summary calculations is zero road grade, which will significantly effect the power draw and thus run time.

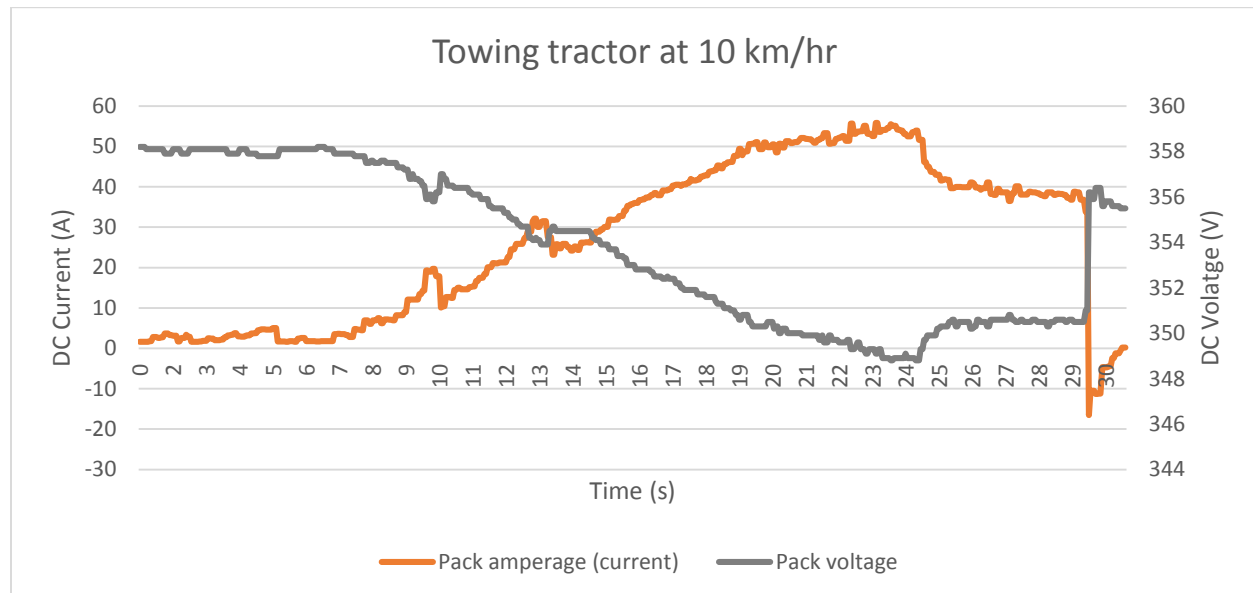


Figure 81 Towing tractor at 10km/hr

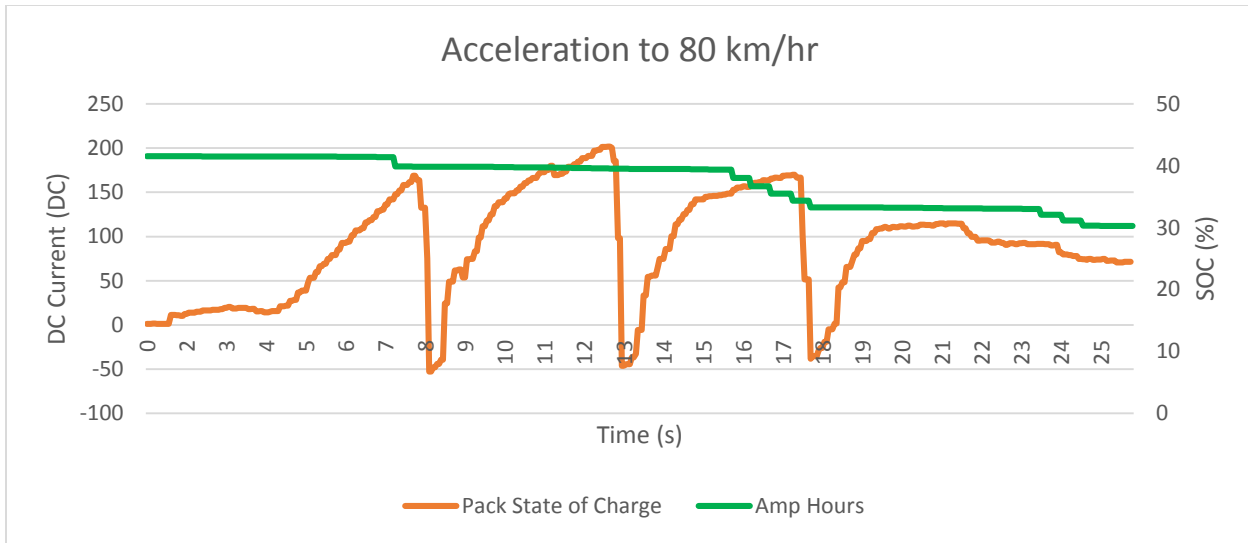


Figure 82 Acceleration to 80km/hr

The above figure 81 shows a total loss of 11% SOC over a 21 second acceleration. $V_{av} = 345V_{dc}$

	Voltage dc,av (V)	Current $dc, average$ (A)	Time (s)	Energy(kJ)
1 st gear	345	80	5	138
2 nd gear	345	100	4.5	155
3 rd gear	345	100	4	138
4 th gear	345	100	6.5	224
Total				655

Table 18 Energy consumed through different gears

Which yields a decrease in SOC in the order of 0.5% from table 18, therefore is being misinterpreted by a factor of 20.

4.3.6 Cooling

The temperature for the inverter and motor require constant monitoring to ensure safe operating regions are always being operated in. The upper threshold temperatures for these two components are 160°C and 105°C for the motor and inverter respectively. Thermal limitations are put in place to limit current to zero at 140°C and 80°C for the motor and inverter respectively should the liquid cooling loops be insufficient or fail. An example of the temperature reached from the inverter and motor combination over a short, but intensive discharge current (480A) below in figure 82. The figure shows the motor has a higher thermal inertia than the inverter, thus takes longer to respond to changes in temperature. This can be depicted both in the initial spike in inverter module 'D' temperature from 28 to 39°C (over 28 seconds and a decrease from 48.6 to 40.7°C (change of 8°C) in 18 seconds.

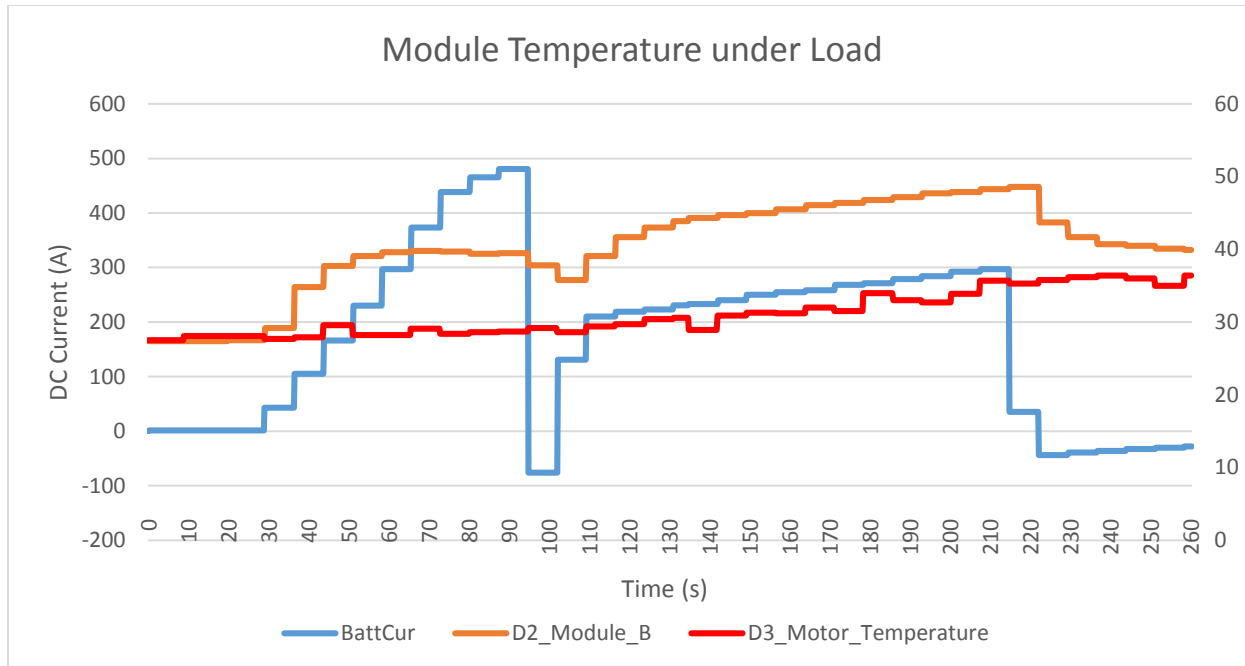


Figure 83 Inverter and motor Thermal profile

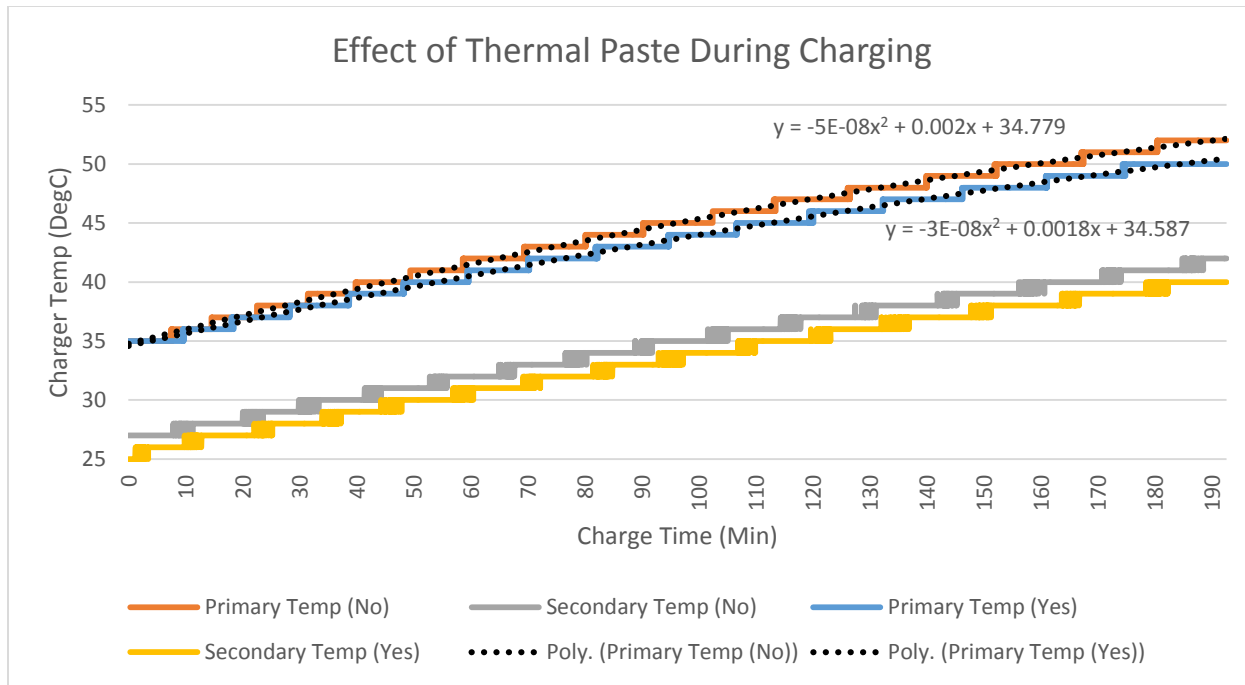


Figure 84 Thermal paste effects on charger

During charging, the Eltek charger dissipates a maximum of 220W of heat. Figure 83 shows that the thermal paste reduces heat conduction away from the charger at higher temperatures by 2°C approximately 50°C operating temperature on the primary sensor.

5.0 Discussion

This project covered many different aspects of engineering, project, electrical and mechanical. The vehicle is now in a state where it can be driven and tested.

5.1 Issues Faced

All major components except the DCDC converter were sourced from different countries. The support was less than favorable when issues with components arose, and it is difficult or impossible to remedy a solution if communications fail. Two companies that were used to source components from gave wrong specifications and sent wrong products, contributing to massive delays in commissioning. A 3 month delay occurred when the wrong batteries were sent, which left the team waiting for the right set to be sent.

Documentation for the EVCM also fell short as to what was expected –wiring the EVCM was on hold for months as no wiring diagram was supplied with the module, step through initiation documents to setup parameters once in MotoTune or reference documentation for the hundreds of variables in MotoTune. Contact was finally made with the company months after issues were raised.

Although these issues were significant hurdles, it gave insight into detailing crucial project elements regarding. The issue with documentation should have been sorted before purchasing took place. Diligence is paramount when dealing with companies based in other countries – as the inclination to have good customer rapport seems to be less than when both parties are on the same continent.

5.2 Future for HiCEV

HiCEV requires refining and general tidying of systems. The project is currently at a phase where the systems can be tested safely as cooling is being used and lubrication in the motor bearings.

The aim for the undergraduate student project this year is twofold; certification of the vehicle to meet the LVVTA standards and refining of vehicle system performance.

6.0 Conclusion

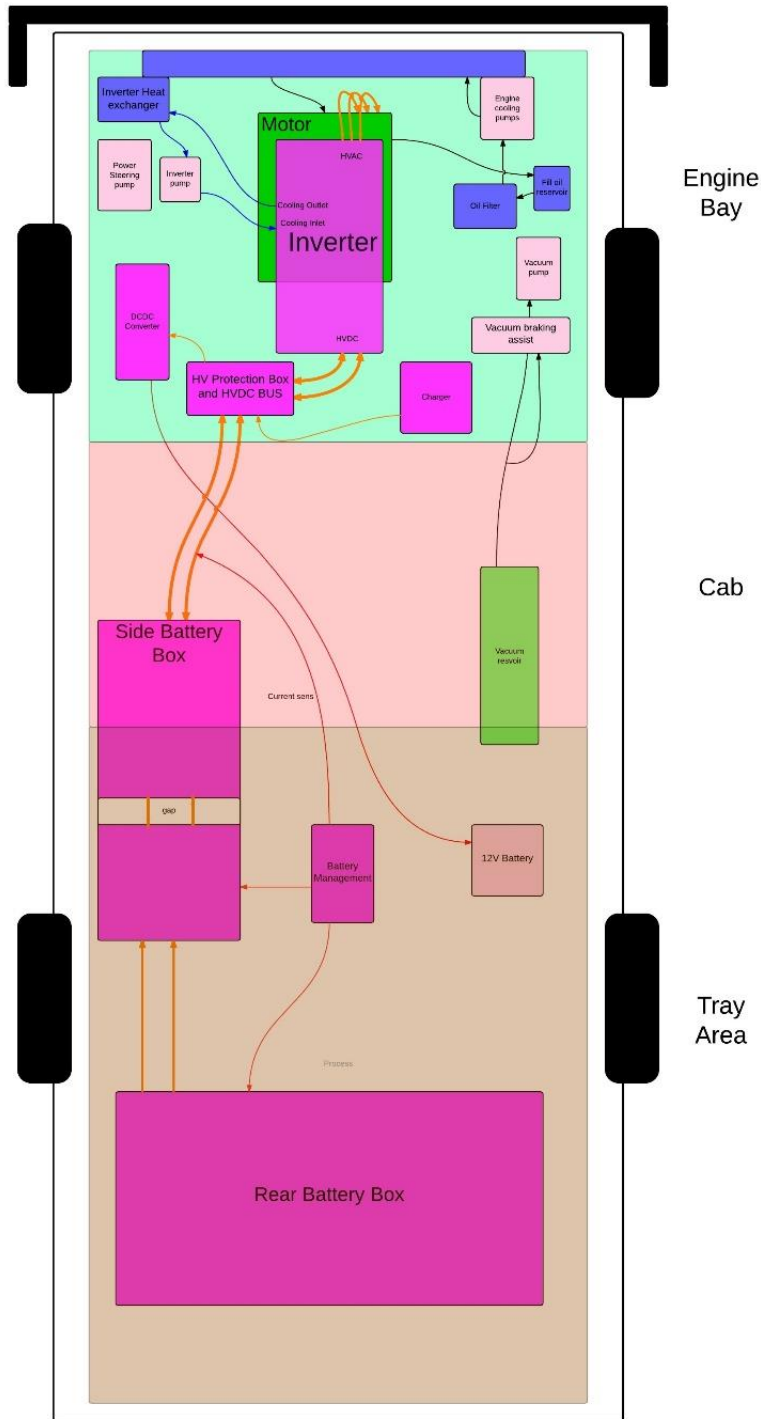
The aim of this project was to design and prototype a high country electric vehicle (HiCEV) for farming applications. HiCEV was the result of a farmers desire to reduce his farms dependency on fossil fuels and to promote electric vehicles in the agricultural sector of NZ.

The prototype specification design converged on the solution of a single electric motor, coupled to the pre-existing manual gearbox. The core of this build is a robust IPM motor driven by a FOC inverter and EVCM controller.

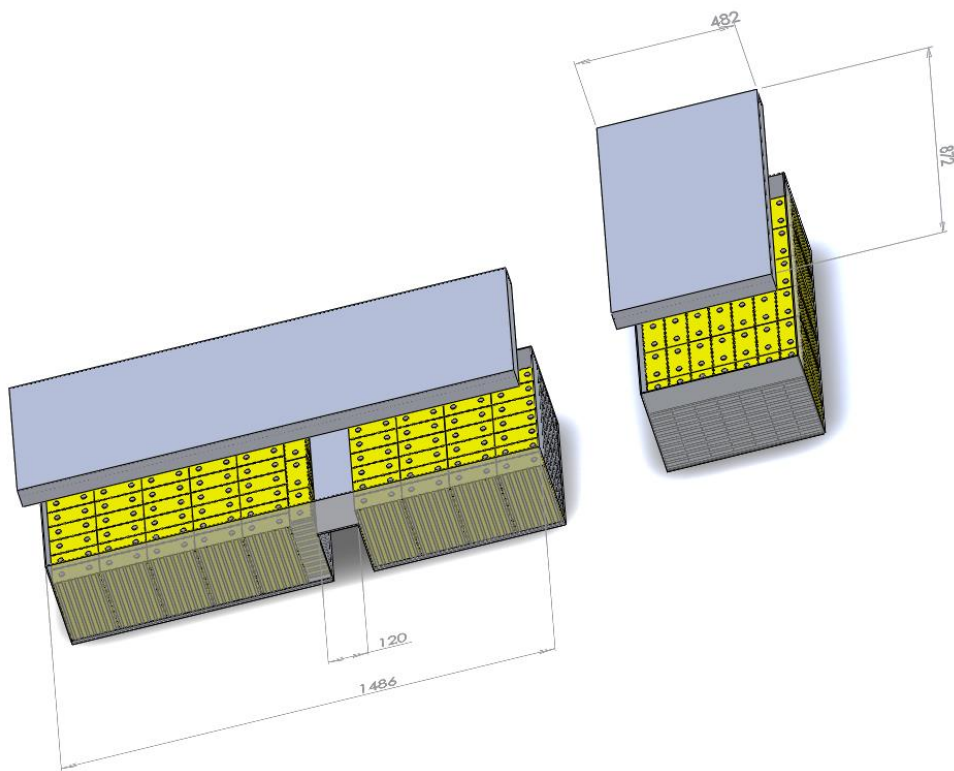
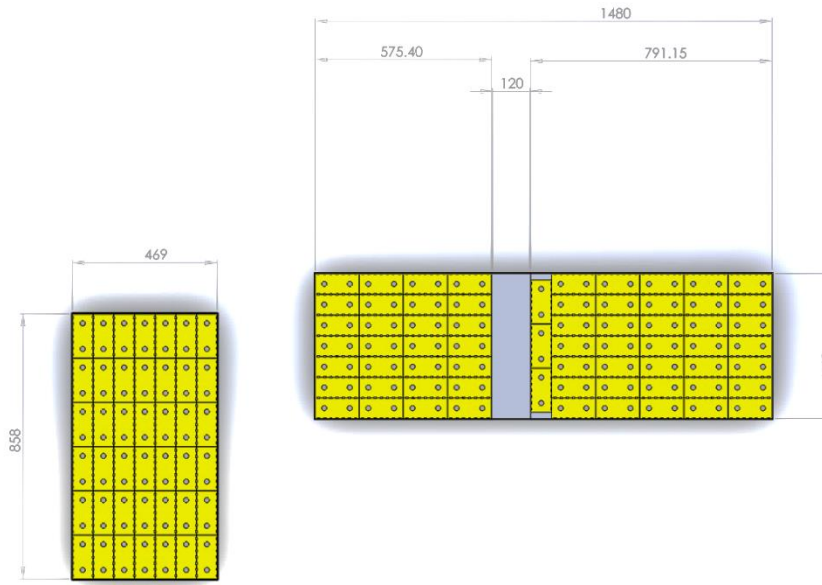
Development of the prototype has reached the state where commissioning main systems of motor, inverter and battery management has been completed and performance testing is starting to commence. Further work will be in finishing the subsystems integration, programming the EVCM performance parameters and aiming for certification of the vehicle by the end of the year.

7.0 Appendix

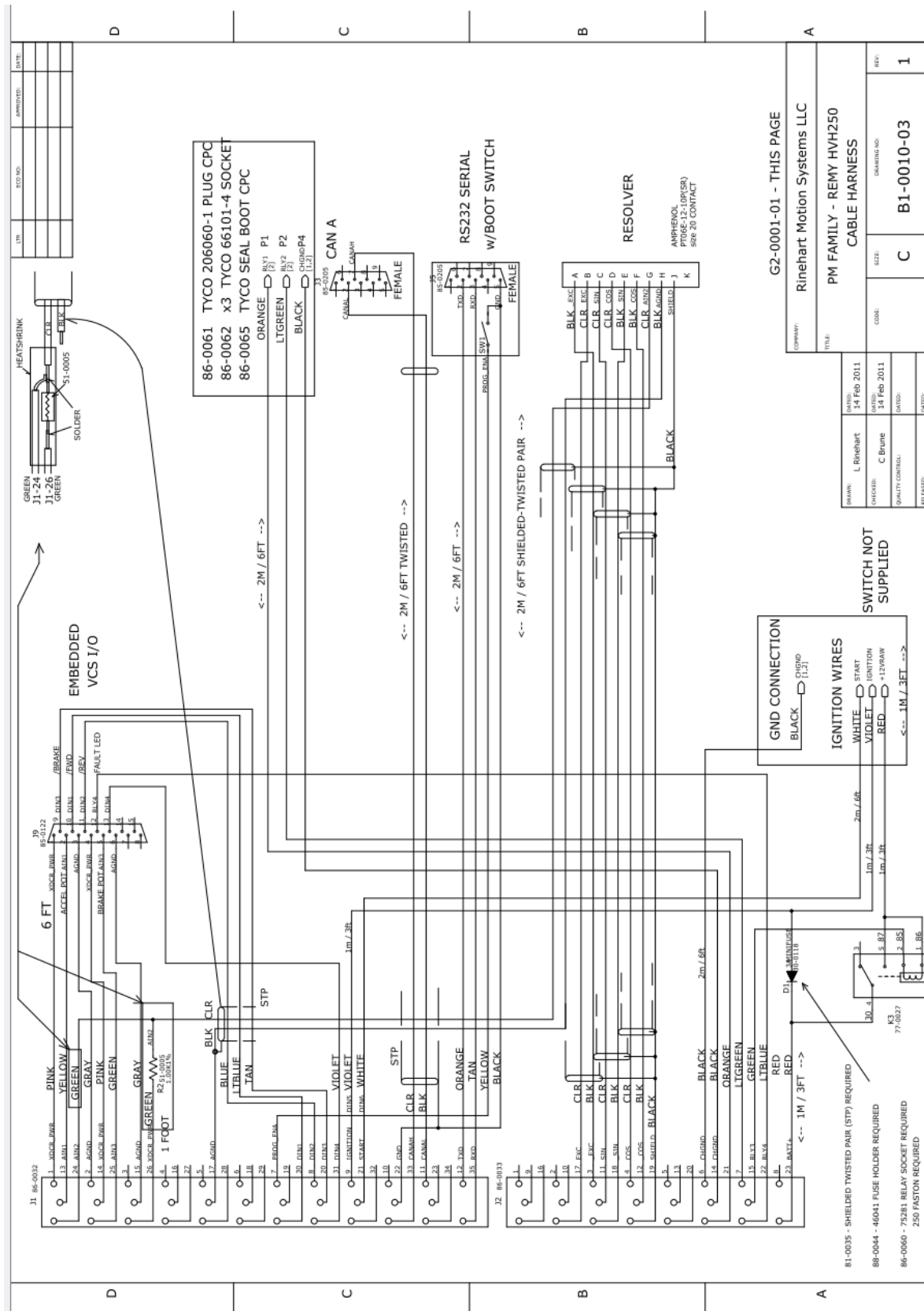
7.1 Birds eye view of component layout



7.2 CAD model of battery boxes



7.3 Rinehart Wiring Diagram



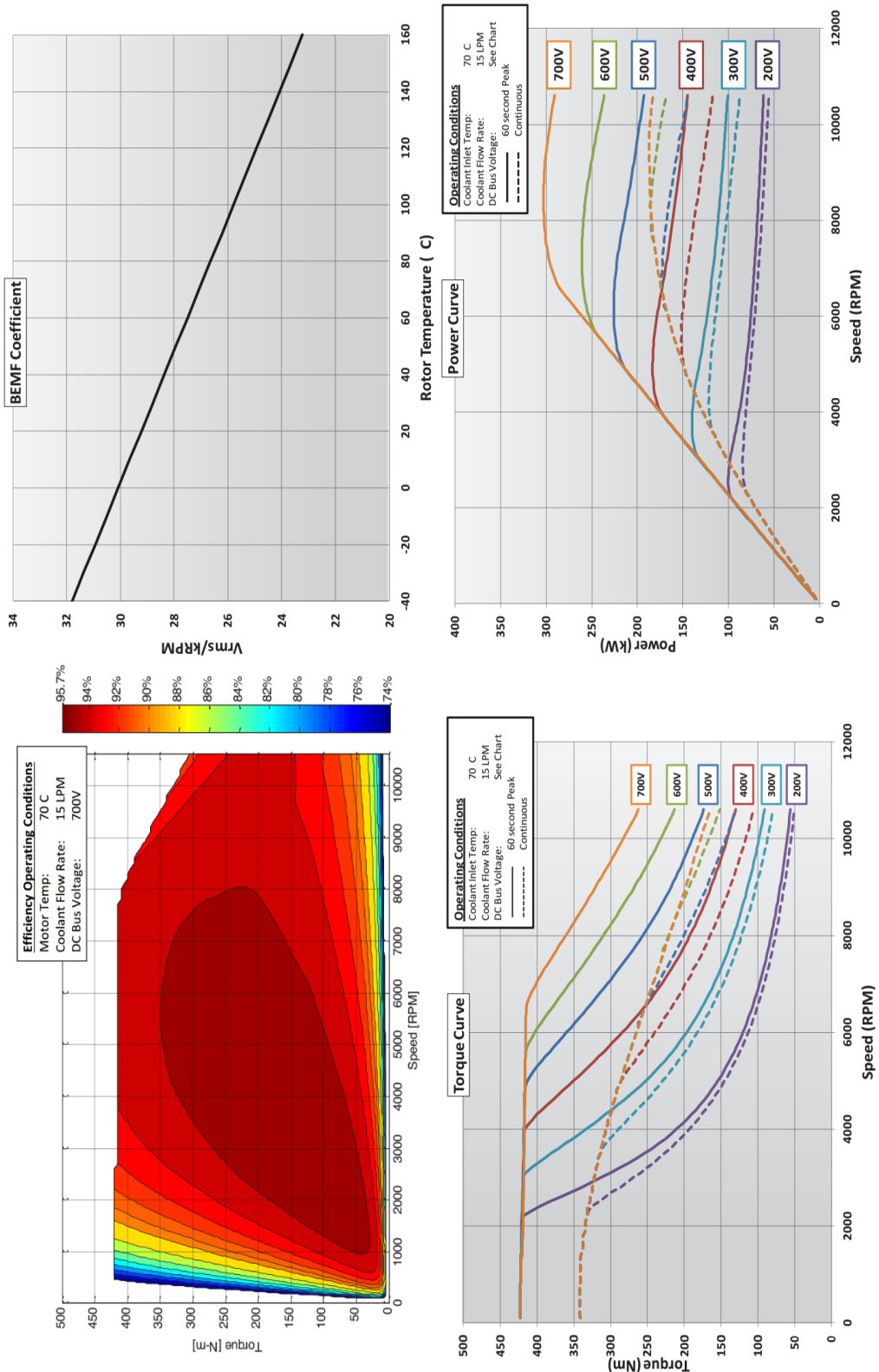
7.4 Inverter Loom Mapping

Origin	Header	Connector Type	Pin #	Pin Name	Description	Destination Component	End Pin #	Cable size (AWG)	Cable Description	Est. Length (m)	Used
Inverter	J1	770854-1	1	XDCR_PWR	+5V @ 80mA max						No
			13	AIN1	Analog Input 1 0-5VFS, Accelerator						No
			24	AIN2	Analog Input 2 0-5VFS	Motor Resolver Header, Temp Sens	G	16-20	Multi Core Shielded	1.5	Yes
			2	AGND	Analog Ground	Motor Resolver Header, ANGD	H	16-20	Multi Core Shielded	1.5	Yes
			14	XDCR_PWR	+5V @ 80mA max						No
			25	AIN3	Analog Input 3 0-5VFS, Brake						No
			3	AIN4	Analog Input 4 0-5VFS, Not assigned						No
			15	AGND	Analog Ground						No
			26	XDCR_PWR	+5V @ 80mA max	Inverter, AIN2 (resolver connection), w Resistor	--	16-20	Multi Core Shielded	1.5	Yes
			4	AOUT	Analog Output (0 - 5V)						No
			16	AIN6	Analog Input 6 0-5VFS						No
			27	RLY6	High-side Relay Driver						No
			5	RTD1	PT100 or PT1000 RTD						No
			17	AGND	Analog Ground						No
			28	XDCR_PWR	5V @80mA max						No
			6	RTD2	PT100 or PT1000 RTD						No
			18	AIN5	Analog Input 6 0-5VFS						No
			29	RLY5	High-side Relay Driver						No
			7	/PROG_ENA	Serial Boot Loader enable	PROGRAMMING, DB9,RS232	5	16-20	Yellow, single core	2	yes
			19	AGND	Analog Ground						No
			30	DIN1	Digital Input 1 – STG(1)						No
			8	DIN2	Digital Input 2 – STG						No
			20	DIN3	Digital Input 3 – STG						No
			31	DIN4	Digital Input 4 – STG						No
			9	DIN5	Digital Input 5 – STB(2)						No
			21	DIN6	Digital Input 6 – STB						No
			32	DIN7	Digital Input 7 – STB						No
			10	DIN8	Digital Input 8 – STB						No

		22	GND	Ground	PROGRAMMING, DB9,RS232 CANA Shield	5	16-20	Black (green), single core	2	yes
		33	CANA_H	CAN Channel A Hi	J3, DB9	7	16-20	Shielded, Twisted Pair	0.3	yes
		11	CANA_L	CAN Channel A Low	J3, DB10	2	16-20	Shielded, Twisted Pair	0.3	yes
		23	CANB_H	CAN Channel B Hi						No
		34	CANB_L	CAN Channel B Low RS-232 Transmit						No
		12	TXD	RS-232 Receive	PROGRAMMING, DB9,RS232	2	16-20	Orange, Single core, multi strand	2	Yes
		35	RXD	RS-232 Transmit	PROGRAMMING, DB9,RS232	3	16-20	Tan, Single core, Multi strand	2	Yes
J2	770854-1	1	XDCR_PWR	+5V @ 80mA max 9						No
		9	ENCA	Encoder Channel A input						No
		16	ENCB	Encoder Channel B input						No
		2	ENCZ	Encoder Channel Z input (Index)						No
		10	GND	GND						No
		17	EXC	Resolver excitation output	Motor Resolver	B	16-20	Shielded, Twisted Pair, red collar	1.5	Yes
		3	EXC_RTN	EXC_RTN Resolver excitation return	Motor Resolver	A	16-20	Shielded, Twisted Pair, red collar	1.5	Yes
		11	SIN	Resolver Sine winding +	Motor Resolver	C	16-20	Shielded, Twisted Pair, green collar	1.5	Yes
		18	/SIN	Resolver Sine winding -	Motor Resolver	E	16-20	Shielded, Twisted Pair, green collar	1.5	Yes
		4	COS	Resolver Cosine winding +	Motor Resolver	D	16-20	Shielded, Twisted Pair, blue collar	1.5	Yes
		12	/COS	Resolver Cosine winding -	Motor Resolver	F	16-20	Shielded, Twisted Pair, blue collar	1.5	Yes
		19	SHIELD	Resolver Shield	Motor Resolver	J	16-20	Shielded, Twisted Pair, bare	1.5	Yes
		5	HALL_A	Hall Encoder Chan, A						No
		13	HALL_B	Hall Encoder Chan, B						No
		20	HALL_C	Hall Encoder Chan, C						No
		6	GND	Main 12V return	12V Return / Vehicle Chassis	GND	16-20	black, single strand	0.3	Yes
		14	GND	Main 12V return	Relay GND	GND	16-20	black, single strand	0.3	Yes
		21	RLY1	Hi-Side Relay Driver	Precharge relay driver	+	16-20	green, single strand	0.5	Yes
		7	RLY2	Hi-Side Relay Driver	Main Relay Drive	+	16-20	yellow, single strand	0.5	Yes
		15	RLY3	Lo-Side Relay Driver			16-20	blue, single strand	0.5	Yes

22	RLY4	Lo-Side Relay Driver		16-20	brown, single core		Yes
8	BATT+	Main 12V power source	12V Main PWR (batt), switched	Batt	16-20	Red, dual core	0.3
23	BATT+	Main 12V power source	12V Main PWR (batt), switched	Batt	16-20		0.3
23	CANB_H	CAN Channel B Hi			16-20		no

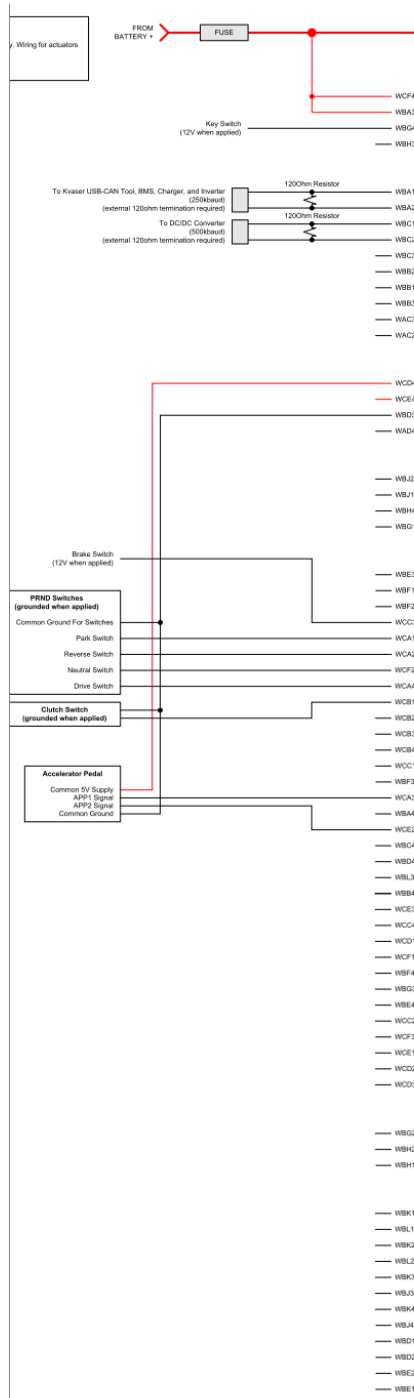
7.5 Motor Performance Diagrams



7.6 Class D Specifications

Section	Description	Requirement
5.7	Insulation Volume Resistivity	10 ⁹ Ω /mm min.
5.8	Pressure at High Temperature	'0.8N @150°C no dielectric breakdown
5.9	Strip Force / Adhesion	Per customer agreement
5.10	Low Temperature Winding	3 tns 2.5kg - 40°C no dielectric breakdown
5.11	Impact	100gm @-40°C no breakdown
5.12.4.1	Sandpaper Abrasion	.2kg 350mm min
5.12.4.2	Scrape Abrasion	Per customer agreement
5.13	Long-Term Heat Aging	150°C 3000 hours
5.15	Thermal Overload	200°C 6 hours
5.16	Shrinkage by heat	2mm max. 150°C
5.17	Fluid Compatibility	Gasoline 15% max. Diesel Fuel 15% max. Engine Oil 15% max. Ethanol 15% max. Power Steering 30% max Automatic Transmission 25% max. Engine Coolant 15% max Battery Acid no breakdown
5.19	Ozone Resistance	45°C 85% Relative Humidity 70 hours, Ozone 50 +/- 5 ppm 1kV 1 min. (no breakdown)
5.20	Resistance to hot water	not less than 10-5 ohm-mm
5.21	Temperature /Humidity Cycling	40 - 8 hours cycles -40°C and 125°C 80 - 100% relative humidity
5.22	Resistance to Flame Propagation	70 sec. max. 50mm unburned Diesel Fuel 15% max.

Engine Oil 15% max.



Ethanol 15% max.

Power Steering 30% max

8.0 Bibliography

- [1] M. Ramsey, "Wall Street Journal," [Online]. Available: <http://www.wsj.com/articles/aston-martin-may-build-electric-rapide-sports-car-in-2-3-years-1427744700>.
- [2] Tesla Motors, "Tesla Motors," [Online]. Available: <http://www.teslamotors.com/models>.
- [3] "Hitachi Construction Machinery - Americas," [Online]. Available: <http://hitachiconstruction.com/eh3500acii.html>.
- [4] John Deere, "John Deere, 644K Hybrid Wheel Loader," [Online]. Available: https://www.deere.com/en_US/products/equipment/wheel_loaders/644k_hybrid/644k_hybrid.page?.
- [5] "FIA Formula-e Championship," [Online]. Available: <http://www.fiaformulae.com/en/guide/overview.aspx>.
- [6] "Glenthorne Station," [Online]. Available: <http://www.glenthorne.co.nz/recreational-activities/station-to-station-tramps>.
- [7] "EECA energywise," [Online]. Available: <http://www.energywise.govt.nz/your-vehicle/new-technologies/electric-vehicles>.
- [8] M. A. M. a. D. W. G. Chris Mi, "HYBRID ELECTRIC VEHICLES," in *Principals and Applications with Practical Perspectives*, Wiley, 2011, p. 470.
- [9] "Drive Electric," [Online]. Available: <http://driveelectric.org.nz/>.
- [1] "Ministry of Transport," [Online]. Available: <http://www.transport.govt.nz/assets/Uploads/Research/Documents/2013-Fleet-report-final.pdf>.
- [1] "EECA," [Online]. Available: <https://www.energywise.govt.nz/on-the-road/electric-vehicles/>.
- [1] U. o. Waikato, "Energy Infomatics," [Online]. Available: <http://ei.cms.waikato.ac.nz/index.php/projects/v2g/>.
- [1] "Ministry of Transport," [Online]. Available: <http://www.transport.govt.nz/research/othertransportresearch/electricvehicles/>.
- [1] R. Cho, "PHYS.ORG," [Online]. Available: <http://phys.org/news/2015-06-batteries.html>.
- [4]

- [1] "Air New Zealand," [Online]. Available: <http://www.airnewzealand.co.nz/press-release-2016-air-new-zealand-electrifies-ground-fleet>.
- [1] U. o. Michigan, "Center for Sustainable Systems," [Online]. Available:
 6] http://css.snr.umn.edu/css_doc/CSS01-07.pdf.
- [1] D. Wratt, "NIWA," [Online]. Available: <https://www.niwa.co.nz/our-science/climate/information-and-resources/clivar/greenhouse>.
- [1] S. L. Dr Allan Miller, "Electric Vehicles in New Zealand," [Online]. Available:
 8] http://www.theenergyconference.org.nz/uploads/98897/files/Presentations/Allan_Miller__Scott_Lemon.pdf.
- [1] "U.S. Energy Information Administration," [Online]. Available:
 9] https://www.eia.gov/energyexplained/index.cfm?page=electricity_home.
- [2] "Washington University," [Online]. Available: <http://courses.washington.edu/me341/oct22v2.htm>.
 0]
- [2] R. R. Gerhold, "Houston Electric Auto Association," [Online]. Available: http://heaa.org/wp-content/uploads/library/DC_vs_AC_motors.pdf.
- [2] M.S.May, "Helwig Carbon Products," [Online]. Available:
 2] http://www.helwigcarbon.com/assets/files/pdf/Articles/ta1_96_2013%20brushes_sprkng_mach%20maint%20single%20pages.pdf.
- [2] "Engineering 360," [Online]. Available:
 3] <http://www.globalspec.com/reference/10796/179909/chapter-3-ac-and-dc-motors-ac-motors-enclosure-types-and-cooling>.
- [2] S. W. Colton, "Desgin and Prototyping Methods for Brushless Motors and Motor Control,"
 4] Massachusetts Institute of Technology, Massachusetts, 2010.
- [2] "Energy Savings with Adjustable Frequency Drives," [Online]. Available:
 5] http://literature.rockwellautomation.com/idc/groups/literature/documents/wp/drives-wp009_en-p.pdf.
- [2] T. Instruments, "Field Orientated Control of 3-Phase AC-Motors," [Online]. Available:
 6] <http://www.ti.com/lit/an/bpra073/bpra073.pdf>.
- [2] "Controller Area Network (CAN) Overview," [Online]. Available: <http://www.ni.com/white-paper/2732/en/>.
- [2] Sewell Development Company, "canbus technology," Sewell Development Company, [Online].
 8] Available: <https://sewelldirect.com/articles/canbus-technology.aspx>.

- [2] "National Instruments," [Online]. Available: <http://www.ni.com/white-paper/2732/en/#toc7.9>
- [3] "Battery University," [Online]. Available:
0] http://batteryuniversity.com/learn/article/whats_the_best_battery.
- [3] IDTechEx, "The Glittering Future of Electric Buses," [Online]. Available:
1] <http://www.idtechex.com/research/topics/electric-vehicles.asp>.
- [3] E. Eason, "World Lithium Supply," [Online]. Available:
2] [<http://large.stanford.edu/courses/2010/ph240/eason2/>] .
- [3] M. Chatsko, "The Motley Fool," [Online]. Available:
3] <http://www.fool.com/investing/general/2015/04/26/the-tesla-gigafactories-are-coming-can-global-lith.aspx>.
- [3] "Orion BMS," [Online]. Available: <http://www.orionbms.com/manuals/pdf/wiring.pdf>.
4]
- [3] "Systems Engineering for Intelligent Transportation," [Online]. Available:
5] <http://ops.fhwa.dot.gov/publications/seitsguide/section3.htm>.
- [3] R. M. Systems, "AC Motor Controller sumamry," [Online]. Available:
6] <http://evwest.com/support/PMxxx%20Datasheet%2001052012.pdf>.
- [3] "Analysis of regenerative braking efficiency," [Online]. Available:
7] <https://confluence.hro.nl/display/RE/Regenerative+braking>.
- [3] "Thunder Sky Winston," [Online]. Available: http://en.winston-battery.com/index.php/products/power-battery/item/wb-lyp100aha?category_id=176.
- [3] "Automobile drag coefficient," [Online]. Available:
9] https://en.wikipedia.org/wiki/Automobile_drag_coefficient.
- [4] "Battery University," [Online]. Available:
0] http://batteryuniversity.com/learn/article/pouch_cell_small_but_not_trouble_free.
- [4] "Trojan Battery," [Online]. Available:
1] http://www.trojanbattery.com/pdf/datasheets/T1275_Trojan_Data_Sheets.pdf.
- [4] "HVH250 Motor Manual," [Online]. Available:
2] http://www.neweagle.net/support/wiki/images/archive/a/a6/20140501174637!HVH250_MotorManual20110408.pdf.
- [4] R. M. S. LLC, "PM100 Series AC Motor Drive," [Online]. Available:
3] http://www.neweagle.net/support/wiki/docs/Rinehart/PM100_User_Manual_3_2011.pdf.

- [4] Eltek, "EV Power Charger CAN Protocol," [Online]. Available:
4] <http://evolvelectrics.com/PDF/Eltek%20CANbus%20Protocol.pdf>.
- [4] R. M. S. LLC, "Resolver Calibration Document," [Online]. Available:
5] <https://app.box.com/s/35n0u8b2sv1cc5pyf86pote73ffgi9xj>.
- [4] ANXIER, "Wire and Cable Ampacity Ratings," [Online]. Available:
6] https://www.anixter.com/en_us/resources/literature/wire-wisdom/wire-and-cable-ampacity-ratings.html.
- [4] U. W. a. Cable, "National Electrical Code," [Online]. Available: <http://www.usawire-cable.com/pdfs/nec%20ampacities.pdf>.
- [4] "Champlain Cable," [Online]. Available: <http://www.champcable.com/product/iso-6722-150-ultra-thin-wall>.
- [4] "United States Environmental Protection Agency," [Online]. Available:
9] <http://epa.gov/climatechange/science/causes.html>.
- [5] "Environmental Protection Agency," [Online]. Available:
0] <http://epa.gov/climatechange/ghgemissions/gases/ch4.html>.
- [5] "Orion BMS Operation Manual," [Online]. Available:
1] http://www.orionbms.com/manuals/pdf/operational_manual.pdf.
- [5] "Interfacing with eltek chargers," [Online]. Available: <http://www.orionbms.com/charger-integration/interfacing-eltek-chargers/>.
- [5] Kalsi, "Shaft deflection, runout, vibration, and axial motion," [Online]. Available:
3] http://www.kalsi.com/handbook/D04_Shaft_deflection_runout_vibration_and_axial_motion.pdf.
- [5] WoodWard, "112-Pin Module Family," [Online]. Available:
4] http://mcs.woodward.com/support/wiki/index.php?title=112-pin_Module_Family#ECM-5554-112-0904.